RESERVOIR ENGINEERING RESEARCH INSTITUTE

Wettability Alteration of Porous Media to Gas-Wetting for Improving Productivity and Injectivity in Gas-Liquid Flows

DE-FC26-00BC15306

Final Report

Contract Date: 9/21/00 – 8/31/03

DOE Program Manager: Mr. Chandra Nautiyal

Principal Investigator: Dr. Abbas Firoozabadi

December 1, 2003

385 Sherman Ave., Suite 2B
Palo Alto, CA 94306

Table of Contents

Disclaimer

This report was prepared as an account of work sponsored by an agency of the United States Government. Neither the United States Government nor any agency thereof, nor any of their employees, makes any warranty, express or implied, or assumes any legal liability or responsibility for the accuracy, completeness, or usefulness of any information, apparatus, product, or process disclosed, or represents that its use would not infringe privately owned rights. Reference herein to any specific commercial product, process, or service by trade name, trademark, manufacturer or otherwise does not necessarily constitute or imply its endorsement, recommendation, or favoring by the United States government or any agency thereof. The views and opinions of authors expressed herein do not necessarily state or reflect those of the United States Government or any agency thereof.

Acknowledgments

The work presented in this final report prepared for the US DOE National Petroleum Technology Office was sponsored by the US DOE Grant DE-FC26-00BC15306 and major oil companies in the period from September 2000 to September 2003. The 3M Corporation also helped with the synthesis of a number of polymers for the purpose of this project.

The work on wettability alteration from strong liquid wetting in gas-liquid systems to intermediate gas wetting is the first report of such an alteration in the petroleum production literature. It has a wide application from well deliverability increase in gas condensate reservoirs to well injectivity in water-alternate-gas (WAG) injection. There are also a number of challenges to overcome in the process of treatment. The good news is that there are two candidate reservoirs that are being considered for the field implementation.

A number of colleagues at RERI have worked on the project of wettability alteration to intermediate gas-wetting. These include Tom Tang, Eric Santiso, Rajinder Kumar and Mashhad Fahes. They have made valuable contributions to the project. During the period of the project, our project managers with DOE were Mr. Purna Halder and Mr. Chandra Nautiyal. Their support allowed us to focus on various aspects of the research.

The major oil companies that supplemented the DOE funding in the period of September 21, 2000 to August 31, 2003 include:

Abu Dhabi National Oil Company (ADNOC)
BP
ChevronTexaco Petroleum Technology Company
ConocoPhillips
ExxonMobil Upstream Research Company
JAPEX
Landmark Graphics Corp.
Maersk Oil and Gas
NIOC R&D
Norsk Hydro Production, A. S.
PEMEX
Petrobras, S. A.
Petronas
Saudi Aramco
Schlumberger Technology Corporation
TotalFinaElf

Abbas Firoozabadi
Principal Investigator

List of Tables

Chapter I

Chapter II

List of Figures

Chapter I

Chapter II

Chapter III

Chapter IV

Summary

The research work on wettability alteration from strong liquid wetting to intermediate gas-wetting which was carried out at RERI in the three year period from September 2000 to August 2003 can be divided into two broad areas: 1 – experiments, and 2 – theory. Chapters I and II cover the experimental aspects of the work and Chapters III and IV include theoretical aspects.

In an earlier work in 2000 (Li and Firoozabadi, 2000), it was demonstrated for the first time that the wettability of a porous rock can be altered from strong liquid wetting in a gas-liquid system to intermediate gas-wetting. The whole process was carried out at room temperature. The implication of such an alteration is that liquid will flow more effectively with a given pressure gradient in gas-liquid flow. An important application is the improved well deliverability in gas condensate wells.

As was stated earlier, the alteration was carried out at room temperature. Our first work in 2000 was mainly the testing of the idea. For real life applications, there are a large number of challenges that have to be met before field implementation of the idea. The effect of temperature and long term durability are among the most important aspects of the current project. A theoretical understanding of the process of wettability alteration will help in the synthesis of the chemicals and the study of the effect of various factors that may not be evaluated at laboratory conditions. The process of wettability alteration to intermediate gas-wetting is basically related to surface phenomena and the decrease of the surface energy. We have taken a long term approach to study the theory. In the following, a brief description of the four chapters gives a picture of accomplishment in the project.

Chapter I presents the effect of treatment using FC-759, a fluoropolymer on wettability alteration from strong liquid-wetting to intermediate gas-wetting. FC-759 is soluble in water. The treatment was carried out at 90°C by immersing the untreated core in the solution containing the polymer. Imbibition and flow tests were performed at room temperature and at 90°C. The results demonstrate the effectiveness in the wettability alteration. As a result of the alteration for a given pressure gradient, there is a substantial increase in the liquid phase mobility and consequently of liquid flow rate.

Chapter II discusses the effect of a high temperature of 140°C on the treatment at reservoir conditions for flow. We have also carried out comprehensive durability testing of the altered wettability for the first time by inspecting as much as 1000 pore volumes (PV) of water and oil into the treated core. Whether a core is treated at room temperature or at 140°C, water can result in loss of chemical effectiveness under high pressure gradient after a large PV injection for most chemicals. Oil, on the other hand, does not desorb the chemicals. As a result of desorpton, the effectiveness of wettability alteration to oil-wetting is reduced substantially. After this observation we embarked on a rigorous attempt to test a number of different polymers synthesized for the purpose of the project. The synthesis was done by 3M Corporation. Only one of the chemicals showed resilience for durability testing. The

chemical C has the properties to be effective especially for wettability alteration for water-gas systems.

There are two condensate reservoirs that have been selected for the purpose of pilot testing. One of these reservoirs is at a temperature of 140°C. The other reservoir is at 90°C. Two oil companies are showing strong interest to pursue the work for field applications.

In addition to the tests performed with water and hydrocarbons such as normal decane, we have also performed tests with a real condensate liquid for gas-liquid systems. The results for the normal-decane and condensate liquid are very similar.

Chapters III and IV present the effect of curvature on interfacial tensions, and the computation composition of the interface for gas-liquid systems which are considerably less complicated than the same effect, and the same computations in fluid-solid systems. These are the first steps in the understanding of interfaces. Wettability is often expressed in terms of contact angle, and contact angle is related to the interfacial tension between the fluid-fluid and fluid-solid phases.

Chapter III discusses the effect of curvature on the interfacial tension of bubbles and droplets. This effect is important in the modeling of the early part of the imbibition in intermediate wetting where kinetic effects are important. We have observed in the imbibition for intermediate-wet systems, a delay in imbibition. The work on effect of curvature is geared toward the understanding of delay (or induction) in imbibition.

Chapter IV presents a model for the computation of the composition at the interface for gas-liquid systems. In the future, such a model can be extended to fluid-solid interfaces.

Chapter 1 - Wettability Alteration to Intermediate Gas-Wetting in Porous Media at Elevated Temperatures

Tom Tang, Reservoir Engineering Research Institute

Abbas Firoozabadi, Reservoir Engineering Research Institute

Abstract

Wettability alteration to intermediate gas-wetting in porous media by treatment with FC-759, a fluoropolymer polymer, has been studied experimentally. Berea sandstone was used as the main rock sample in our work and its wettability before and after chemical treatment was studied at various temperatures from 25 to 93^{o}C. We also studied recovery performance for both gas/oil and oil/water systems for Berea sandstone before and after wettability alteration by chemical treatment.

Our experimental study shows that chemical treatment with FC-759 can result in: (1) wettability alteration from strong liquid-wetting to stable intermediate gas-wetting at room temperature and at elevated temperatures; (2) neutral wetting for gas, oil, and water phases in two-phase flow; (3) significant increase in oil mobility for gas/oil system; and (4) improved recovery behavior for both gas/oil and oil/water systems.

This work reveals a potential for field application for improved gas-well deliverability and well injectivity by altering the rock wettability around wellbore in gas condensate reservoirs from strong liquid-wetting to intermediate gas-wetting.

Introduction

Wettability alteration in water-oil systems in relation to oil recovery performance has been studied extensively in the past several decades[1-10]. However, wettability alteration in gas-liquid systems (that is, gas-oil and gas-water) through chemical treatment has only been studied recently. Li and Firoozabadi[11] and Tang and Firoozabadi[12] investigated wettability alteration from strong liquid-wetting to intermediate gas-wetting using fluorochemical polymers, FC-722 and FC-759. They showed that a stable intermediate gas-wetting can be established in Berea sandstone and chalk at room temperature. Through wettability alteration, the liquid-phase mobility for a gas-liquid system increases significantly, showing potential to improved gas well deliverability in gas condensate reservoirs. In references 11 and 12, the wettability alteration in intermediate gas-wetting has been studied at room temperature. One major goal of this work is the study of the effect of wettability alteration at high temperatures encountered in gas reservoirs. In this work, we will first present the experimental and the chemical treatment process followed by imbibition and coreflooding tests.

Experimental

Fluids and Rocks

Normal decane ($n\text{-}C_{10}$) with specific gravity of 0.73 at T=25°C was used as the oil phase in most experiments. In some tests, we used normal tetradecane ($n\text{-}C_{14}$). The measured viscosity of $n\text{-}C_{10}$ was 0.92 cp at T=25°C and 0.51 cp at T=90°C. In the presentation of results, when we use the term oil, it means that $n\text{-}C_{10}$ is used in the tests. Distilled water dissolved with 0.2% NaCl (brine) was used as the water phase. The specific gravity of brine was 1.012. The viscosity of brine was 1.012 cp at T=25°C and 0.54 cp at T=90°C. Air was used as the gas

phase. Berea sandstone with air permeability of 320 md and a porosity of 20% was used in most experiments. Two dimensions of Berea were used in this work. One had a length of about 5-6 cm and a diameter of 2.54 cm; this group was mainly used for spontaneous imbibition tests. The other one had a length of 18 cm and a diameter of 2.54 cm; this group was mainly used for core flooding tests. Kansas outcrop chalk with an air permeability of 1.5 md and a porosity of 32% was used in some experiments for the purpose of examining the results for a second rock type. The length of chalk samples was about 6-7 cm and diameter was 2.54 cm. Relevant data of the rock properties are listed in Table 1.

Chemical Treatment

FC-759 and FC-722 polymers manufactured by 3M Specialty Materials were used to alter the wettability of Berea and chalk samples from strongly liquid-wetting to intermediate gas-wetting. These chemicals have the specific functional groups which serve different purposes. Among these chemicals, FC-759 was used for most of this study because it was developed for coating on the surface of porous media[13]. Figure 1 shows the chemical structure of FC-759. The fluorochemical group provides water and oil repellency; the silanol and anionic groups chemically bond onto the rock surfaces providing a durable treatment; the anionic and nonionic groups make the polymer hydrophilically soluble. In addition, some Berea samples were treated with 1% stearic acid solution. The sample was saturated and aged with 1% stearic acid solution (1% stearic acid dissolved in normal decane) at room temperature for 10 days. The wettability of the rock treated with 1% stearic acid shows a very weak water-wetting for a water/oil system[10].

In a previous work[12], we reported two processes to alter rock wettability from strongly liquid-wetting to intermediate gas-wetting: process-1 and process-2. In this work, the core samples were treated using process-2. For this process, the core sample with about 10-15% initial water saturation was first saturated with chemical solution using an evacuating system. Then, it was submerged in the same chemical solution; the container was sealed and aged at T=90°C for 3 days. After aging, the core sample was cooled to room temperature and was displaced with dry air to remove all liquids. The core sample, either dry or with some initial water saturation (re-established), was then used for imbibition or flooding tests. In process-2, unlike process-1, we do not heat the dry core at high temperature for stabilizing the chemical adsorption (that is, process-1).

Imbibition and Coreflooding Process

The air-saturated core was hung under an electronic balance and placed in either oil or water to carry out spontaneous imbibition tests (see Figure 2a). For the tests conducted at room temperature, the core was hung on the balance all the time and change in the weight of the core sample vs. time was recorded; for the test conducted at elevated temperature, the core sample and the container were placed in an oven at the test temperature. The weight of the core sample was measured using the electronic balance vs. time.

Coreflooding tests were carried out in the temperature range of about 25°C to 90°C. Figure 2b shows a schematic of the apparatus for coreflooding tests. The core sample was covered with FTP heat-shrinking tubing and placed in a visual coreholder. It was positioned horizontally to avoid gravity effect. A confining pressure of 300 psig was used. In some tests, gas was injected at constant inlet pressure; in others, oil (or water) was injected at constant

rate. The produced gas and oil (or water) were separated in the separator installed at the outlet; the gas and oil (or water) production rates were measured vs. time. The pressure-drop across the core was measured using a Validyne differential pressure transducer. For the tests performed at 90°C, the injected liquids were heated in the pre-heater which was made of a 20-ft coiled copper tubing with an inside diameter of 1 mm before entering the core.

Results

Wettability Alteration to Intermediate Gas-Wetting

In this section, we will present some aspects of wettability alteration from strong liquid-wetting to intermediate gas-wetting using the chemical treatment process that was described above. Gas recovery and oil imbibition rate by spontaneous oil imbibition are used to characterize the wettability state of the core before and after chemical treatment.

Uniformity of Altered Wettability

Figure 3a shows the core samples (B20-B23) used to examine the uniformity of the altered wettability by chemical treatment. Four cylindrical cores were treated with 10% FC-759 at T=93°C. After chemical treatment, three of them were cut to make different shapes and fresh surfaces for oil imbibition. Core B23 was not cut; core B21 was cut from the middle along radius; core B22 was cut from the middle along the axial direction; and core B21 was cut from the two ends (see Figure 3a). These four cores were then used for spontaneous oil imbibition testing at room temperature. Figure 3b presents the relevant experimental data for these four cores. T_a represents the aging temperature and T_t represents the test temperature. In order to assess the change in wettability, imbibition data for the untreated Berea sample (B1) is also

presented as a reference. The results shown in Fig. 3b reveal that both oil imbibition rate and final gas recovery are similar for the four treated cores. Increase in imbibition surface areas for cores B20-B22 does not raise oil imbibition rate, indicating that the altered wettability by chemical treatment is uniform throughout the cores.

Effect of Initial Wettability State

Berea samples with three wettability states, strongly water-wet, weakly water-wet, and weakly oil-wet were treated with 8% FC-759 to examine the effect of initial wettability state on wettability alteration to intermediate gas-wetting by FC-759 treatment. Untreated Berea sample (B2) was used as a reference for strongly water-wet sample. The measured Amott Index to water (I_w) for core B2 was 1.0. In order to alter the wettability to a weakly water-wet core, Berea sample (B3) was pre-treated with 1% stearic acid solution using the procedure described by Tang and Firoozabadi[10]. The measured Amott Index[14] to water (I_w) was 0.18 for core B3 after it was pre-treated with stearic acid solution. For the weakly oil-wet core sample, Berea sample (B4) was pre-treated with the crude oil from Kagel field, Rio Blanco, Co. The dry core sample was saturated with crude oil and aged at T=90^{o}C for 10 days. Thereafter, the core sample was flooded with hot normal decane until the effluent was colorless. Then, the core was heated for 8 hours at T=105^{o}C to stabilize the adsorption of polar oil components. The measured Amott Index to water (I_w) was zero and to oil (I_o) was about 0.1 for core B4 after treated with the crude oil. The core samples with different initial wettability states (strongly water-wet, weakly water-wet and weakly oil-wet) were then treated with 8% FC-759 using the procedure described above. After the cores were treated with 8% FC-759, they were used for spontaneous oil imbibition tests with zero initial water saturation at room temperature.

Figure 4 presents the measured imbibition data for the three Berea samples (B2, B3, and B4). The final gas recovery by spontaneous oil imbibition was about 8% for treated core B2 (initially water-wet), 10% for treated core B3 (initially weakly water-wet), and 15% for treated core B4 (initially weakly oil-wet). The wettability alteration to intermediate gas-wetting using 8% FC-759 treatment was mildly influenced by the initial wettability state of the cores. The trend of the data in Figure 4 suggests that adsorption of FC-759 is not much affected by other polar oil components adsorbed onto the rock surfaces. Clean rock provides the surfaces for FC-759 treatment for the most pronounced wettability alteration. However, the presence of other polar species is not detrimental to wettability alteration to intermediate gas-wetting by FC-759 treatment.

Effect of Initial Liquid Saturation

Figure 5a shows the gas recovery by spontaneous oil imbibition for the core treated at various initial water saturations. The final gas recovery decreases with increase in initial water saturation, indicating a positive effect of initial water saturation on chemical treatment with FC-759. For all the three cores, the final gas recovery was less than 10%. A substantial decrease in imbibition rate and final gas recovery are observed due to wettability alteration from strongly liquid-wetting to intermediate gas-wetting. These results are in agreement with our previous study for the treated cores at zero initial water saturation [12] and provide strong evidence that wettability alteration to intermediate gas-wetting can be achieved for the cores with about 10-20% initial water saturation.

In the wellbore of gas condensate reservoirs, liquid-condensate dropout could be as high as 60%[15]. Therefore, investigation of the effect of initial oil saturation on wettability alteration

by FC-759 is of interest. Berea sample (B17) initially saturated with about 10% oil was treated with 10% FC-759 using a treatment procedure similar to the other tests. Thereafter, the core was dried and used for oil imbibition test. Figure 5b shows that gas recovery increased quickly to about 5% at the beginning of the test. After that, the oil imbibed into the core gradually. The oil imbibition continued to the end of the test. The gas recovery by spontaneous oil imbibition at the end of the test was about 33%. Higher gas recovery might have been obtained should we have continued the test. Thus, one may imply that initial oil saturation could reduce the effectiveness of wettability alteration.

In gas condensate reservoirs there is generally some initial water saturation prior to liquid dropout. For field application, further study of the wettability alteration with coexistence of both water and oil saturation is useful. Three cores (B16, B18, and B19) were used for this purpose. We fixed the initial water saturation at 10% and changed the initial oil saturation from zero to 40%. Then the chemical was injected into the cores and the cores were aged at 93^{o}C for three days. After the cores were dried, they were used for imbibition tests. Figure 5c shows the imbibition data for these three cores (B16, B18, and B19). The results reveal that the oil imbibition rate and final gas recovery increases with increase in initial oil saturation at a constant initial water saturation of 10%. Comparison of Figs. 5b and 5c reveals that initial water saturation improves the wettability alteration by FC-759.

Effect of Temperature

In order to study the effect of temperature, we performed spontaneous imbibition tests conducted at various temperatures from 25^{o}C to 93^{o}C. The treated-core sample was placed in a container with a sealed cap and filled with oil. The container was kept in an oven at test

temperature, except for quick measurement of core weight. The imbibition in an untreated core (B5) was used to establish a reference for studying the effect of temperature on imbibition behavior. For core B5, increase in temperature from 25 to 90°C only showed a small increase in imbibition rate (Figure 6a). Figure 6b shows the data for B15, a Berea core treated with 1% stearic acid solution. The results show that the oil imbibition rate and the final gas recovery were high – both at T=25 and 90°C. The results also show that stearic acid, which can establish a weakly water-wetting on Berea sandstone for a water/oil system, can not establish an intermediate gas-wetting in Berea sandstone for a gas/oil system. Figure 6c shows the experimental data obtained for core B6 when treated with 2% FC-722 twice, at T=25, 55, 75, and 88°C. Oil imbibition rate and the final gas recovery increased systematically with increase in temperature. The imbibition rate at T=88°C was very high; the final gas recovery was 52%, showing a liquid-wet behavior. In order to examine desorption of the chemical from the rock surfaces due to increase in temperature, we dried and weighed core B6 after the tests. The measured data showed that no desorption occurred because the weight of the core remained unchanged. Thereafter, we performed a spontaneous oil imbibition test with core B6 at T=25°C (defined as run-2 in Figure 6c). The core sample behaved as intermediate gas-wetting again. The final gas recovery for run-2 was only 11%, which was nearly the same as that for run-1. This behavior implies that increase in temperature may increase surface energy which improves oil imbibition. Figure 6d shows the data for core Berea B7 treated with 10% FC-759 twice, at T=25, 55, 70, and 93°C. The results show that oil imbibition rate and final gas recovery were less influenced with temperature in the 25 to 93°C range. In fact, from T=25 to 70°C, the oil imbibition performance did not change appreciably. Even at 93°C, the oil imbibition rate was slow and the final gas recovery was about 27%. FC-759 is more effective

than FC-722 at high temperatures, indicating that chemical structure is a dominant factor for wettability stability.

Effect of Oil

We compared the oil imbibition behavior in the treated Berea at T=93^{o}C using both normal tetradecane (n-C_{14}) and normal decane (n-C_{10}). Figure 7 shows the data for the treated and untreated cores. For the untreated core, the oil imbibition rate was slower for n-C_{14}; the final gas recovery was the same for n-C_{10} and n-C_{14}. For the treated core, both oil imbibition rate and final gas recovery were lower for n-C_{14}. This result implies that the treated core may behave somewhat differently with different oils. We have embarked on a set of experiments using condensate liquids in our tests to study fluid flow in treated cores. The results will be published in the near future.

Wettability Features of the Treated Cores by FC-759 for Water/Oil System

For cores (B8 and C2) treated with 8% FC-759, we also studied wettability features for the water/oil system. Figure 8a presents the experimental data for water recovery by spontaneous oil imbibition in a 100% water saturated cores, B8 and C2. This figure shows that oil can not imbibe into the water-saturated cores, revealing that the cores B8 and C2 are not preferentially oil-wet. Next, we dried the core samples and saturated them with oil. The oil-saturated cores were then placed in water to perform spontaneous water imbibition testing. Figure 8b presents the oil recovery by spontaneous water imbibition in the oil-saturated cores B8 and C2. About 7% oil was recovered by spontaneous water imbibition from these two cores, indicating that the cores B8 and C2 were not preferentially water-wet either.

The above results reveal that when the core samples (Berea and chalk) were treated with FC-759, it behaved neutrally wet for a water-oil system: neither oil nor water preferentially wets the rock surfaces. The established neutral wetting on Berea sandstone and chalk is stable based on measurements from tests of long duration (we do not present the results here for the sake of brevity).

Implications of Wettability Alteration to Intermediate Gas-Wetting

In a recent work[12], we showed that gas/liquid flow could be improved significantly through wettability alteration from strong liquid-wetting to intermediate gas-wetting at room temperature. In this work, we study further the effect of wettability alteration to intermediate gas-wetting on (1) recovery efficiency for both gas/oil and water/oil systems, (2) gas and oil relative permeabilities, and (3) injectivity of water or oil. The recovery efficiency tests were performed at room temperature only, whereas relative permeability measurements are conducted both at room temperature and at high temperature.

Two Berea samples, B10 and B11, with a length of 18 cm and a diameter of 2.54 cm were repeatedly used in the following tests. B12 was treated with 8% FC-759 twice and B11 was not treated. All the tests were performed with the coreholder positioned horizontally. The cores were 100% saturated with one phase and the second phase was injected to displace the resident phase.

Recovery for Gas/Oil System

The data of gas recovery by oil injection in the untreated (B11) and treated (B10) cores saturated with air are presented in Figure 9a. Oil was injected at a constant rate of 3 cm^3/min.

The data show that for the treated core with FC-759, the gas recovery at oil breakthrough increased from 60 to 80%; the final gas recovery increased from 80 to 90%. The corresponding pressure-drop data for the tests with cores B11 and B10 are presented in Figure 9b. The maximum pressure drop was about 17.5 psi for the untreated core (B11) and about 7.2 psi for the treated core (B10). After oil breakthrough, the pressure-drop gradually decreased and stabilized at 7.6 psi for the untreated core (B11) and at 5.6 psi for the treated core (B10). Decrease in pressure-drop after wettability alteration indicates an increase in oil injectivity in porous media.

Recovery for Oil/Water System

Figure 10a shows the results for water injection in 100% oil-saturated cores. The water injection rate was 4 cm^3/min. For the treated core (B10), the oil recovery at water breakthrough was about 56% and the final recovery was about 72%; about 16% oil was produced after water breakthrough, indicating the invading phase (water) was not preferentially wetting the rock surface. For the untreated core (B11), the oil recovery at water breakthrough was about 53% and the final recovery was about 54%. The oil recovery after water breakthrough was negligible, indicating a typical process of wetting phase (water) displacing a non-wetting phase (oil). This result is consistent with the results obtained by Tweheyo et al[16]. The pressure-drop data presented in Figure 10b also indicate a decrease after wettability alteration. The maximum pressure-drop for the untreated core (B11) was 6.5 psi and it then stabilized at 5.6 psi after water breakthrough. For the treated core (B10), the maximum pressure-drop was 2.9 psi and it then stabilized at 1.4 psi after water breakthrough. The pressure drop decreased about 3.5 times

after wettability alteration, indicating a significant increase of water injectivity in the oil saturated core. This result is in line with the work reported by Penny et al (1983)[8].

Figure 11a shows the experimental data for oil injection in water-saturated cores. The oil injection rate was 4 cm^3/min. For the untreated core (B11), water recovery at oil breakthrough was about 30%, and the final recovery was about 50%. Nearly two-fifths of the recovered water was produced after oil breakthrough, indicating a non-wetting phase (oil) displacing a wetting phase (water). For the treated core (B10), the water recovery at oil breakthrough was about 51% and the final recovery was about 62 %. This behavior also indicates that the oil phase (the invading phase) was not preferentially wetting the rock. The corresponding pressure-drop data for oil displacing water are presented in Figure 11b. The maximum pressure-drop for the untreated core was about 3.4 psi; it then stabilized at 2 psi. For the treated core, the maximum pressure-drop was about 1.7 psi and it then stabilized at 0.8 psi. The oil injectivity in the water-saturated core increased 2 times with the alteration of wettability.

The results above show that after wettability alteration from strong liquid-wetting to intermediate gas-wetting, gas recovery by oil injection, oil recovery by water injection, and water recovery by oil injection were improved significantly. In addition, oil injectivity in the gas-saturated core, oil injectivity in water-saturated core, and the water injectivity in the oil-saturated core were improved significantly. All these results imply that wettability alteration through FC-759 treatment can also be applied to oil reservoirs and aquifers for the purpose of improving water and oil injectivity and productivity in water-oil flow.

Reduction of Oil Saturation in Porous Media by Dry Gas Injection

In some gas condensate reservoirs, liquid dropout accumulation near the wellbore can cause sharp decline in gas production[16,17]. Removal of liquids from the wellbore has been a challenge. In this work, we study the effect of wettability alteration on oil removal from a core by injecting dry gas. Two Berea samples, B13 (treated with 10% FC-759 twice) and B14 (untreated) were saturated with oil (n-C_{10}). Then they were subjected to dry air injection at a constant pressure gradient of 0.056 psi/cm. The oil saturation was measured by weighing the core; thus the measured oil saturation is an average value. The tests were carried out at T=25 and 90^{o}C.

Figure 12a presents the average oil saturation (n-C_{10}) vs. time for the treated and untreated cores at T=25^{o}C. Oil saturation in both cores decreased quickly from 100 to about 60% during the first 20 minutes. Then, oil saturation decreased slower. The oil saturation in the treated core (B13) remained lower than that in the untreated core (B14), showing higher oil mobility in the treated core. At injection time t=200 minutes, the oil saturation in the treated core (B13) was about 30% and in the untreated core (B14) was about 41%. The final oil saturation in the treated core (B13) was 23%; in the untreated core (B14), was 35%.

Results at T=90^{o}C are presented in Figure12b. At t<200 minutes, the oil saturation decreased with a trend similar to the test at T=25^{o}C. Thereafter, the oil saturation in both cores continued decreasing at a lower rate. The oil saturation in the treated core (B13) was about 20% lower than that in the untreated core (B14). At t=2400 minutes, the oil saturation in the treated core (B13) reached zero and the oil saturation in the untreated core (B14) reached 17%. Comparing the results shown in Figures 12a and 12b, one may assume that at high temperatures, oil

saturation could be decreased further. We assume that in addition to the wettability alteration, the phase-behavior effect also reduces oil saturation in porous media at high temperatures.

Gas and Oil Relative Permeabilities

Figure 13a shows the measured gas and oil relative permeabilities for the untreated core (B14) and treated core (B15) at 90°C. Initial water saturation was zero and the oil phase was normal decane (n-C_{10}). The results show that the wettability alteration from strong liquid-wetting to intermediate gas-wetting resulted in (1) the oil saturation at the point for $k_{ro} = k_{rg}$ reduced from 0.55 to 0.48 PV; (2) the cross point relative permeability increased from 0.04 to 0.1 PV; (3) gas relative permeability decreased, but oil relative permeability increased significantly; and (4) the residual oil saturation decreased from 0.48 to 0.1 PV. These results are in line with those obtained at room temperature (Tang and Firoozabadi[12], 2000). Figure 13b shows the measured gas and oil relative permeabilities for the treated core (B15) at 90°C. Both n-C_{10} and n-C_{14} were used. The results show that the gas relative permeability decreased and oil relative permeability increased when the oil phase was changed from n-C_{10} to n-C_{14}. This trend is in agreement with our imbibition study shown in Figure 7. As was stated earlier, we are currently working with condensate liquids and the results will be the subject of a forthcoming publication.

Discussions and Conclusions

In this work, we have demonstrated that the wettability of Berea and chalk can be altered to intermediate gas-wetting using FC-759 for a temperature range of 25-93°C with initial water and oil saturations. From wettability alteration to intermediate gas-wetting, it is shown that: (1)

improved recovery performance for both gas/oil and oil/water systems; (2) increased oil phase mobility and decrease in residual oil saturation for a gas/oil system; (3) reduced oil saturation in porous media through injecting dry gas at both room and elevated temperatures; and (4) increased oil or water injectivity in water/oil flow.

In addition, in the course of the experiments, we did not observe core damage due to treatment with FC-759. Visual examinations show that fine particles of the Berea and chalk become more stable after treatment with FC-759. Therefore, sand production could also reduce by adsorption of FC-759 onto the rock surfaces.

We are currently searching for new chemicals that are very effective for wettability alteration to intermediate gas-wetting. Also, we are currently focusing on tests at reservoir conditions including using reservoir gas condensate fluids. The results will be published in due time.

Acknowledgements

This work was supported by the US DOE grant DE-FG22-96BC14850 and the members of the Reservoir Engineering Research Institute (RERI). Their support is appreciated. We thank Mr. R. Jahanian for his assistance in the experimental work.

References

1. MORROW, N. R., CRAM, P.J., McCAFFERY, F.G., Displacement Studies in Dolomite with Wettability Control by Octanoic Acid, *Soc. Pet. Eng. J.*, Aug., 1973, pp. 221-232.
2. MORROW, N.R., LIM, H.T., and WARD, J.S., Effect of Crude Oil Induced Wettability Changes on Oil Recovery, *SPEFE*, Feb., 1986, pp. 89-103.

3. OWENS, W.W. and ARCHER, D.L., The Effect of Rock Wettability on Oil-Water Relative Permeability Relationships, *JPT, Trans, AIME*, 251., July 1971, pp. 873-878.

4. KOVSECK, A.R., WONG, H., and RADKE, C,J., A Pore-Level Scenario for the Development of Mixed Wettability in Oil Reservoirs, *AIChE, J.*, Vol. 39, No.6., June 1993, pp.1072-1085.

5. CUIEC, L.E., Evaluation of Reservoir Wettability and Its Effect on Oil Recovery, *Surfactant Science Series, Interfacial Phenomena in Petroleum Recovery*, Morrow N.R., ed., Marcel, Dekker, Inc., 1990, pp.319-375.

6. MAINI, B.B., IONESCU, E., BATYCKY, J.P., Miscible Displacement of Residual Oil-Effects of Wettability on Dispersion in Porous Media. *JCPT*, May-June, 1986. pp.36-41.

7. LEGENS, C., PALERMO, T., TOULHOAT, H., FAFET, A., and KOUTSOUKOS, P.. Carbonate Rock Wettability Changes Induced by Organic Compound Adsorption. *J. Pet. Sci. Eng*., Vol. 20, 1998, pp.277-282.

8. PENNY, G. S., SOLIMAN, M. Y. CONWAY, M.W. and BRISCOE, J. E., Enhanced Load Water-Recovery Technique Improves Stimulation Results, *paper SPE 12149* presented at *the 68th ATCE*, San Francisco, CA, October 5-8., 1983.

9. FLEURY, M., BRANLAND, P., LENORMAND, R., ZARCONE, C., Intermediate Wettability by Chemical Treatment. *J. Pet. Sci. Eng*., Vol. 24, 1999. pp.123-130.

10. TANG, G. and FIROOZABADI, A., Effect of Pressure Gradient and Initial Water Saturation on Water Injection in Water-Wet and Mixed-Wet Fractured Porous Media, SPE Reservoir Evaluation & Engineering, Dec. 2001, pp. 516-524.

11. LI, K. and FIROOZABADI, A., Experimental Study of Wettability Alteration to Preferential Gas-Wetting in Porous Media and Its Effects. *SPE Reservoir Evaluation and Engineering*, April, 2000, pp.139-149.
12. TANG, G. and FIROOZABADI, A., Relative Permeability Modification in Gas-Liquid Systems through Wettability to Intermediate Gas-Wetting, Paper *SPE 62934* presented at *the 2000 ATCE*, Dallas, TX., 1-4 Oct., 2000 (b).
13. LINERT, J.G., A New Water-Soluble Fluoropolymer Silanol and its Application in Stone and Concrete Protection, *Proceedings of 1997 Waterborne, High-Solids, and Powder Coating Symposium*, New Orleans, LA, Feb.5-7, 1997.
14. AMOTT, E., Observations Relating to the Wettability of Porous Rock, *Trans, AIME*, 1959, 216, pp.156-162.
15. TWEHEYO, M. T., HOLT, TORSETER, T., An Experimental Study of the Relationship between Wettability and Oil Production Characteristics. *J. Pet. Sci. Eng*., Vol. 24, 1999, pp.179-188.
16. HINCHMAN, S.B. and BARREE, R.D., Productivity Loss in Gas Condensate Reservoirs, paper SPE 14203 presented at the 60th Annual Technical Conference and Exhibition of SPE, Las Vegas, NV, Sept., 22-25, 1985.
17. EL-BANBI, A.H. and McCAIN Jr, W.D., Investigation of Well Deliverability in Gas-Condensate Reservoirs, paper PSE 59773 presented at the 2000 SPE/CERI Gas Technology Symposium, Calgary, Alberta, Canada, 3-5 April, 2000.

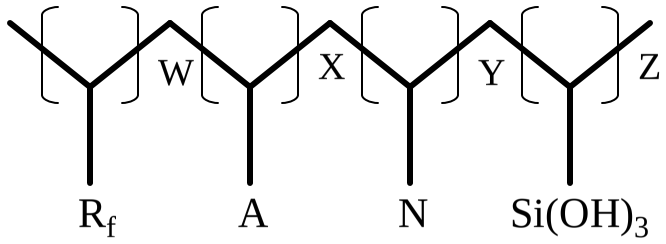

R_f-Fluorochemical

A -Anionic group

N -Nonionic group

W≠X≠Y≠Z

Fig.1 Chemical Structure of FC-759 (Linert, 1997)

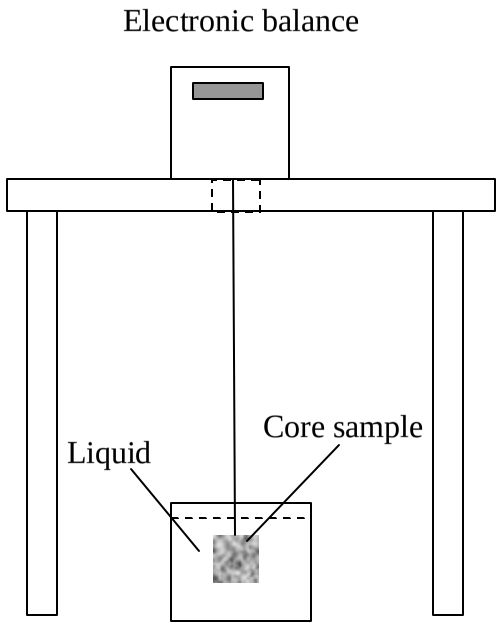

Fig.2a Schematic of the Apparatus for Spontaneous Imbibition Tests

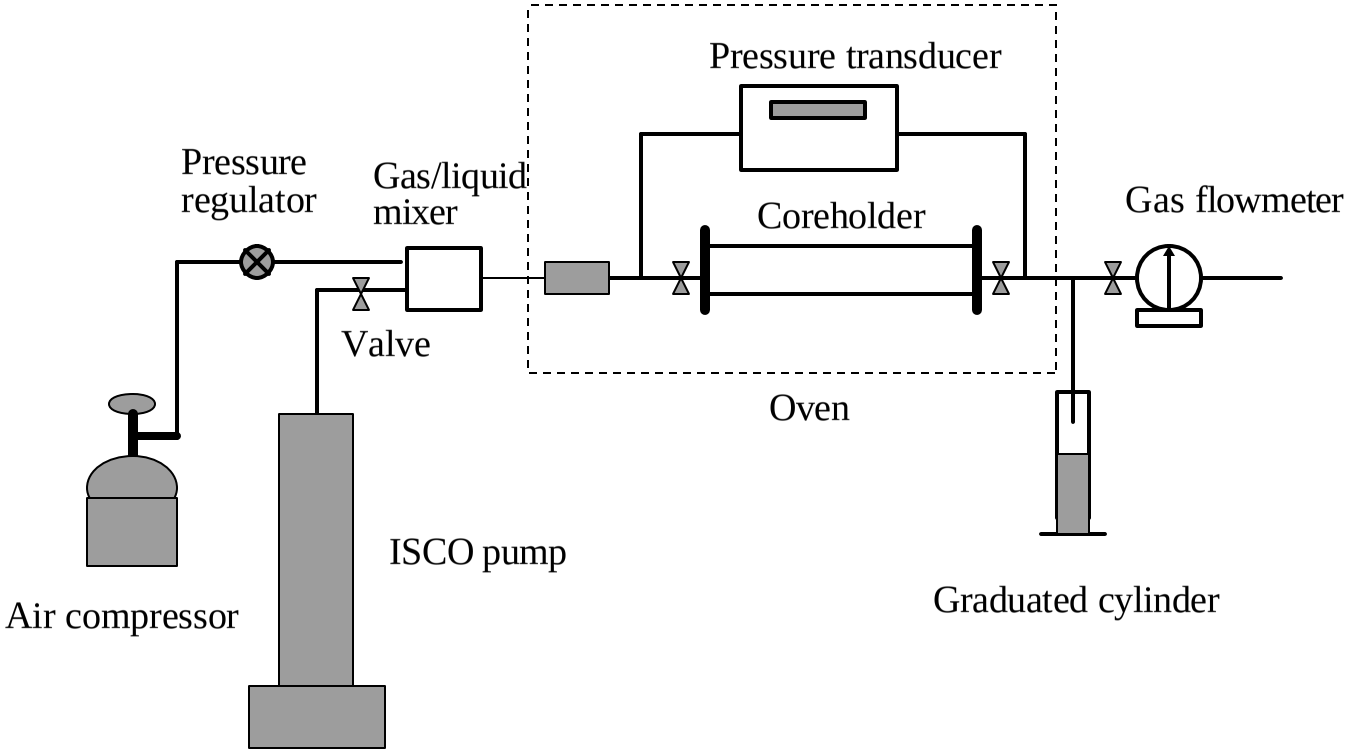

Fig.2b Schematic of the Apparatus for Coreflooding Tests

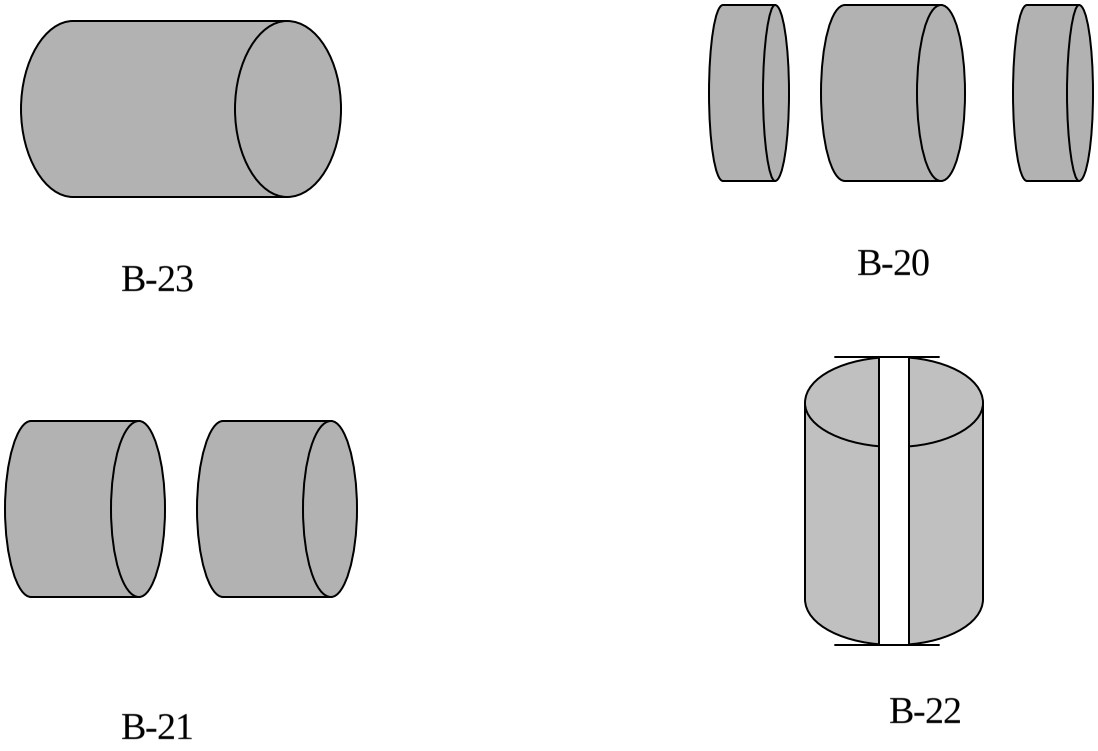

Figure 3a Schematic of the Cores after Cutting

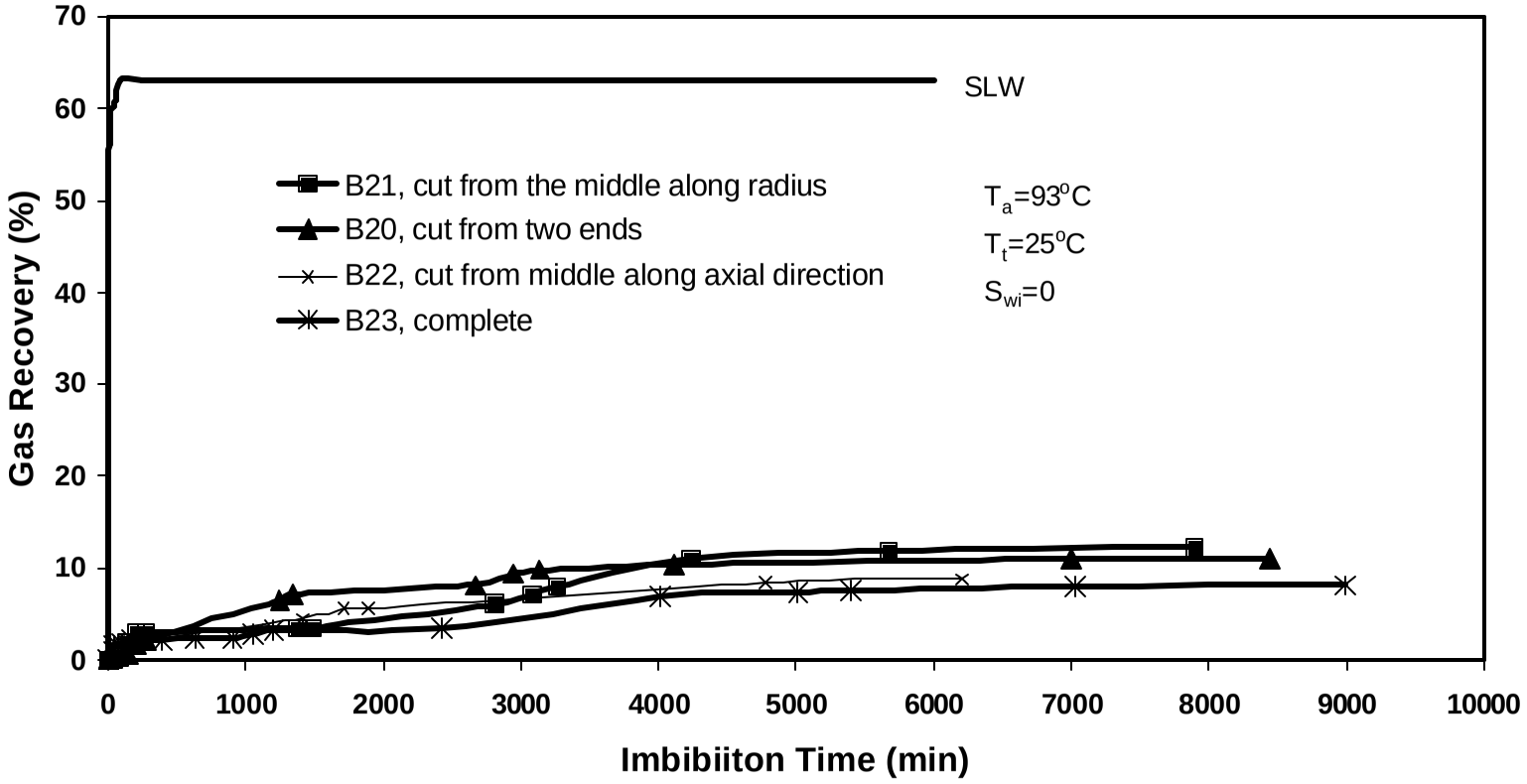

Fig. 3b Gas Recovery by Spontaneous Oil Imbibition for Cores Treated with 10% FC-759 before and after Cut

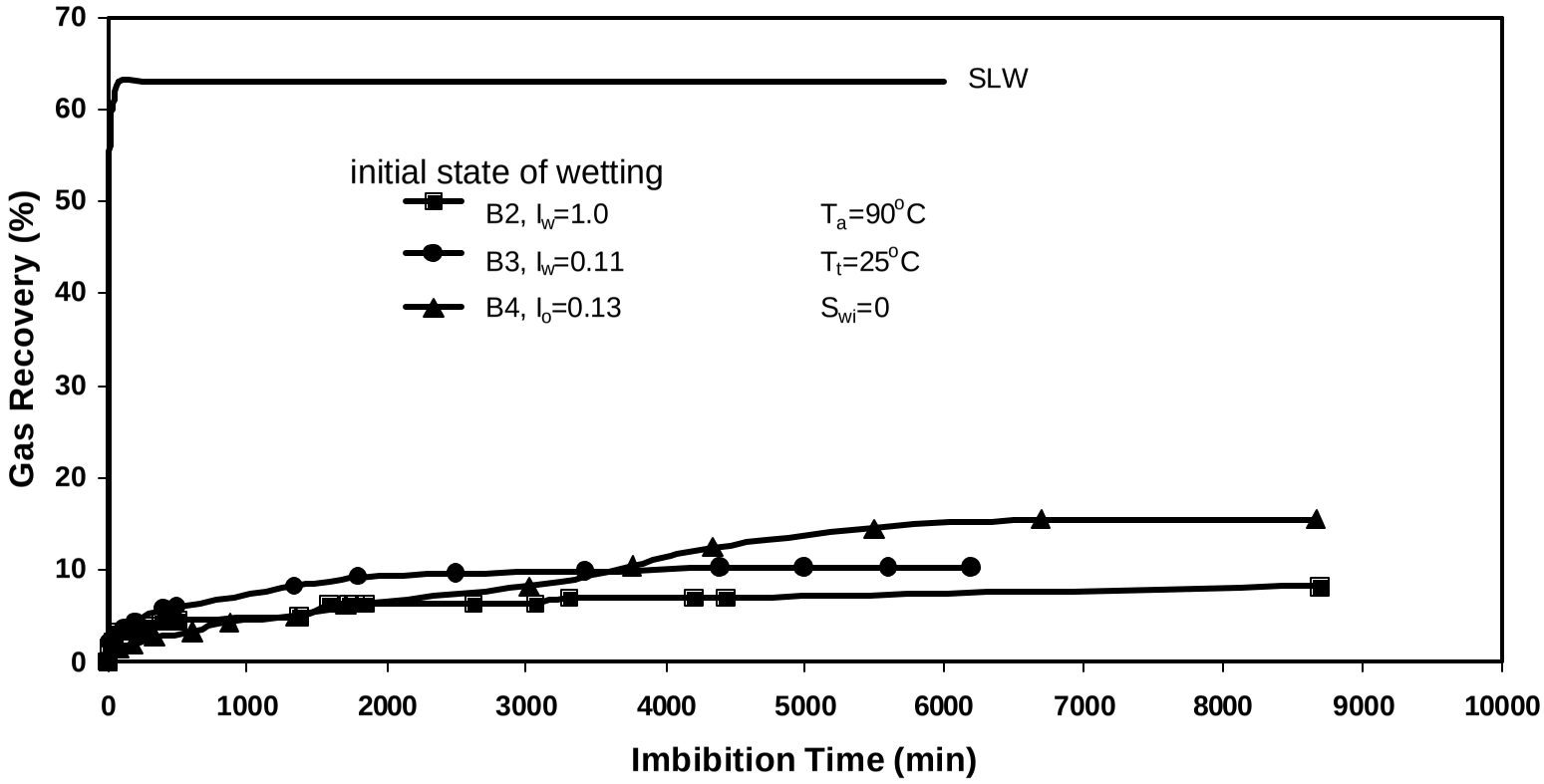

Fig.4 Effect of Initial Wettability on Wettability Alteration by 8% FC-759

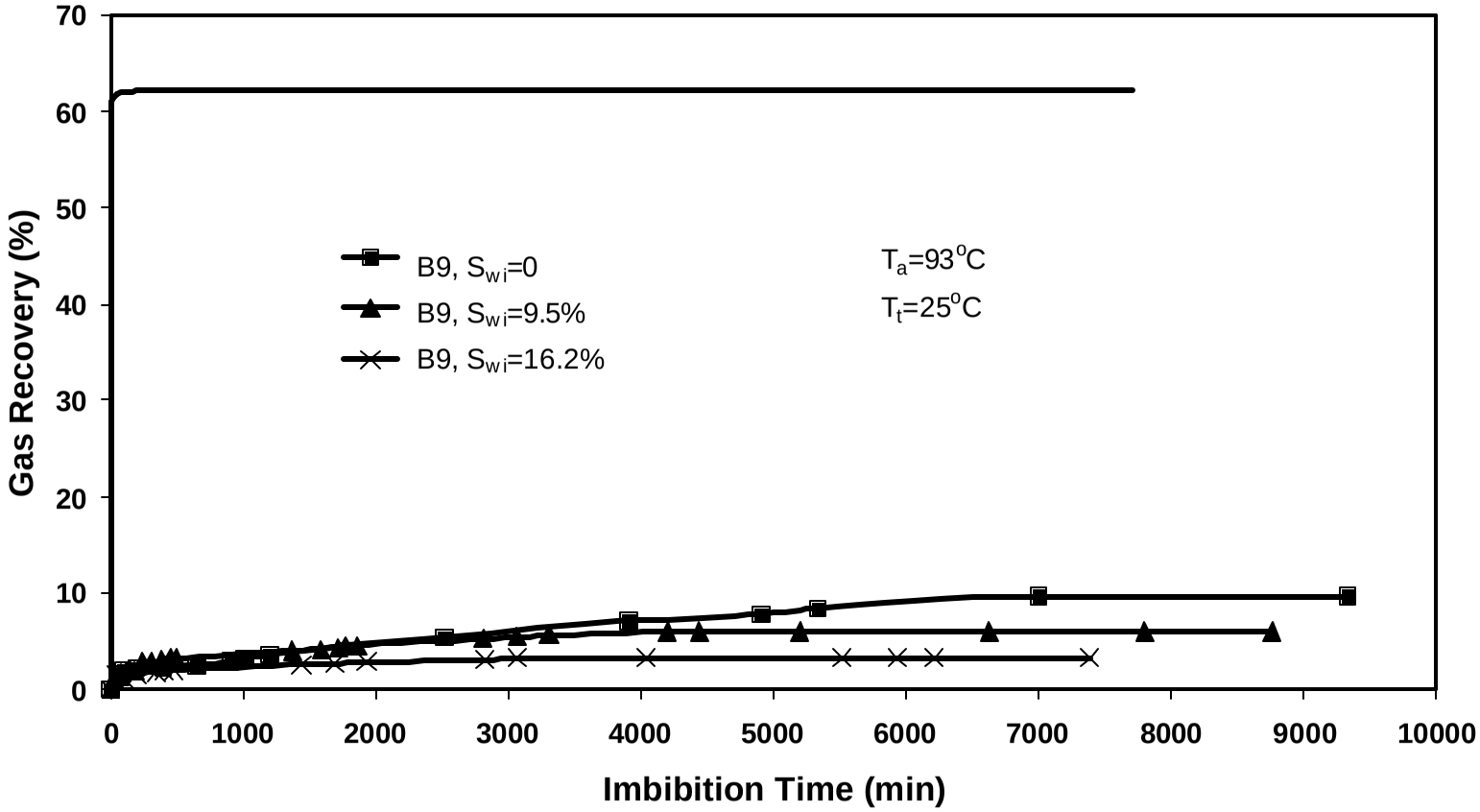

Fig.5a Effect of Initial Water Saturation on Wettability Alteration by 8% FC-759

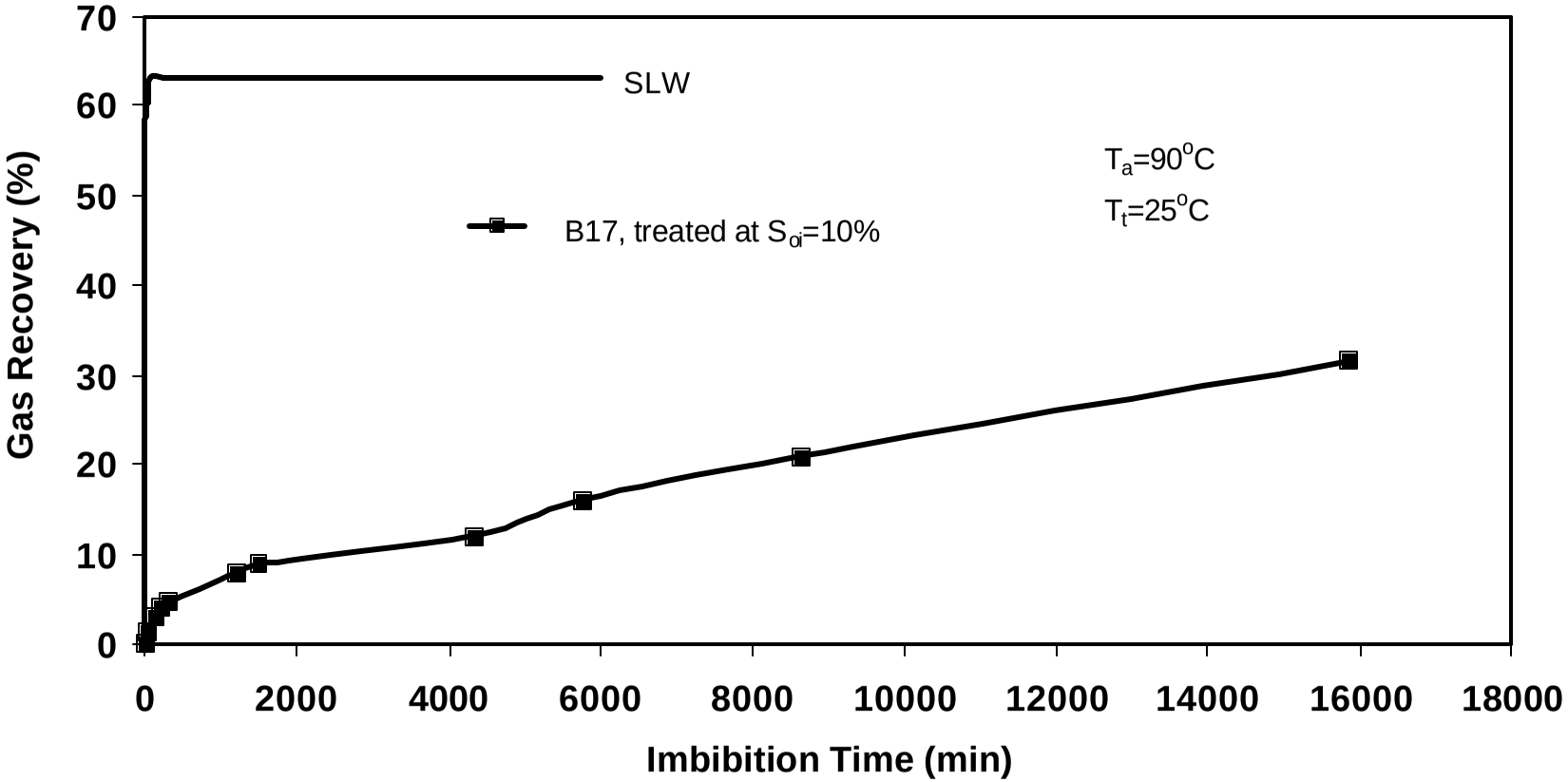

Fig.5b Effect of Initial Oil Saturation on Wettability Alteration by 10% FC-759

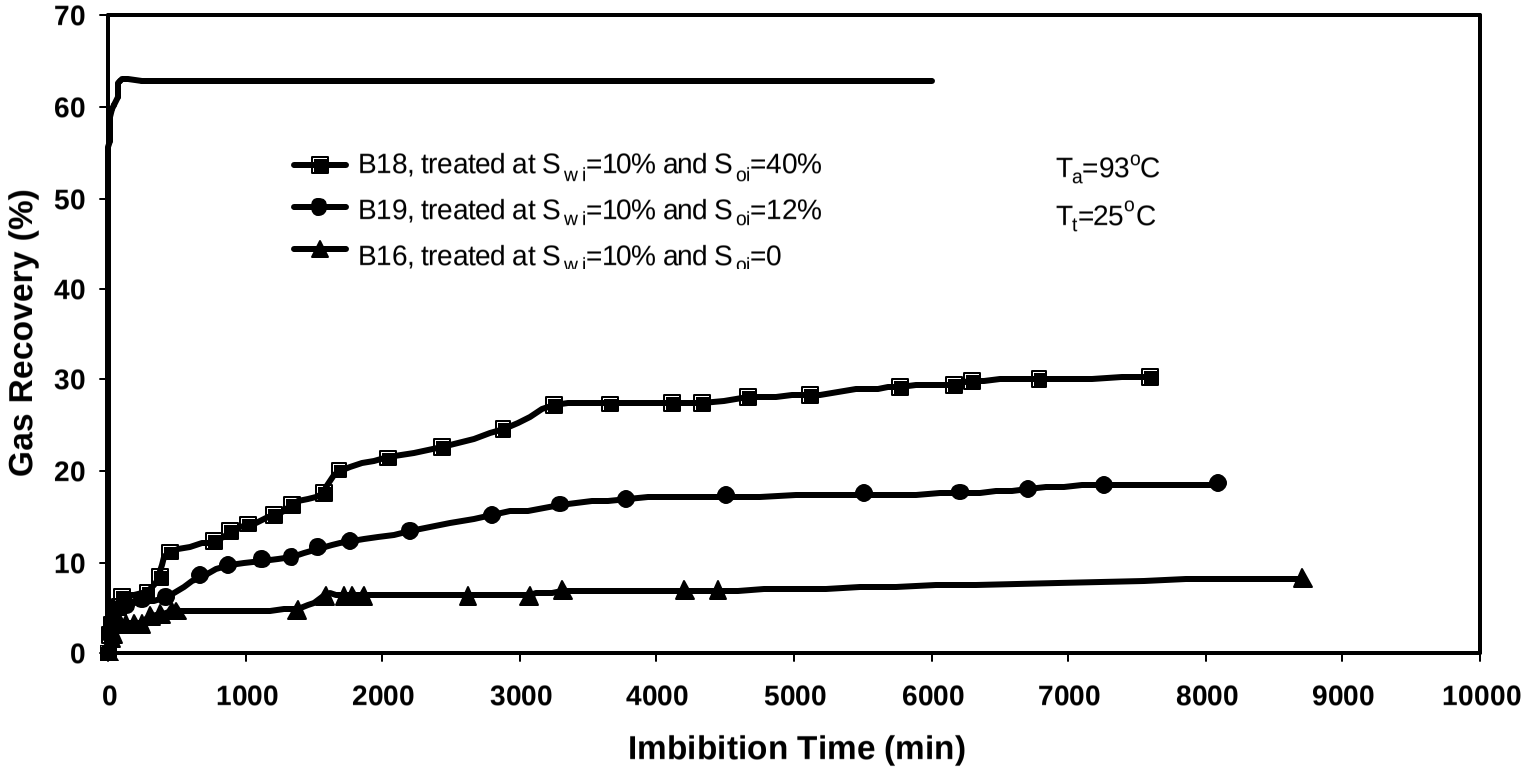

Fig.5c Effect of Initial Water and Oil Saturation on Wettability Alteration by 10% FC-759

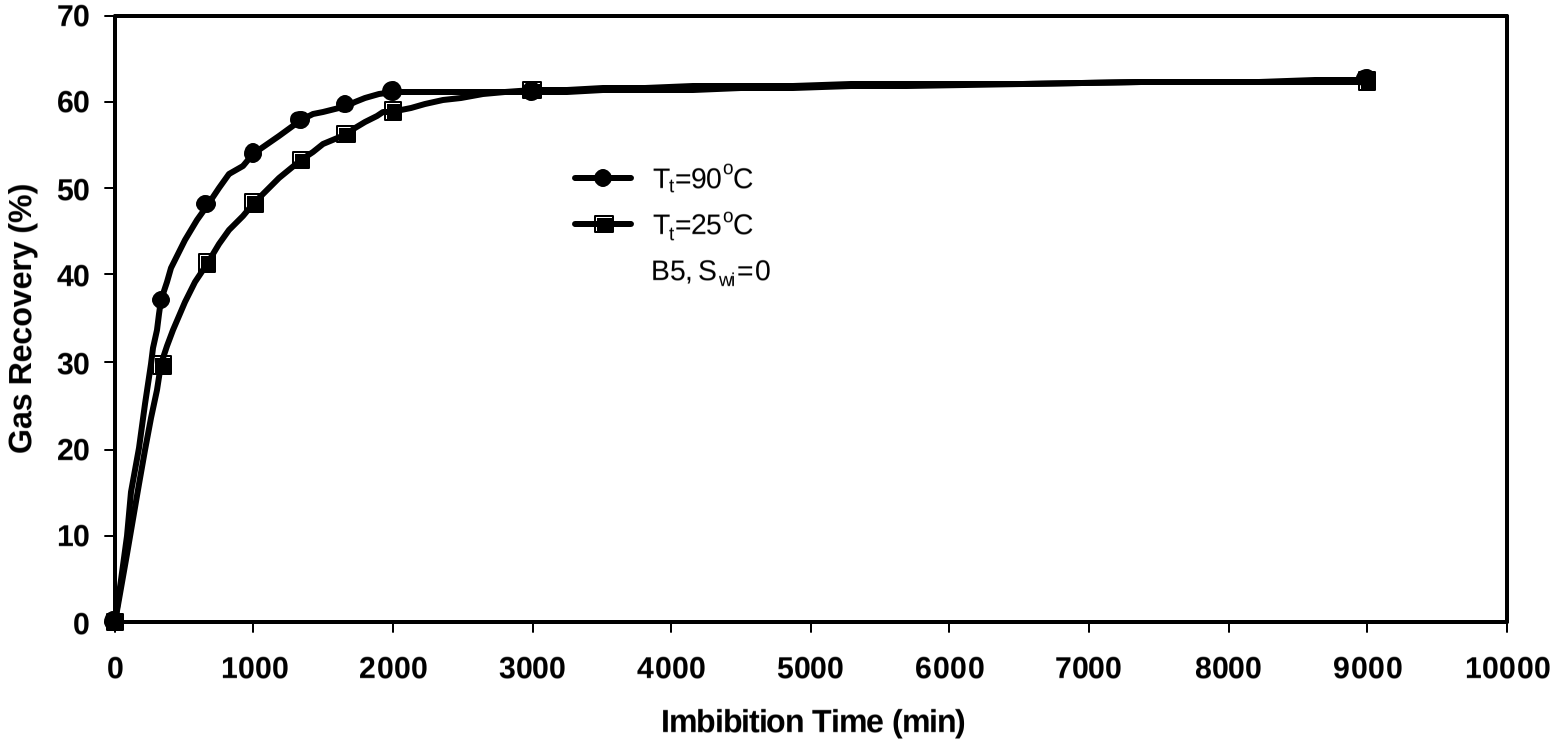

Fig.6a Effect of Temperature on Spontaneous Oil Imbibition for Untreated Berea

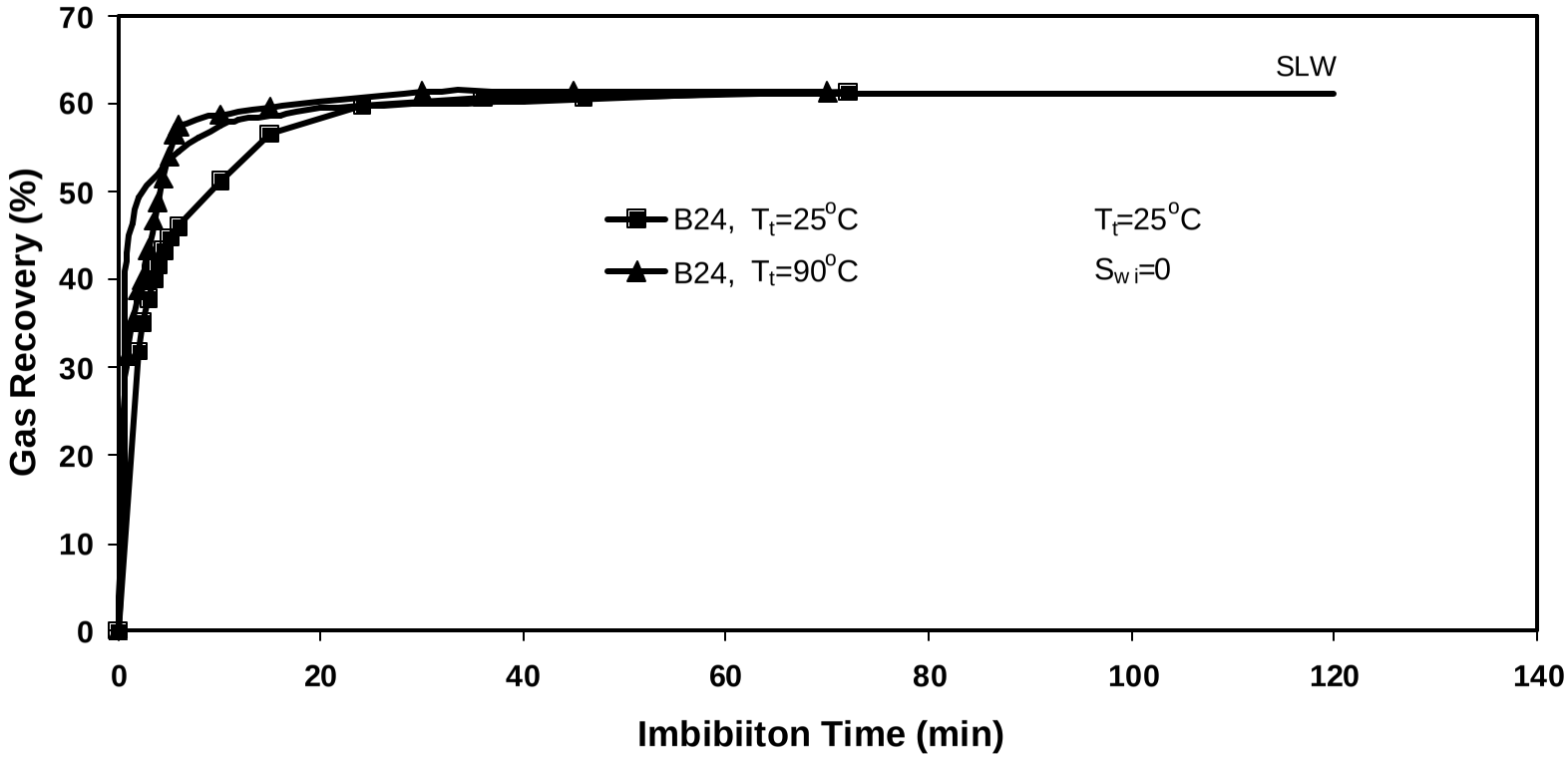

Fig. 6b Effect of Temperature on Spontaneous Oil Imbibition in Berea Treated with 1% Stearic Acid

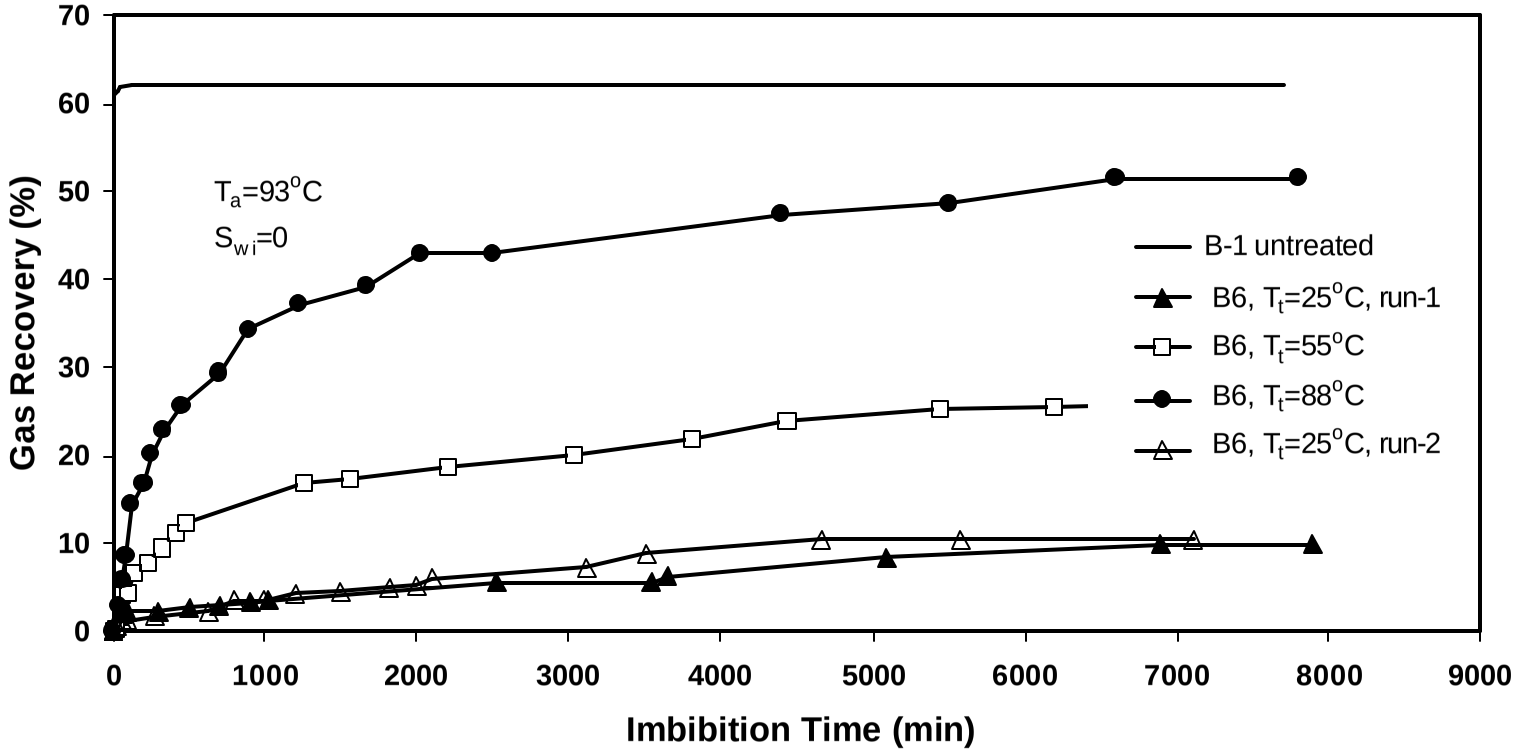

Fig.6c Effect of Temperature on Spontaneous Oil Imbibition for Berea Samples Treated with 2% FC-722.

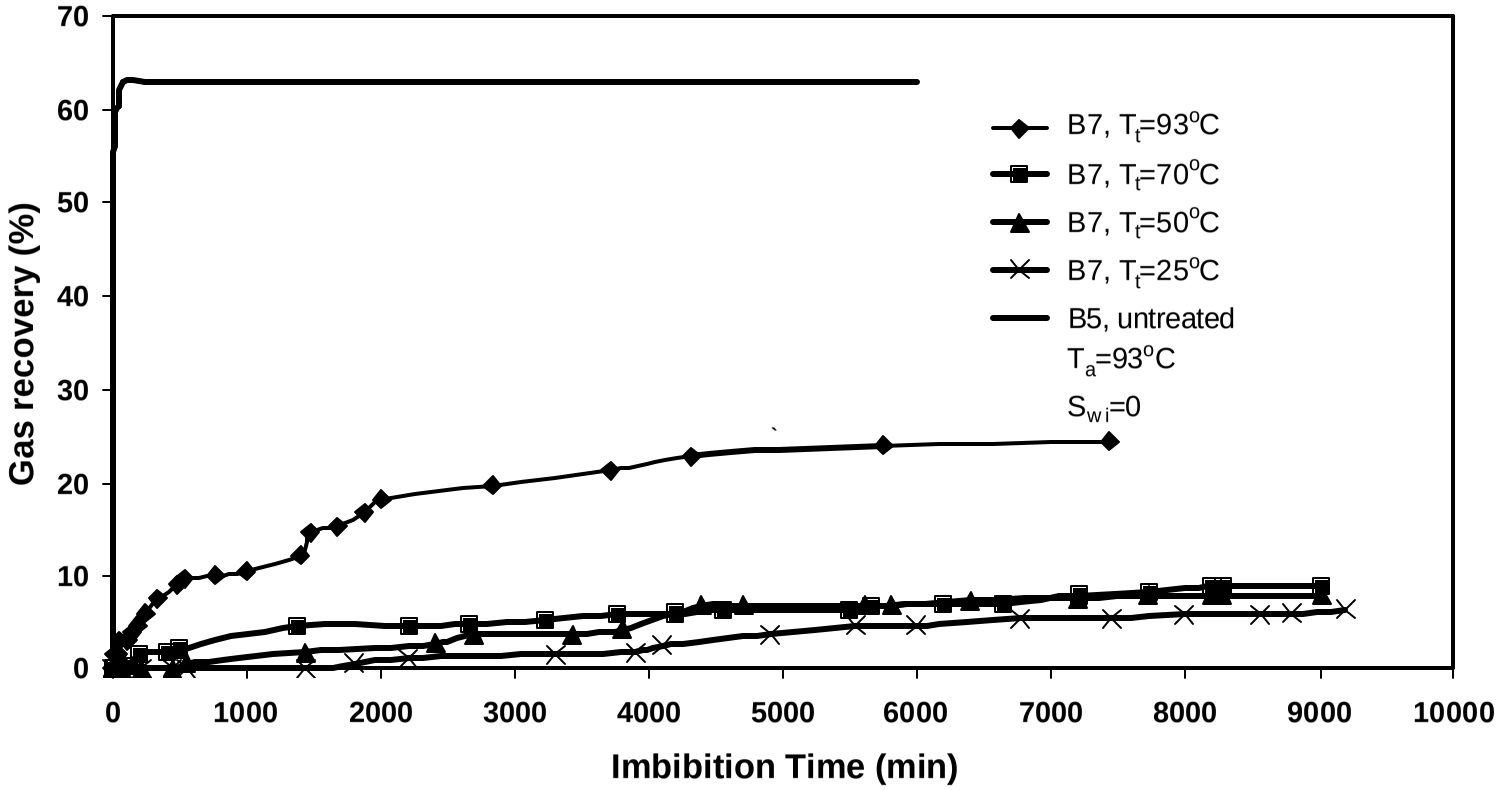

Fig.6d Effect of Temperature on Spontaneous Oil Imbibition for Berea Sample Treated With 10% FC-759

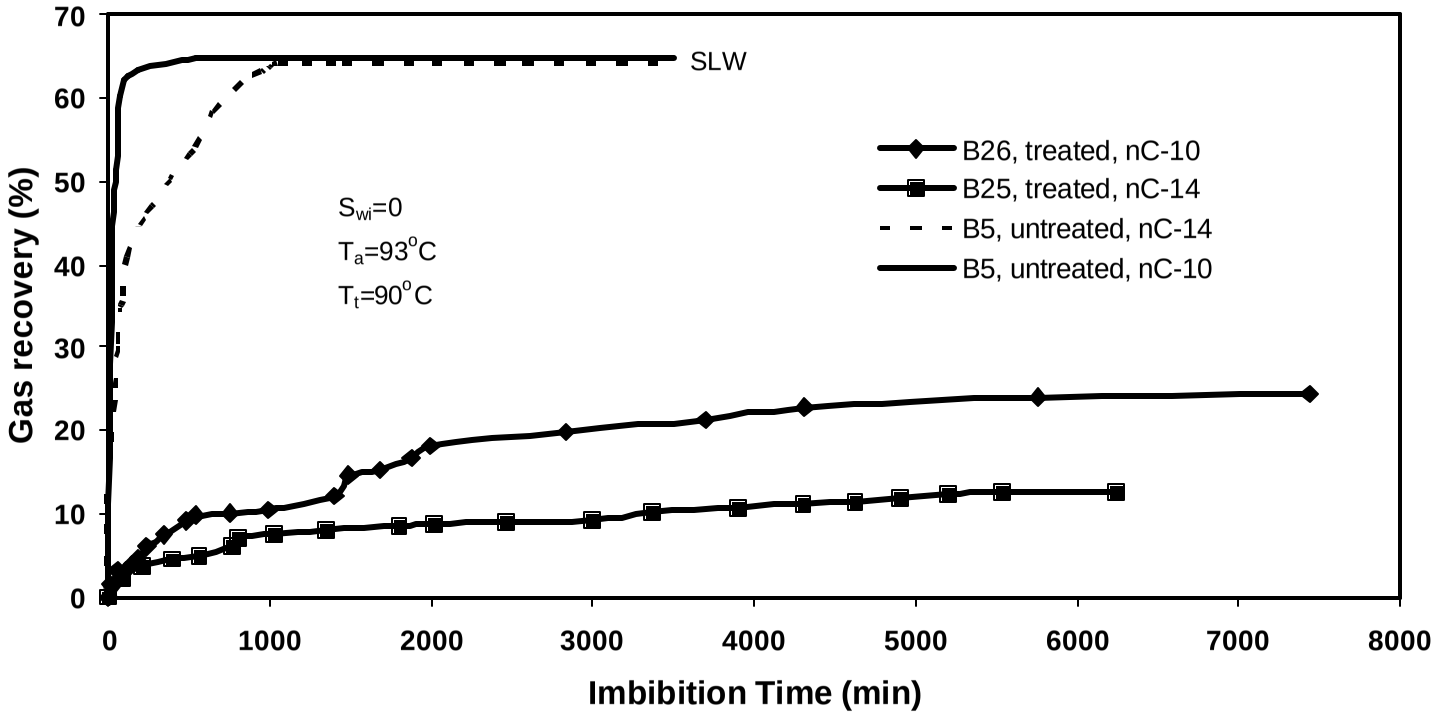

Fig.7 Spontaneous Imbibition of nC_{10} and nC_{14} for Berea Sample Treated with 10% FC-759

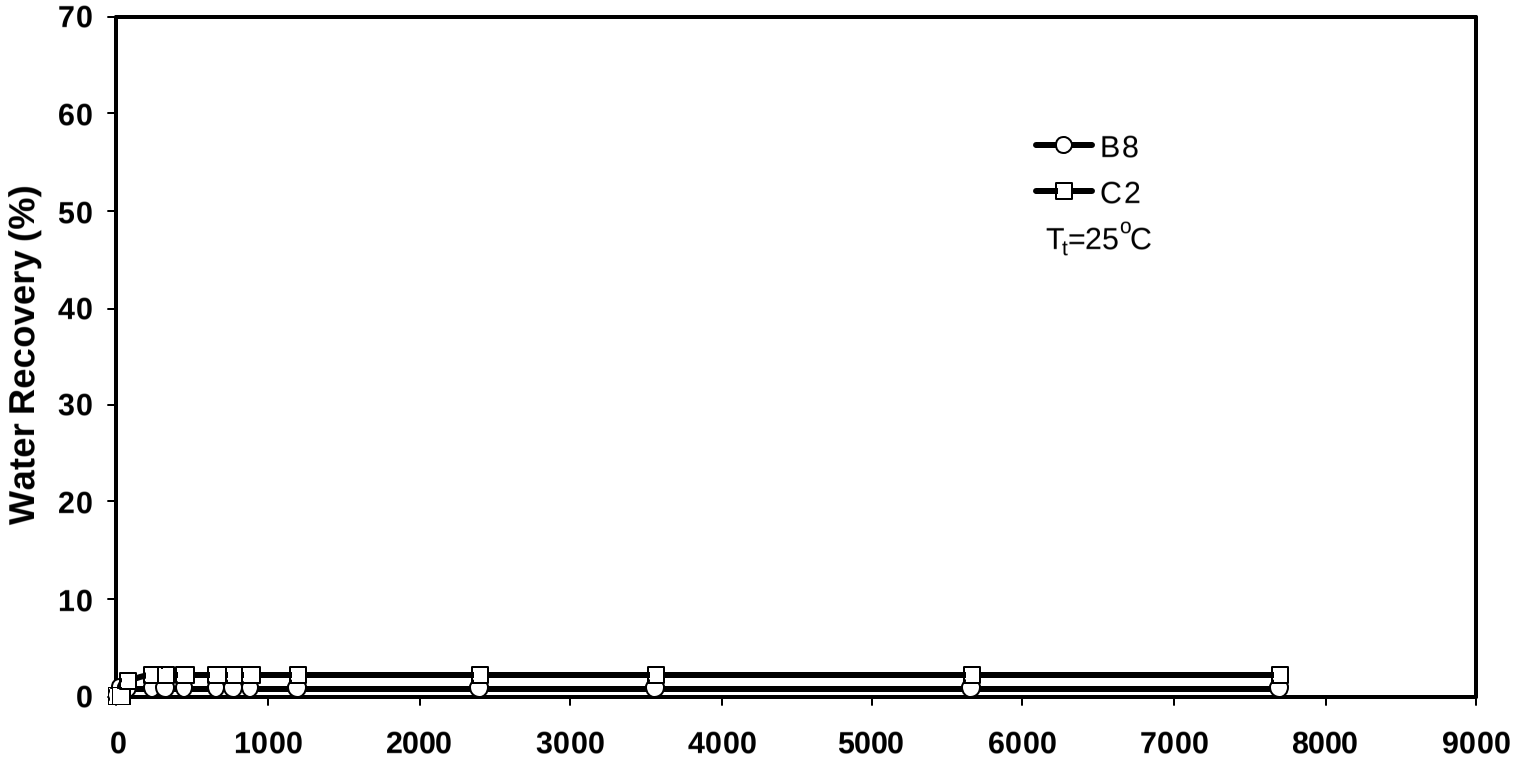

Fig.8a Water Recovery by Spontaneous Oil Imbibition for the Cores Treated with 8% FC-759

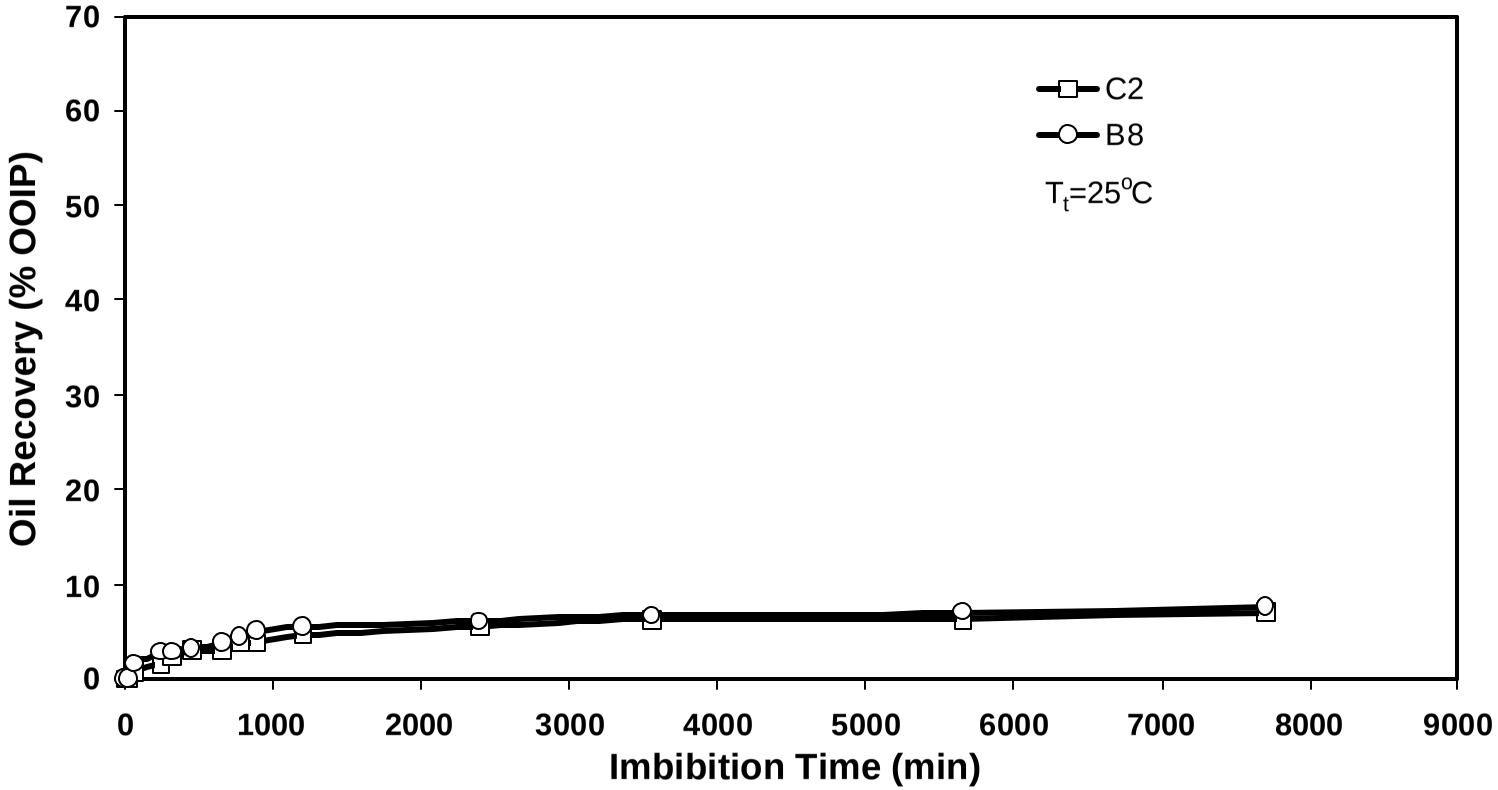

Fig.8b Oil Recovery by Spontaneous Water Imbibition for the Cores Treated with 8% FC-759

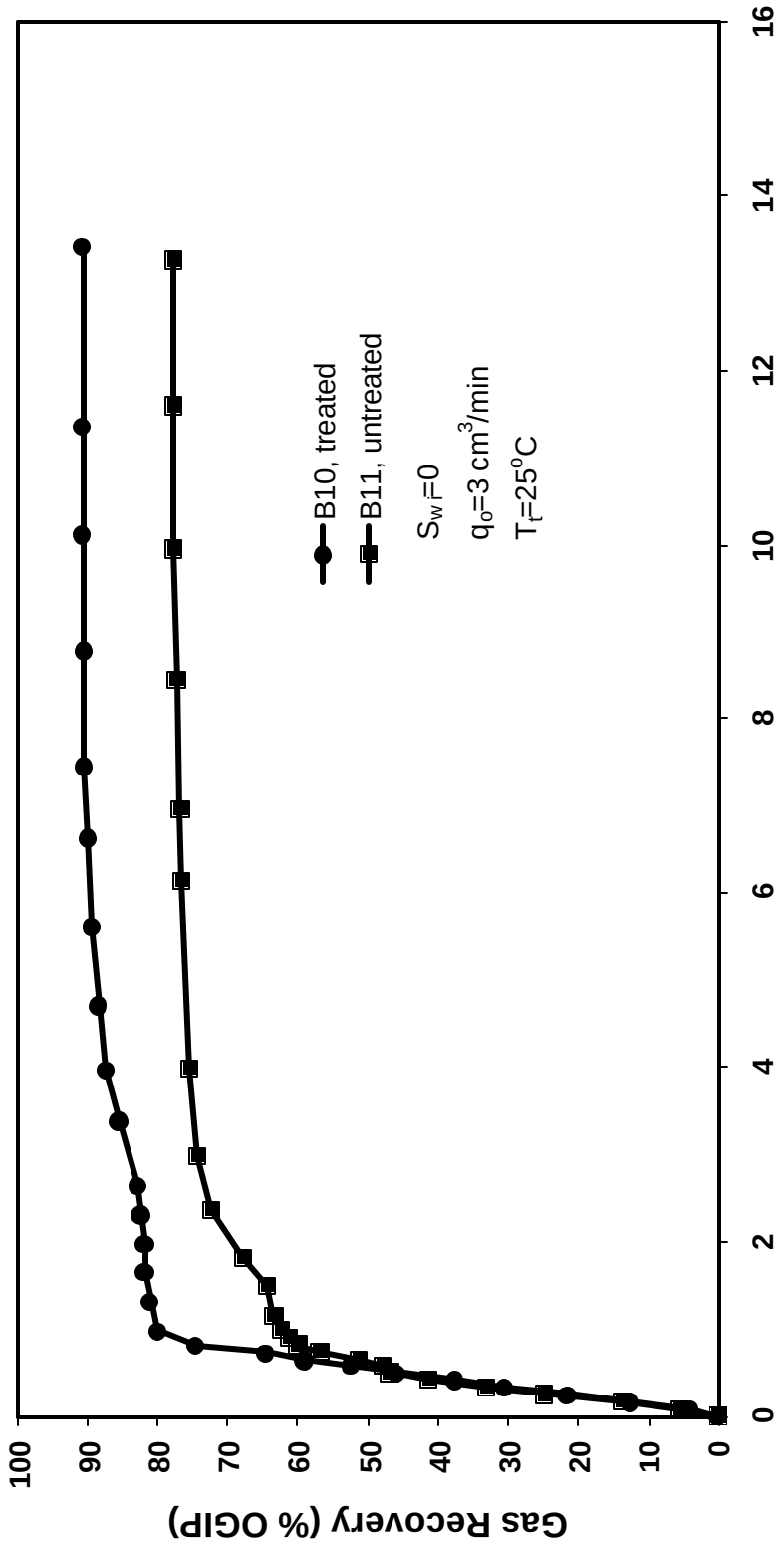

Fig.9a Effect of Wettability Alteration on Gas Recovery by Oil Injection.

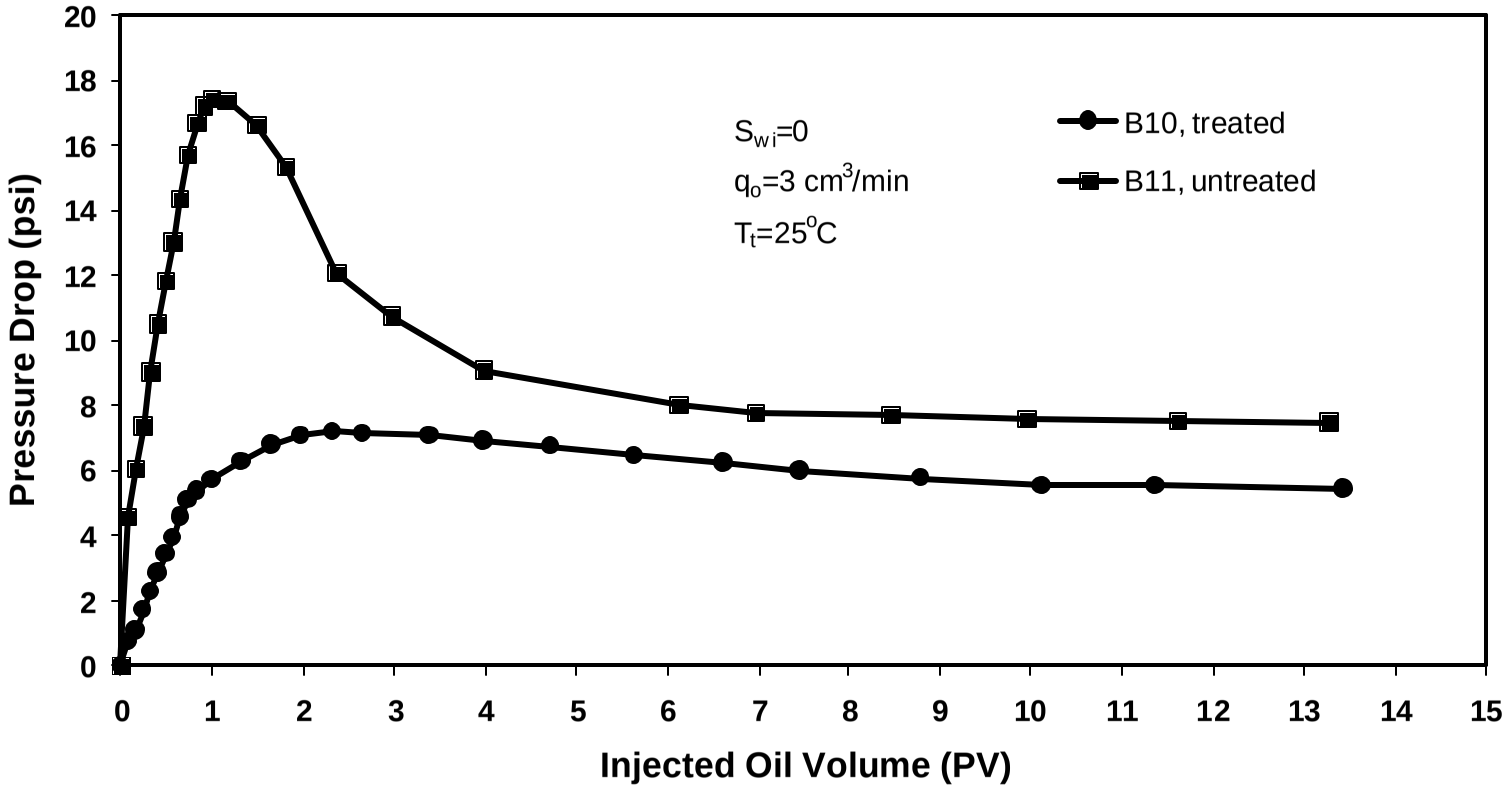

Fig. 9b. Effect of Wettability Alteration on Pressure Drop for Oil Injection in Gas Saturated Berea

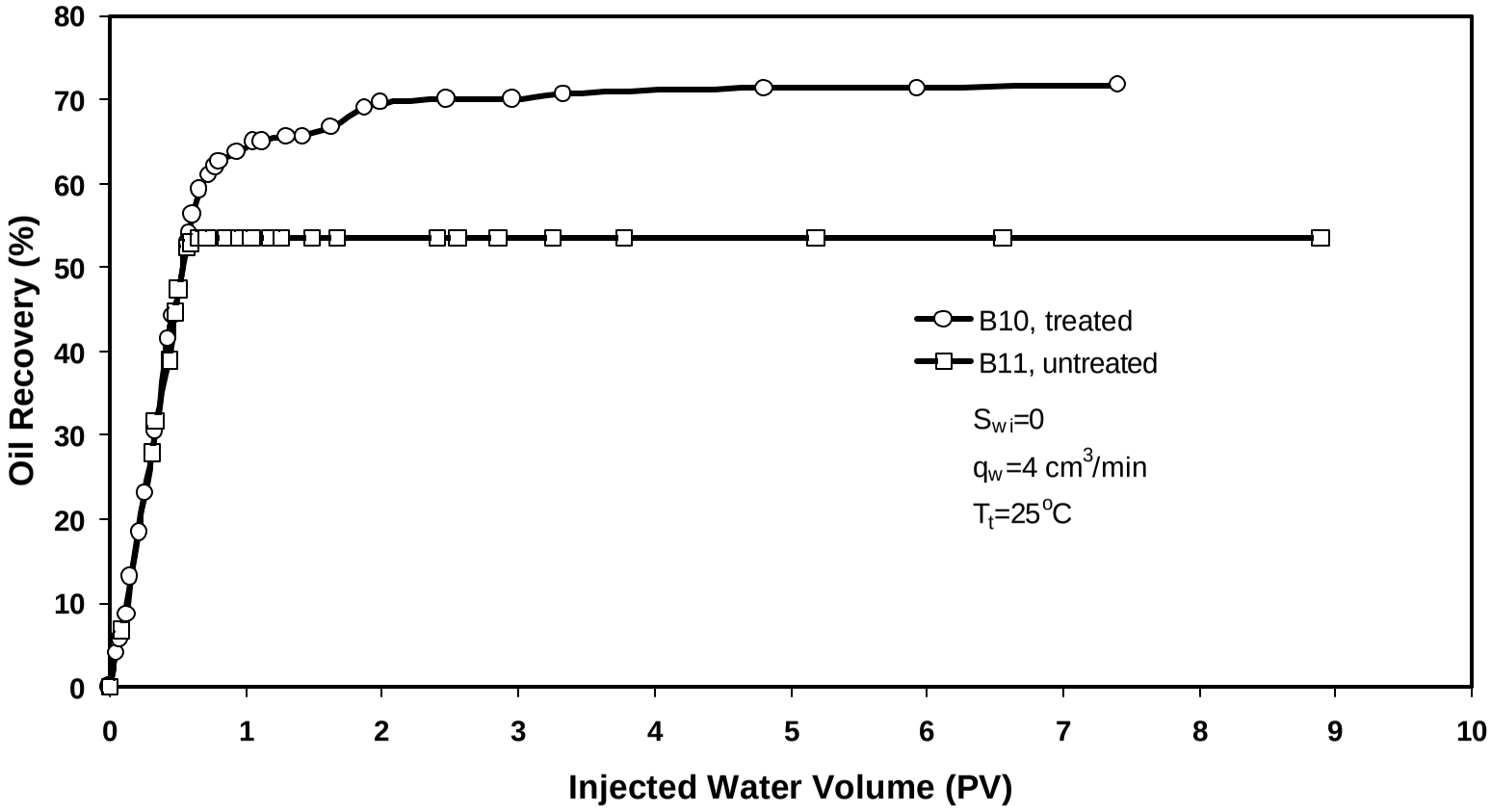

Fig.10a Effect of Wettability Alteration Oil Recovery by Water Injection

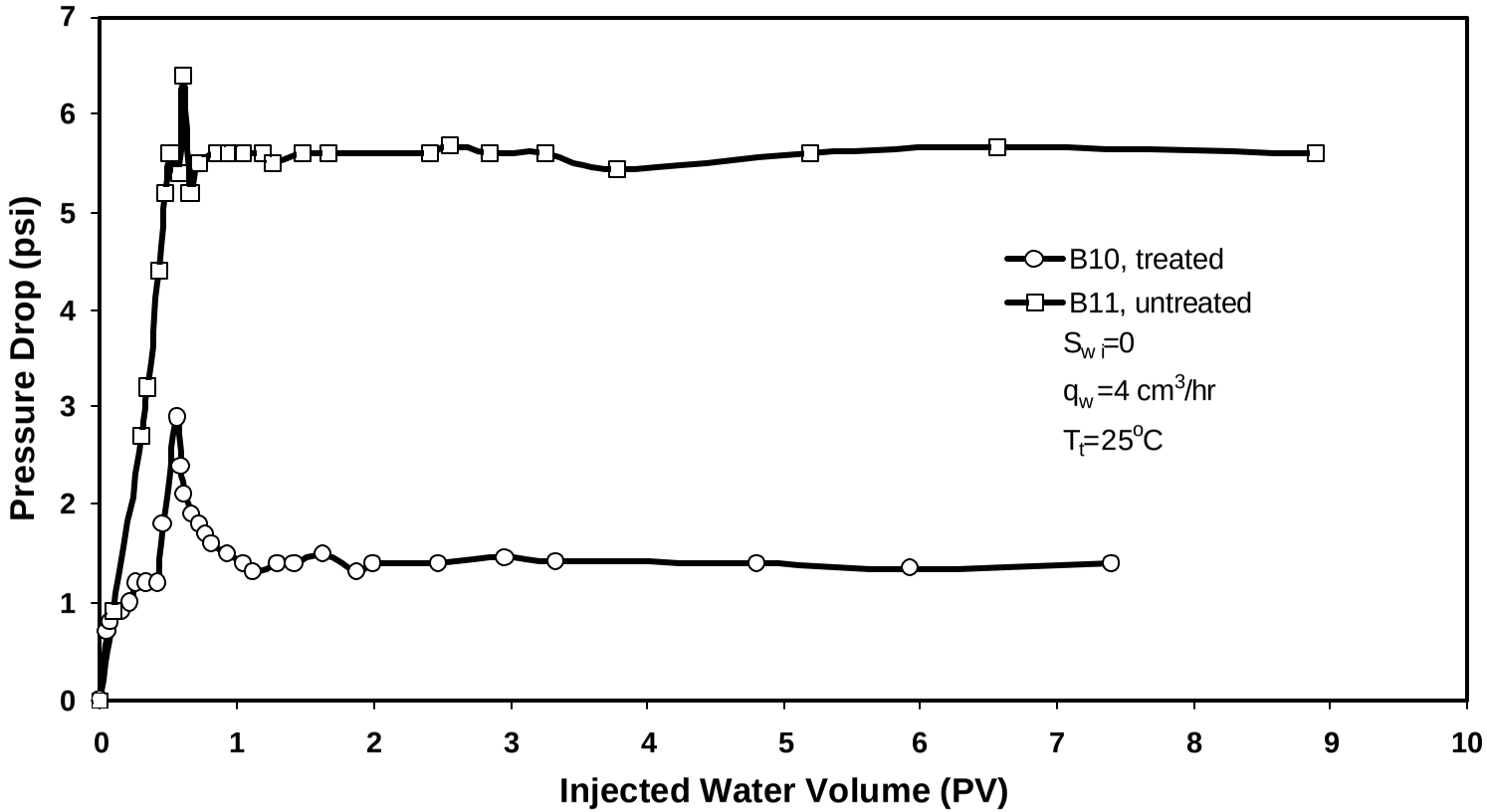

Fig.10b Effect of Wetability Alteration on Pressure Drop for Water Injection in Oil Saturated Cores

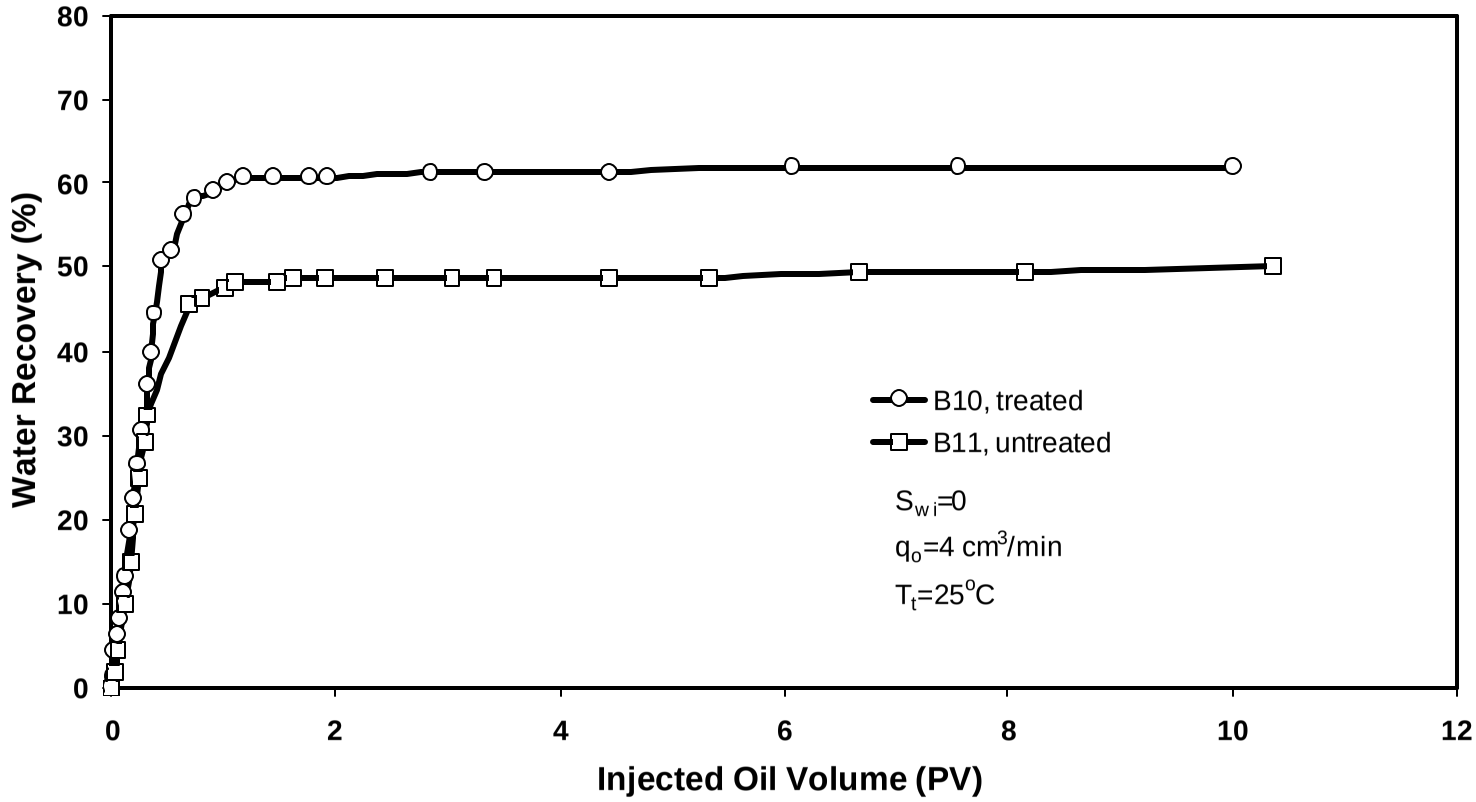

Fig.11a Effect of Wettabiltiy Alteration on Water Recovery by Oil Injection in Water Saturated Cores

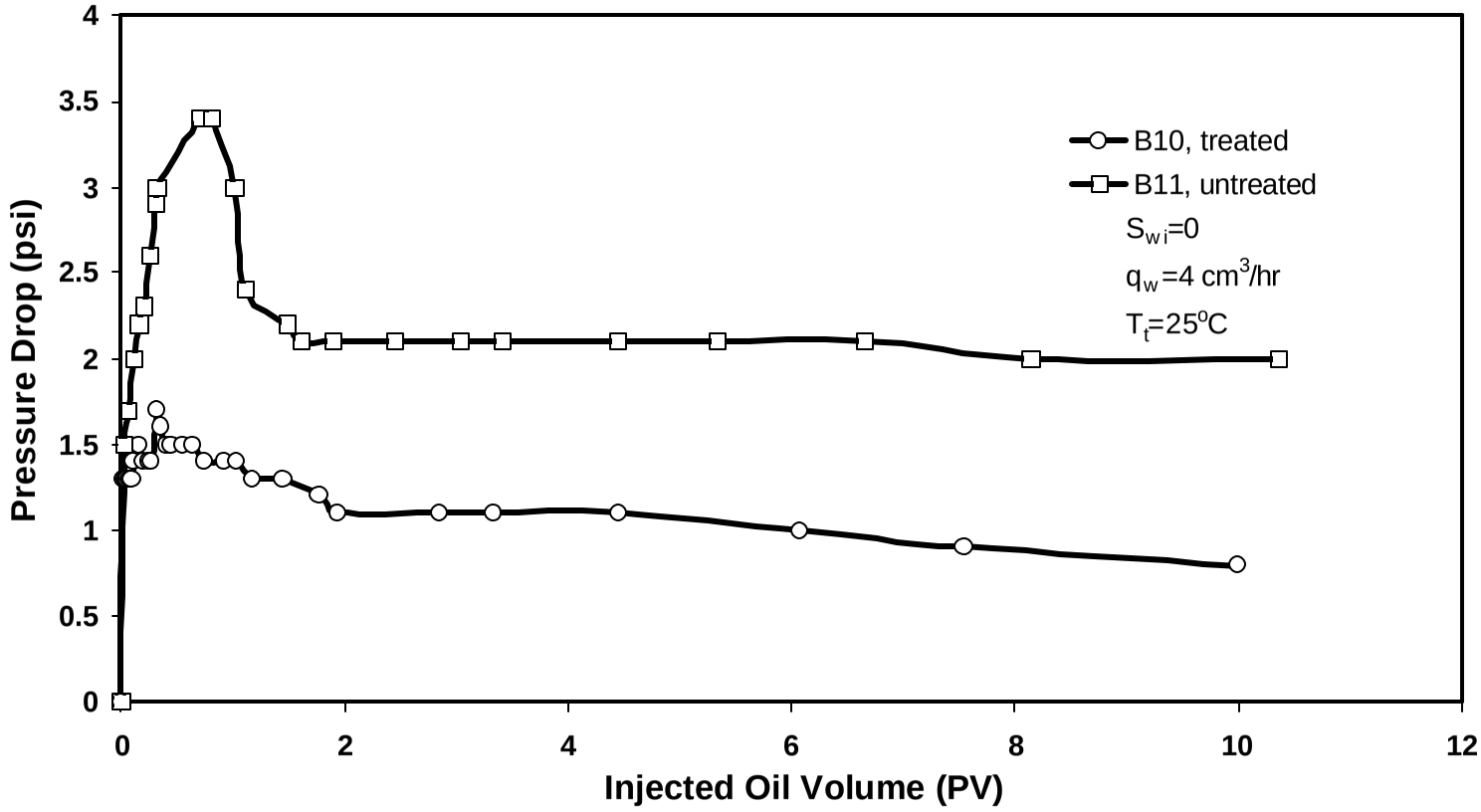

Fig.11b Effect of Wettability Alteration on Pressure Drop for Oil Injection in Water Saturated Cores

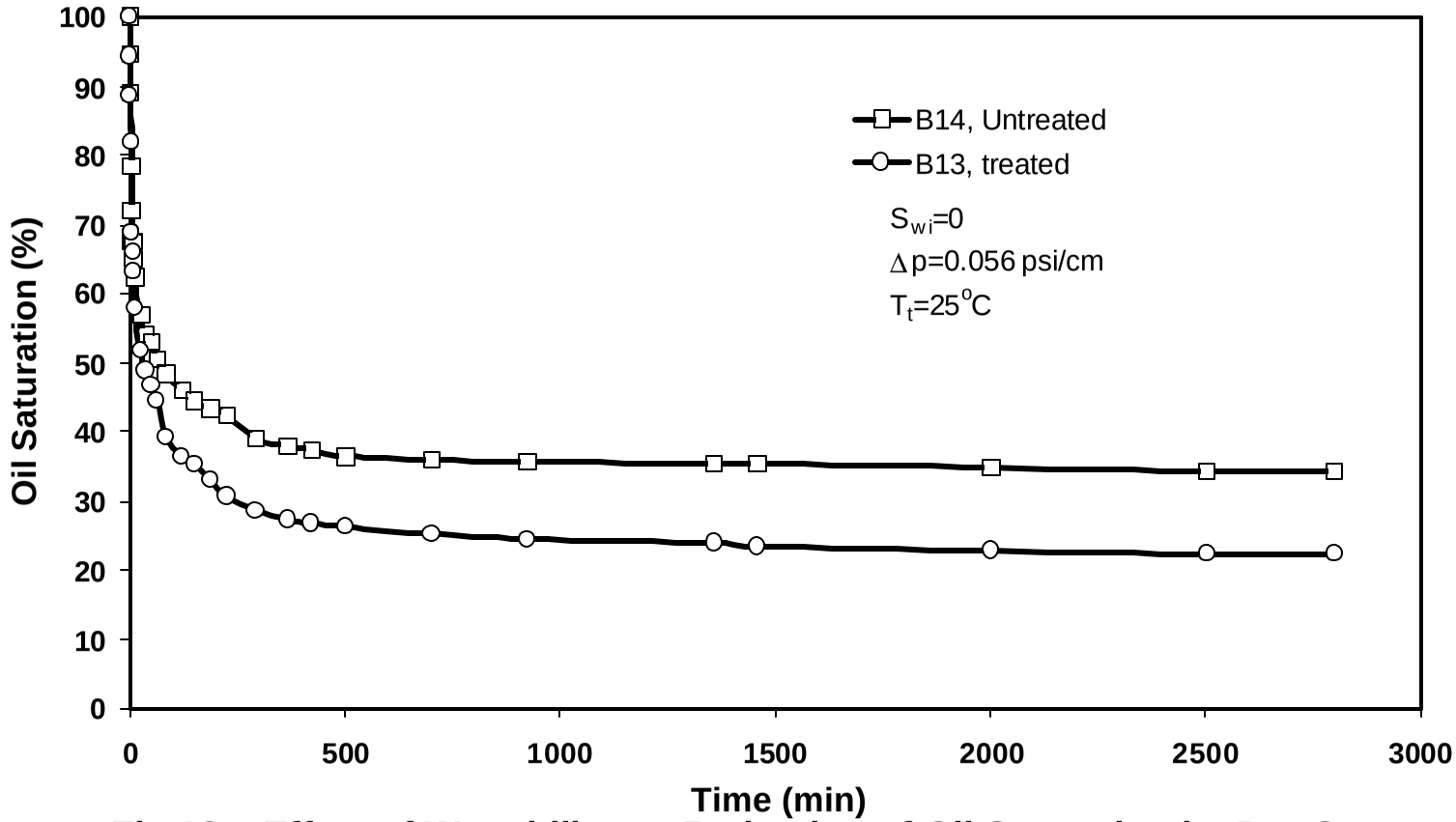

Fig.12a Effect of Wettability on Reduction of Oil Saturation by Dry Gas Injection at Room Temperature

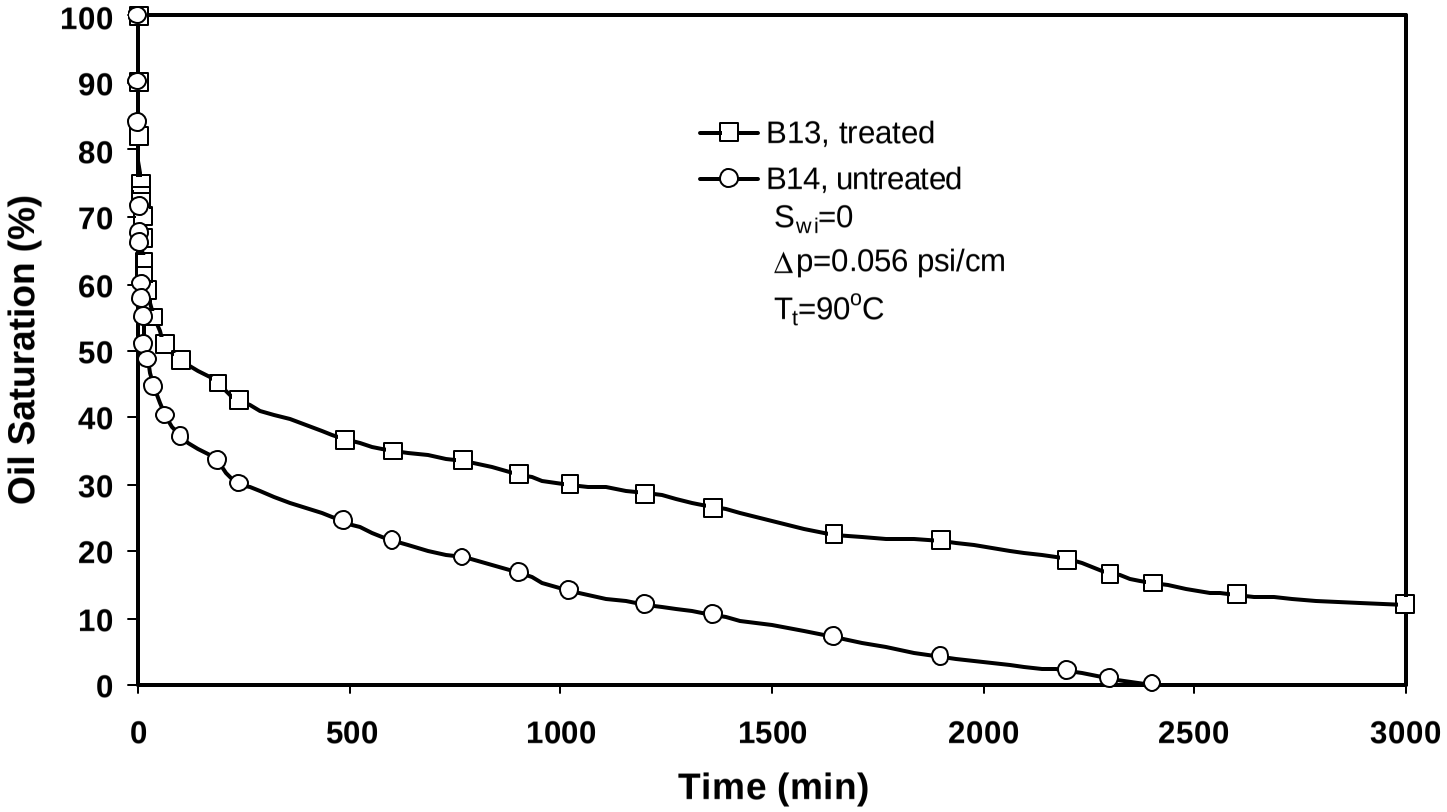

Fig.12b Effect of Wettability on Reduction of Oil Saturation by Dry Gas Injection at High Temperature

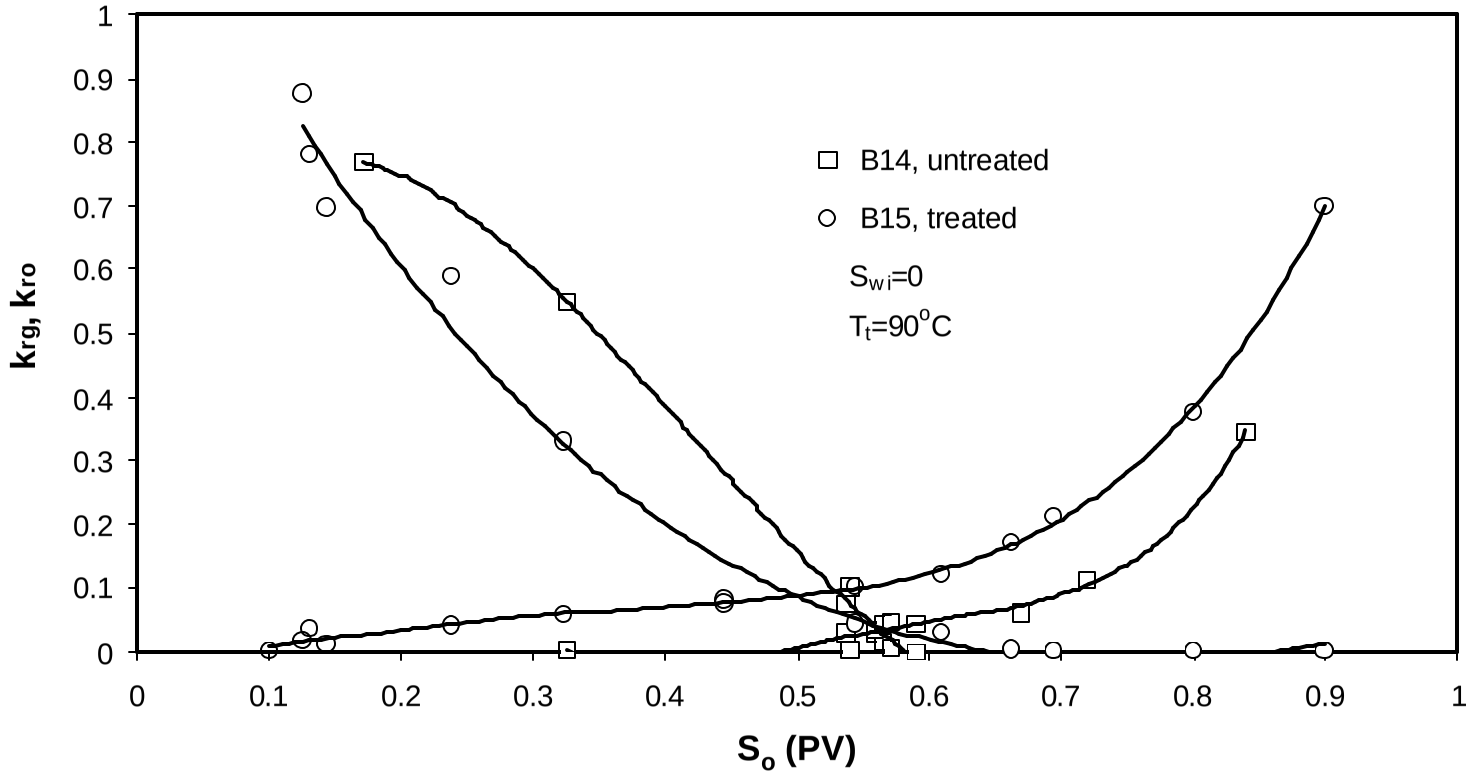

Fig.13a Gas and Oil Relative Permeabilities for Treated and Untreated Cores at T=90°C: nC-10

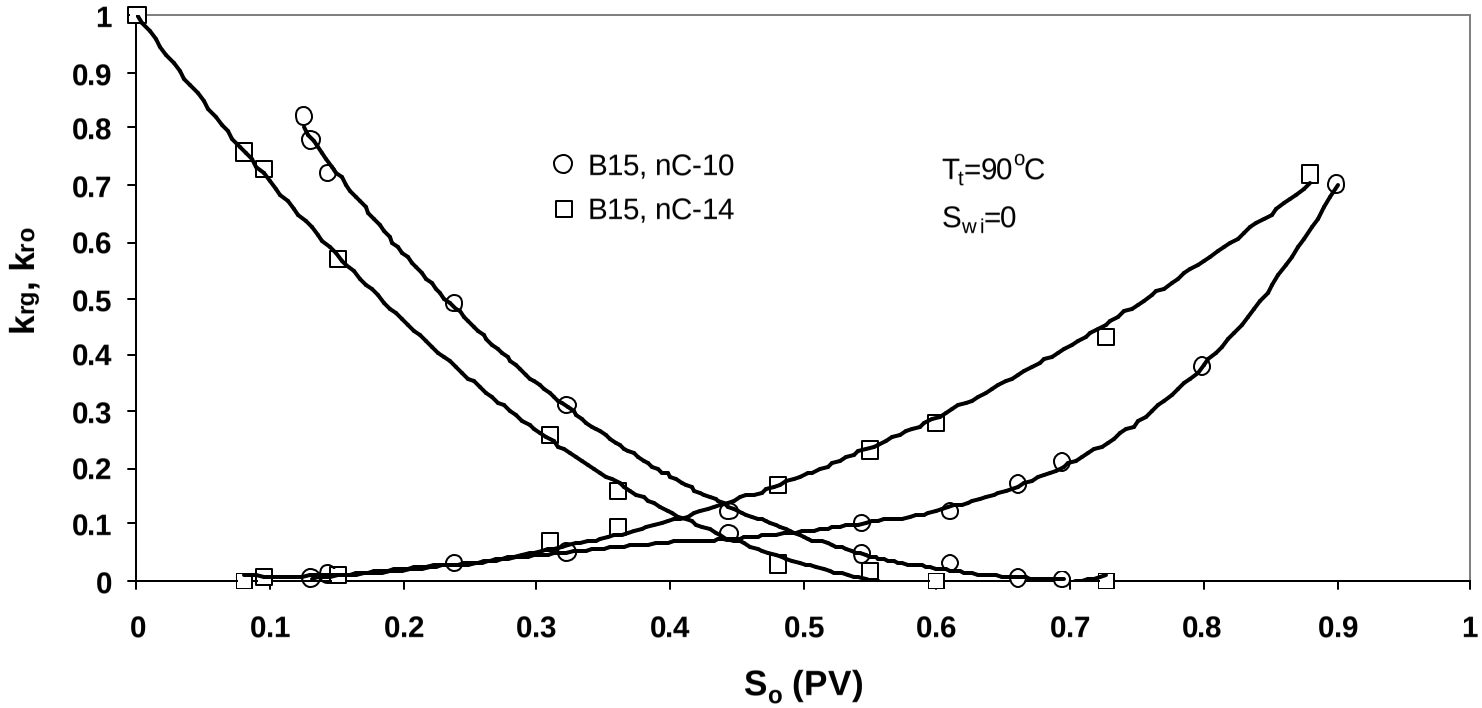

Fig.13b Gas and Oil Relative Permeabilities for Treated Berea at T=90°C for nC-10 and nC-14

Table 1 Core Properties and Other Relevant Data

Core	k_a (md)	f (%)	L (cm)	d (cm)	T_r (^oC)	Chemical treatment	Fluid system
B1	316	20.1	5.8	2.5	25/93	-	g/o
B2	308	20.0	5.7	2.5	25	-	g/o
B3[a]	310	20.3	6.2	2.5	25	8% FC-759	g/o
B4[b]	301	20.5	5.9	2.5	25	8% FC-759	g/o
B5	321	20.3	6.1	2.5	25/90	-	g/o
B6	311	20.1	5.7	2.5	25/55/88	2% FC-722	g/o
B7	323	20.5	6.2	2.5	25/50/70/93	10% FC-759	g/o
B8	317	20.1	5.9	2.5	25	8% FC-759	w/o
B9	296	19.9	6.2	2.5	25	10% FC-759	g/o
B10	322	22.4	18.0	2.5	25	8% FC-759	g/o
B11	318	22.2	18.2	2.5	25	-	g/o, w/o
B13	308	22.0	17.8	2.5	25/90	10% FC-759	g/o
B14	321	21.9	18.1	2.5	25/90	-	g/o
B15	310	21.8	18.4	2.5	90	10% FC-759	g/o
B16	293	20.1	6.2	2.5	25	10% FC-759	g/o
B17	289	20.0	5.8	2.5	25	10% FC-759	g/o
B18	303	20.1	6.0	2.5	25	10% FC-759	g/o
B19	327	20.5	5.6	2.5	25	10% FC-759	g/o
B20[c]	310	20.3	6.2	2.5	25	10% FC-759	g/o
B21[c]	289	20.0	5.7	2.5	25	10% FC-759	g/o
B22[c]	312	20.4	6.1	2.5	25	10% FC-759	g/o
B23	309	20.3	6.2	2.5	25	10% FC-759	g/o
B24	279	19.9	6.0	2.5	25	10% FC-759	g/o
B25[d]	311	20.1	6.3	2.5	93	10% FC-759	g/o
B26	301	20.0	6.0	25	93	10% FC-759	g/o
C-2	1.31	31.2	6.7	2.2	25	8% FC-759	g/o, w/o

Note: [a] pretreated with stearic acid; [b] pretreated with crude oil; [c]cut cores; [d]n-C_{14} was oil phase

Chapter 2 - Wettability Alteration to Intermediate Gas-Wetting for Gas-Water Systems at Reservoir Conditions

M. Fahes, and A. Firoozabadi, Reservoir Engineering Research Institute (RERI)

Abstract

We have altered the wettability of rocks by treatment at temperatures of 140°C, 90°C and at room temperature of 24°C. The treatment at those temperatures were at simulated reservoir conditions(the treatment was carried out by injection of the solution into the cores). There are currently two candidate reservoirs for the study of treatment on well deliverability. The reservoir with 140°C temperature provides the toughest challenge and that is the reason we have focused on the treatment at this temperature. Out of some 8 polymers which were mainly synthesized for the purpose of this project, only one chemical which is called chemical C is judged to be suitable for its effectiveness on wettability alteration to intermediate gas-wetting in gas-water systems. It also shows the promise for wettability alteration to gas-oil systems. We are currently studying the process of pre-treatment with some other chemicals to increase the chemical treatment effectiveness and durability.

In this work, we have focused, for the first time, on long term treatment durability by injecting water and oil in large quantities after the treatment. The new finding is that

all chemicals show resilience with respect to oil injection. But water can desorb the chemicals after large volume injection. Chemical C is an exception.

Introduction

There are various evidences that the accumulation of water and hydrocarbon liquids in the near wellbore region reduces gas well deliverability in gas condensate reservoirs with low permeability. Alteration of wettability from liquid wetting to intermediate gas wetting is perhaps the most promising approach to enhance gas well deliverability. The enhancement results from a significant increase in liquid mobility.

The idea of wettability alteration from liquid wetting to intermediate gas wetting was proposed by Li and Firoozabadi in 2000 (Li and Firoozabadi, 2000). In the work of Li and Firoozabadi, the effect of wettability alteration on gas and oil, and gas and water imbibition was studied at room temperature. The treatments were also carried out at room temperature. Tang and Firoozabadi extended the work of Li and Firoozabadi to imbibition and relative permeability measurements at room temperature (Tang and Firoozabadi, 2002). Part of the treatment process was performed at a temperature of 100°C.

Tang and Firoozabadi also performed imbibition and injection testing in the temperature range of 70 to 80°C (Tang and Firoozabadi, 2003). (The cores were not treated at the imbibition and injection testing temperature of 70 and 80°C). The results

showed that there was a decrease in the effectiveness for one chemical, and another chemical stayed effective at 80°C.

The main purpose of this work is the treatment and flow studies at high reservoir temperatures which include injecting the chemical and aging the core both at reservoir conditions of temperature. One candidate reservoir has a temperature of 140°C, and a second candidate reservoir has a temperature of 90°C. Another major goal is to examine the durability of the treated rock after a long time.

This report is structured along the following format. We first describe briefly the cores and various chemicals used in the treatment. Then the treatment process is presented. We did treat the cores at two different temperatures, 140°C and a room temperature of 24°C, to examine the difference in effectiveness between the treatment temperatures. Water washing that was performed to test the durability of the chemical treatment is then described. Next the results of water imbibition are presented first for the cores treated at high temperature and then for those treated at room temperature. In the last section the results for decane imbibition are discussed. The report is ended with few concluding remarks.

Cores and Chemicals

The Berea cores used in the experiments are about 1 inch in diameter and about 3.5 inch in length. The permeability ranges between 150 and 900 md. The fractional porosity is 0.21. Table 1 shows the properties of the different cores.

Eight chemicals which were synthesized for our project by 3M Corporation were tested to study their effect on water and decane spontaneous imbibition in the Berea cores. The method and conditions of treatment were often similar, and the process of treatment was selected such that it represents the conditions at the reservoir. The cores were treated at one of the three temperatures 140°C, 90°C, or the room temperature of 24°C. The aging time varied from three hours to three days.

All the chemicals used in the treatment process are of the fluoropolymer type with different functional groups. They are all water soluble except FC-722, which has a different solvent. The composition of each of the chemicals was designed to serve a certain function. A-chemical and FC-759 are similar in terms of building blocks; they consist of the fluorochemical group that provides the water and oil repellence, the silanol and anionic groups that chemically bond onto the rock surfaces, and the anionic and nonionic groups that make the polymer soluble in the aqueous solution before chemical bonding to the rock substrate. D-chemical and L-chemical include the maximum amount of fluorochemical that can be incorporated before the molecule becomes unstable. G-chemical has a building block that would improve water repellency. B-chemical has a building block that would make the material tough. EGC-1700 is similar in structure to FC-722 but is water soluble. Table 2 includes some properties of those chemicals.

We used tap water in imbibition and water injection experiments. Normal decane represented the oil phase in the oil/gas systems. Air was used as the gas phase. We have

also conducted imbibition experiments with a real gas condensate liquid from a gas reservoir in Texas. Results are very similar to normal decane.

Treatment Procedure

We use two different setups to treat the cores. At high temperature we use the high-pressure high-temperature Temco core-holder shown in Figure 1-a. At room temperature we use the visual core-holder shown in Figure 2.

High Temperature Treatment - We pack the dry core in the Temco core-holder inside a viton sleeve, and then we use the pump to fill the body of the core-holder with water and apply an overburden pressure of 1000 psi, which is held constant during the treatment and aging process. We then start the heating by setting the temperature of the oven at 140°C (or 90°C, depending on the experiment). After the set temperature is established, 4 pore volumes (PV) of the chemical solution are injected at the core inlet; a minimum pressure of 150 psi is maintained at the core outlet to avoid vaporization. After an aging time of one to three days, nitrogen is injected from the inlet to remove the excess liquid. The core is then taken out of the core holder and placed in the oven at 140°C to dry it for adsorption and imbibition measurements. The setup is shown is Fig 1-b.

Room Temperature Treatment - We place the core between two steal end-caps and we cover it with cylindrical heat-shrink tubing, then we pack it in the visual core holder and we fill the body of the core holder with nitrogen at an overburden pressure of 450 to 500 psi. After that we inject 3 to 4 PV of the chemical solution at the inlet and the core is

aged with the solution for a period of three hours to three days. Nitrogen is then injected to remove excess liquid and the core is dried in the oven at 140°C

Washing

In order to study the durability of the chemical treatment, the treated cores were flooded with water and normal decane where thousands of PV of water (in water flooding) were injected into the core while packed in the visual core holder. The main goal was to test whether the alteration in wettability will withstand excessive liquid injection.

The rate of injection varied from 7 to 30 cc/min depending on the permeability of the core. The pressure drop across the core was as high as 80 psi in some of the tests. After injecting water (or normal decane), the core was removed from the core holder and placed in the oven at a temperature of 140°C to dry and then spontaneous imbibition was performed. In some of the tests a decrease in the dry weight of the core was recorded. The decrease is believed to be due to removal of either adsorbed or unadsorbed chemical.

In most cases after extensive washing, there was very little effect on imbibition by water; in few cases there was a small increase in the imbibition. Decane imbibition, on the other hand, increased after washing the core with water. Some cores were washed several times to check if multiple washing will affect the imbibition. Decane was also injected into some of the cores to examine the difference with water flooding. The results will be presented later with the details of injection rate and pressure drop.

Apparatus and Imbibition Measurement

The setup used for imbibition is shown in Fig 3. The core is held by a thread and placed in the liquid, while hanging below an electronic balance. The mass is then recorded verses time with the aim of knowing how much water will imbibe into the core. In the figures presented in this report we plot the fractional liquid saturation verses time, where the liquid saturation at a given time is calculated from:

$$S_L = \frac{M - M_i}{r \times V_P}$$

M_i = mass of the core-thread at time zero when the core was initially placed in the liquid

M = mass of the core-thread-liquid at a given time

V_P = pore volume of the core (about 9.5 cc for most cores)

ρ = liquid density

There is no practical way that would allow us to read the initial mass because when the core is placed in the liquid the mass changes instantly. This initial mass is calculated at the end of the experiment after measuring the mass of the liquid inside the core when it is removed from the water cylinder.

Imbibition Results

We have performed an extensive set of imbibition experiments using treated cores. The imbibition tests were performed in both water and normal decane. We present in this section the results of water imbibition for the cores treated at high temperature,

then for the cores treated at room temperature. After that the results of decane imbibition are presented.

Water Imbibition

Treated cores treated at 140°C/90°C **-** We have performed a number of water imbibition tests at room temperature using treated cores at 140°C with polymers FC-759, A, B, C, D and L dissolved in water, and with FC-722 dissolved in C_6F_{14}. We also performed few imbibition tests with cores treated at 90°C with EGC-1700 dissolved in HFG-7100. The results of the imbibition tests are presented in the following.

FC-759 - The core MB1 was treated with 8% FC-759 at 140°C. It was first treated for one day but decane imbibition was high (decane imbibition tests will be described later). We then treated the core for a second time for one day; decane imbibition was substantially lower this time. Next we performed water flooding (water washing). The decane imbibition increased again. The core was treated for a third time, aged for three days, and again decane imbibition decreased. Water imbibition was then conducted on the core for the first time, and after 6 hours of imbibition the water saturation was only 6% (see Fig 4). After drying the core we injected 2 liters of water at a rate of 10 cc/min, we dried the core in the oven and measured water imbibition again, after 18 hours water saturation was 10%. We then injected 3.5 liters of water at a rate of 15 cc/min where the pressure drop across the core was 64 psi. Water imbibition was then performed again with the dry core, and after 6.5 hours the water saturation was 8%. As a final step we washed the core with decane; we injected 1.5 liters at a rate of 20 cc/min, the pressure

drop was 28 psi. Water imbibition was then performed, and after 8 hours, water saturation was 9%. These series of tests with extensive flooding (washing) repeatedly with water, and decane demonstrate that the chemical is effective for the alteration of wettability to intermediate gas-wetting for the water-gas system.

D-chemical - The core MB3 was treated with 8% D-chemical. In the first treatment the core was aged for three days at 140°C. The imbibition of water was very high, after 2 hours of imbibition the water saturation was 65% (see Fig 5). The core was treated a second time and aged for 6 days at 24°C, then water imbibition test was performed and after 8 hours the saturation was 6.5%. Nest we injected 3 liters of water into the core at a rate of 20 cc/min; the pressure drop was 20 psi. A water imbibition test was conducted again; after 17 hours of imbibition the water saturation was 9%. The core was treated a third time at 140°C in an attempt to improve decane imbibition (results to be presented later). In the water imbibition test, after 37 hours the water saturation was 25%. We interpret the results with this chemical as lack of effectiveness of treatment at 140 C in the alteration of wettability to intermediate gas wetting in the gas-water system.

A-chemical - The MB2 core was treated with 8% A-chemical at 140°C with an aging time of three days. Figure 6 shows the results of water imbibition; after 15 hours the saturation was 62%. The core was treated for a second time at 140°C and aged for three days. We observed deposition when viewing the effluent after nitrogen injection for the displacement. This chemical is therefore unsuitable for the alteration of wettability.

B-chemical - The MB5 core was treated with 8% solution of the B-chemical. The first treatment was carried out at 140°C and aged for three days. Water imbibition was then performed; after 2 hours the saturation was 38% (see Fig 6). Two liters of water were then injected into the core at a rate of 20 cc/min; the pressure drop across the core was about 52 psi. We noticed a sharp decrease in the rate of water imbibition; after one hour of imbibition water saturation was 3.7%. The core was then treated a second time, at 24°C and aged for three days. Subsequently three liters of water were injected into the core at a rate of 20 cc/min; the pressure drop was 76 psi. The imbibition of water was then tested; after one hour the water saturation was 3.7%. The core was treated a third time at 140°C for 1 day. The core broke after the treatment. We performed water imbibition with one piece of the broken core; after 9 hours, water saturation was 30%. The rate of imbibition on the broken side was much more than the unbroken side when we place water droplet on the rock surfaces. The result of water imbibition may imply either that the treatment at 140 C was not effective, or can be an indication that the treatment was nonuniform. It also may imply both.

FC-722 - The core MB13 was treated with a 0.4% solution of FC-722 at 140°C. It was treated 4 times. After each treatment we measured the decane imbibition; the results will be presented later. During each treatment the core was aged for one day. In the third treatment some water from the overburden accidentally entered the core at 140°C. Water imbibition was performed after the 4^{th} treatment, after 25 hours water saturation was 20% (see Fig 7). We used then a new core, MB17, and treated it with 0.4% FC-722 at 140°C. The treatment duration was for one day. Water imbibition was tested and after 20 hours

the saturation of water was 9%. We then washed the treated core with 5.2 liters of water at a rate of 30 cc/min; the pressure drop was about 80 psi. Water imbibition was not affected by extensive flooding. After 20 hours of imbibition water saturation was 9.5%. The MB17 core shows a lower water imbibition than MB13. The results of water imbibition for MB13 and MB1 are very similar.

L-chemical - The MB21 core was treated with 8% L-chemical at 140°C. It was aged for 1 day in the first treatment. Water imbibition was then tested, after 20 hours water saturation was 27%. We injected 4.2 liters of water into the core at a rate of 30 cc/min; the pressure drop was 40 psi. The results from the water imbibition shown in Fig. 8 show that the washing did not alter wettability. The core was treated a second time for 1 day at 140°C. As Fig. 8 shows the result from imbibition after the second treatment is the same as the previous two tests. The treatment with the L chemical at 140°C may have some useful features that can be studied in the flow testing.

EGC-1700 - The MB23 core was treated with 1% EGC-1700 at 90°C. In the first treatment it was aged for 1 day. Then we performed the water imbibition; after 21 hours water saturation was 30% (see Fig 9). We treated the core for a second time for 1 day, and water imbibition after 43 hours was 14%.

C-chemical - The MB27 core was treated with 8% C-chemical at 140°C once for 1 day. The water imbibition for this core was lower than all the other cores; after 23.5 hours, the saturation of water was 4.3% (see Fig 10). Water washing was then performed at 140°C

in the Temco core-holder, where 80 cc of water were injected into the core. Water imbibition at room temperature was then performed and after 22 hours water saturation was 6% which shows no measurable effect. We also injected 1.5 liters of decane into the core at room temperature. Water imbibition was not affected by the washing, after 24 hours of imbibition the saturation of water was 6.3%.

Cores treated at room temperature - Cores were treated with chemical B, C, D, L, FC-722 and EGC-1700 at room temperature to examine the treatment effect on imbibition at room temperature. The results for water imbibition at room temperature show the effectiveness of nearly all of the chemicals. Some of the cores were aged for three hours, others overnight.

The imbibition results for the core MB3 treated with D-chemical and the core MB5 treated with B-chemical were presented in the previous section. The same results are also shown again in Fig 11. The core MB7 was treated with 0.4% FC-722 at room temperature and aged overnight. It was then washed 4 times and tested for decane imbibition each time. It was treated a second time at room temperature overnight and again was washed 4 times by water flooding. A water imbibition test was performed . After 18 hours of imbibition the water saturation was 9.5%. Fig 11 shows the imbibition data.

The core MB11 was treated with 8% L-chemical at room temperature. It was aged overnight with the chemical solution. Then water imbibition was tested and after 3 hours

water saturation was 3% (see Fig 12). The core was treated again overnight to improve decane imbibition. After the second treatment 600 cc of water was injected into the core at a rate of 3 cc/min where the pressure drop was 76 psi. Water imbibition was then carried out and after 20 hours, water saturation was 4.3%.

The core MB19 was treated three times with 1% and 2% EGC-1700. The aging period varied from 3 to 12 hours. Water imbibition was tested after the second treatment where after 13.5 hours water saturation was 5%. After the third treatment, the core was washed with water 4 times; the amounts of water injected were 2.8 liters, 5.5 liters, 5 liters, and 4 liters. The results of water imbibition after water washing are shown in Fig 13. Note that the rate of imbibition increased a small amount only after the initial water injection. We also noticed a minor washing of the chemical (from weight measurement when the core was dired) after water washing in the first flooding after the third treatment.

C-chemical was tested for a three hour treatment of the core MB25 at room temperature. Water imbibition was then performed and after 23 hours water saturation was 3.8% (see Fig 14). Then more than 3 liters of water were injected into this core at a rate of 30 cc/min; the pressure drop was around 100 psi. Water imbibition was tested again and after 16 hours water saturation was 4.6%. This chemical had again the best effect on water repellence in cores treated at room temperature.

Decane Imbibition

Of all the chemical that were used in the alteration of wettability in the previous section C-Chemical showed the most effective. We have also performed water imbibition tests at a temperature of 70 C. This chemical keep its effectiveness for wettability alteration at higher temperature too. Next we will examine chemical effectiveness for the decane-gas systems.

Cores treated at 140° C - The FC-759, A, B, C, D and FC-722 chemicals were used to test the effect of chemical treatment at 140°C on decane imbibition.

FC-759 - The core MB1 was treated with 8% FC-759 at 140°C three times and aged from 1 to 3 days, as explained in a previous section. After the first treatment for 1 day decane imbibition was high; after 3.5 and 16.7 hours, decane saturations were 66, and 71%, respectively (see Fig 15). After the second treatment for 1 day, decane imbibition decreased significantly; decane saturations were 16.5, and 28% after 2, and 22.5 hours, respectively. One liter of water was then injected into the core to check how permanent the effect of treatment on decane imbibition is. The rate of imbibition increased again; after 6 and 19 hours decane saturations were 60 and 61.7%,respectively. We treated the core a third time, with an aging period of three days. Decane imbibition decreased again and after 18 hours, decane saturation was 26%. Water washing after the third treatment increased decane imbibition and the results are also shown in Fig 15. The details of the washing were presented in a previous section. In the second and third treatments, a state of preferentially gas weting in the treated core was established for the oil/gas system, but that alteration of wettability was not very strong and it was affected by water washing.

Nevertheless FC-759 was more affective on decane imbibition for high temperature treatment than the other chemicals as we will see in the following.

D-chemical - The details of the treatment of the core MB3 with D-chemical were presented earlier. Fig 16 shows the results of decane imbibition after each of the three treatments (first and third treatments at 140°C; second treatment at 24°C). As the figure shows, D-chemical was not effective for decane repellence when treated at either room temperature or high temperature. As an example, decane imbibition after the third treatment was 65% after 2 hours.

A-chemical - We stated before in the preceding section, the core MB2 was treated twice with 8% A-chemical and that deposition was noticed after the second treatment. The result of decane imbibition after the first treatment was also high; decane saturation was 70% after half an hour (see Fig 17).

B-chemical - The details of the treatment and water washing of MB5 were presented earlier; here we present the decane imbibition at each stage. After the first treatment the decane imbibition in the MB5 core was lower than that in MB2 and MB3. After 1 hour, decane saturation was 51% (see Fig 17) compared to 68% for MB3 and more than 70% for MB2. Water washing did not increase the imbibition. After the second treatment at room temperature, decane imbibition decreased, and the decane saturation was 45% after 2 hours. This time after water washing, decane imbibition increased, and the saturation

was 58% after 2.5 hours. After the third treatment at 140°C the core was broken but we performed decane imbibition for one piece; the result is shown in Fig 17.

FC-722 - The core MB13 was treated with 0.4% FC722 and aged for one day. Decane imbibition was high and after 1 hour of imbibition the decane saturation was 57%, and increased to 63% after 15.5 hours (see Fig 18). After the second treatment decane imbibition decreased and the saturation was 29% after 12 hours. We then injected 7.35 liters of water into the core at a rate of 30 cc/min; the pressure drop 80 psi. Decane imbibition increased and the saturation was 44% after 16.5 hours. After the third treatment some water accidentally entered the core at 140°C and the decane imbibition after that was high, 55% after 14.5 hours. After the fourth treatment decane imbibition did not decrease, it was 62% after 18 hours. The core MB17 (a new core) was treated once with FC-722 at 140°C. Decane imbibition was also high, 70% after 21.5 hours.

C-Chemical - The core MB27 was treated once with C-chemical for 1 day; the decane imbibition was about 54% after an hour and a half (see Fig 19). We may continue to work with this chemical for repeated treatments.

Chemicals L and EGC-1700 were used for high temperature treatment but the data for decane imbibition has not been plotted yet. In contact angle measurements, decane imbibed at the sides of the core; it is likely that the imbibition will be low enough for effective wettability alteration.

Cores treated at room temperature - The chemicals D, B, L, FC-722 and EGC-1700 were tested for their effect on decane imbibition by treatments at room temperature.

The results for B and D chemicals were presented earlier in Figs 16 and 17. FC-722 showed a much stronger effect than chemicals B and D. The MB7 core was treated with 0.4% FC-722 at room temperature for three hours. Decane imbibition was 12% after 1 hour (see Fig 20). Two liters of water were then injected into the core; decane imbibition increased as a result. The saturation was 25.5% after one hour then 28% after 4.5 hours. The core was then washed three more times and the amount of water injected was 2 liters for the 2^{nd} and 3^{rd} washings, and 5.5 liters for the 4^{th} washing. Treating the core again at room temperature overnight decreased the decane imbibition; it was 6.6% after an hour and a half. Water injection again increased the decane imbibition as shown in Fig 21. We injected 6.35 liters, 3.78 liters, 6.4 liters and then 6 liters into the core. It seems that the water injection in the 2^{nd}, 3^{rd} and 4^{th} times did not have a drastic effect on decane imbibition.

MB15 was also treated with 0.4% FC722 at room temperature. It was aged for three hours in the first treatment but decane imbibition was high as shown in Fig 22. After the 2^{nd} and third treatments overnight decane imbibition decreased but water washing results in a significant increase in imbibition.

L-chemical was used to treat MB11 two times at room temperature, each time aged for 1 day. The decane imbibition was high after the first treatment as shown in Fig 23 but it

decreased after the second treatment. About 600 cc of water were injected into the core; decane imbibition increased after washing.

MB19 was treated three times with EGC-1700. Decane imbibition was high after each treatment as shown in Fig 24. This chemical does not seem to be suitable in repelling decane.

Concluding Remarks

- C-chemical showed the best effect on water imbibition in both room temperature and 140°C treatments; a stable gas preferential wetting was established for the water/gas system.
- C-chemical, FC-759 and FC-722 had a mild effect on decane imbibition while A, B, C and D chemicals were not effective.

References

1. LI, K. and FIROOZABADI, A., Experimental Study of Wettability Alteration to Preferential Gas-Wetting in Porous Media and It's Effect, SPE *Reservoir Evaluation & Engineering*, Apr., 2000, p. 139.
2. TANG, G. and FIROOZABADI, A., Relative Permeability Modification in Gas/Liquid Systems Through Wettability Alteration to Intermediate Gas Wetting, SPE *Reservoir Evaluation & Engineering*, Dec., 2000, p. 427.

3. TANG, T. and FIROOZABADI, A., Wettability Alteration to Intermediate Gas-Wetting in Porous Media at Elevated Temperatures, Chapter I, also in *Transport in Porous Media*, Aug., 2003, 52 (2), p. 427.

Fig. 1a - Temco core holder used for high temperature treatment

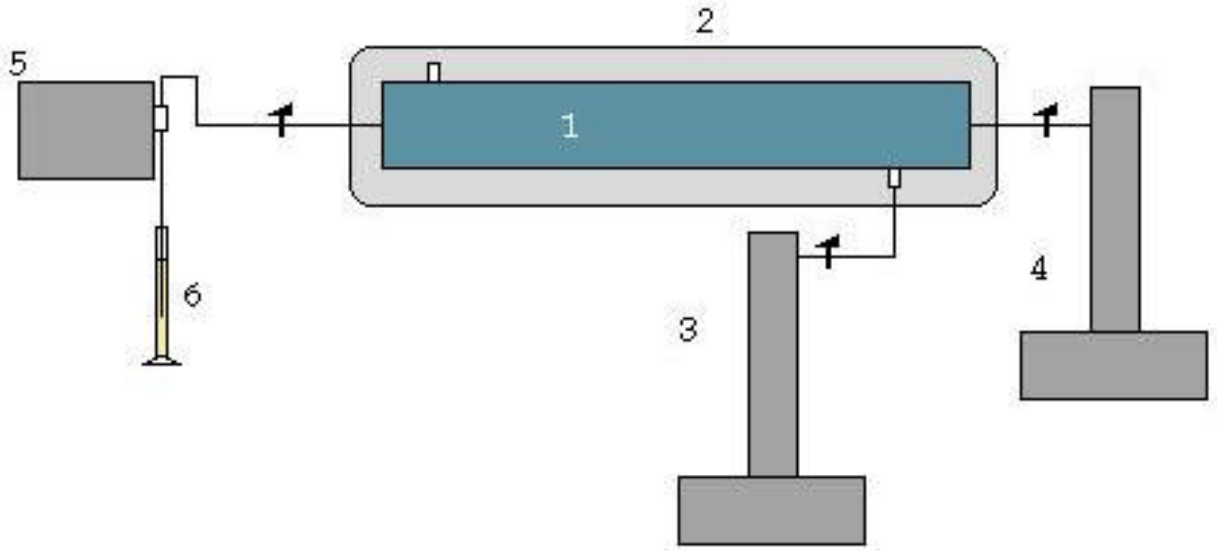

1. Temco core holder
2. Oven
3. Pump used for applying overburden pressure
4. Pump used for applying pressure at the outlet of the core
5. Pump used for injecting the chemical solution
6. Graduated cylinder

Fig. 1b - Setup used for high temperature treatment.

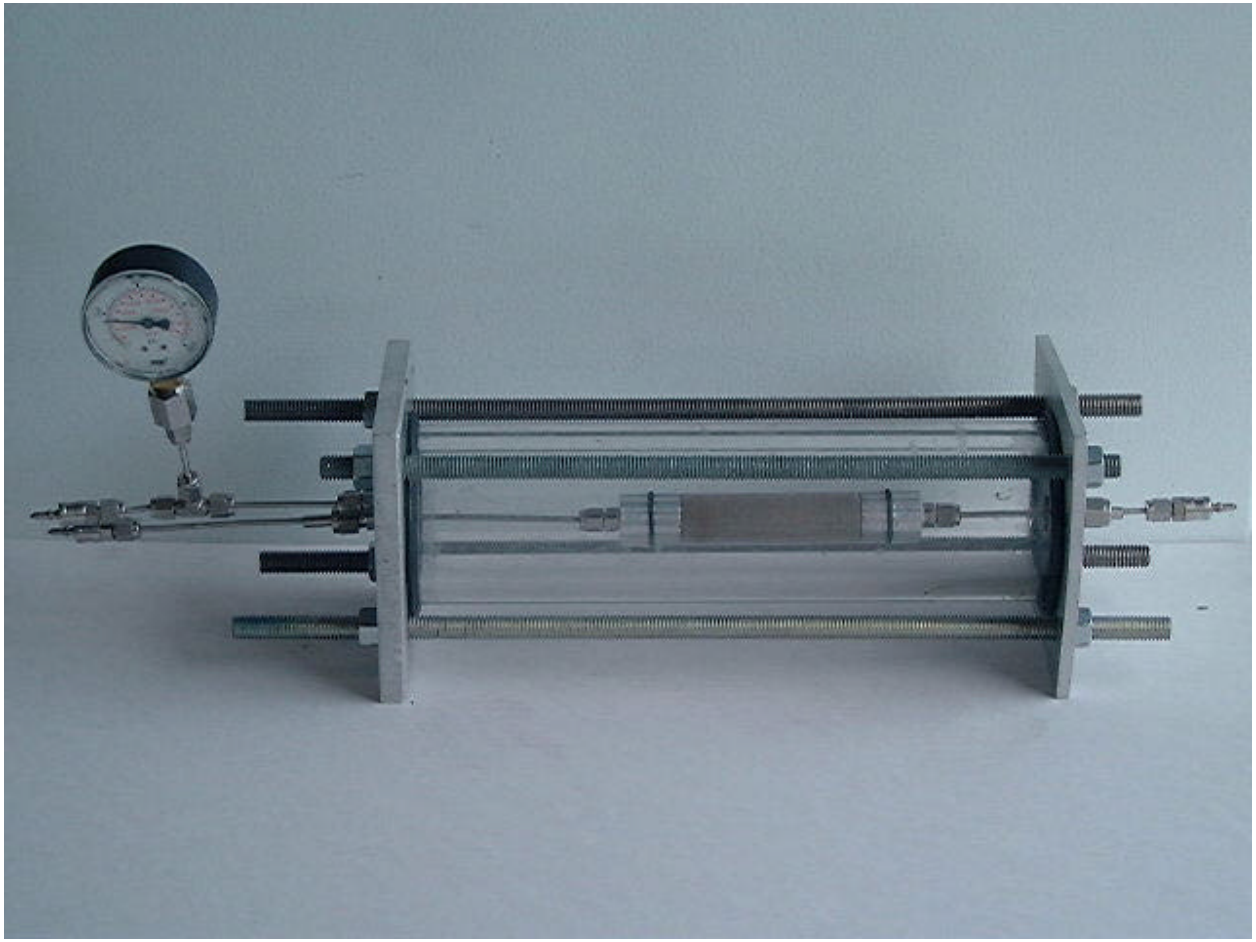

Fig. 2 - Visual core holder used for room temperature treatment, permeability measurements and fluid injection tests.

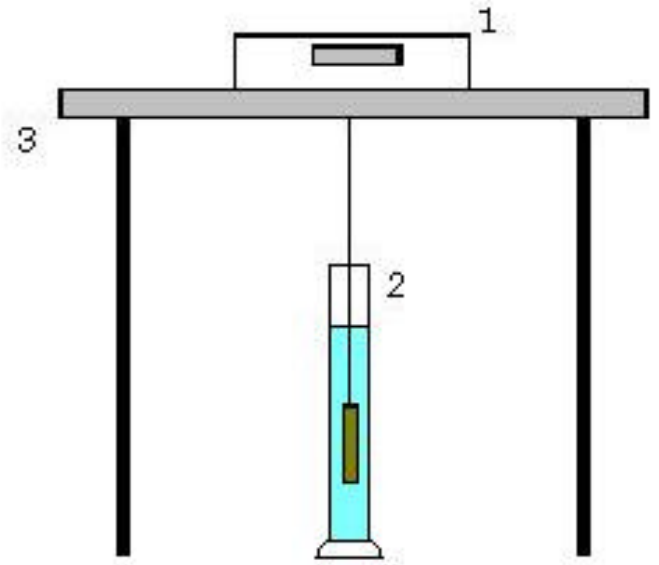

1. Electronic balance
2. Graduated cylinder containing the liquid and the core
3. Table for supporting the balance

Fig. 3 - Setup used for spontaneous imbibition measurement

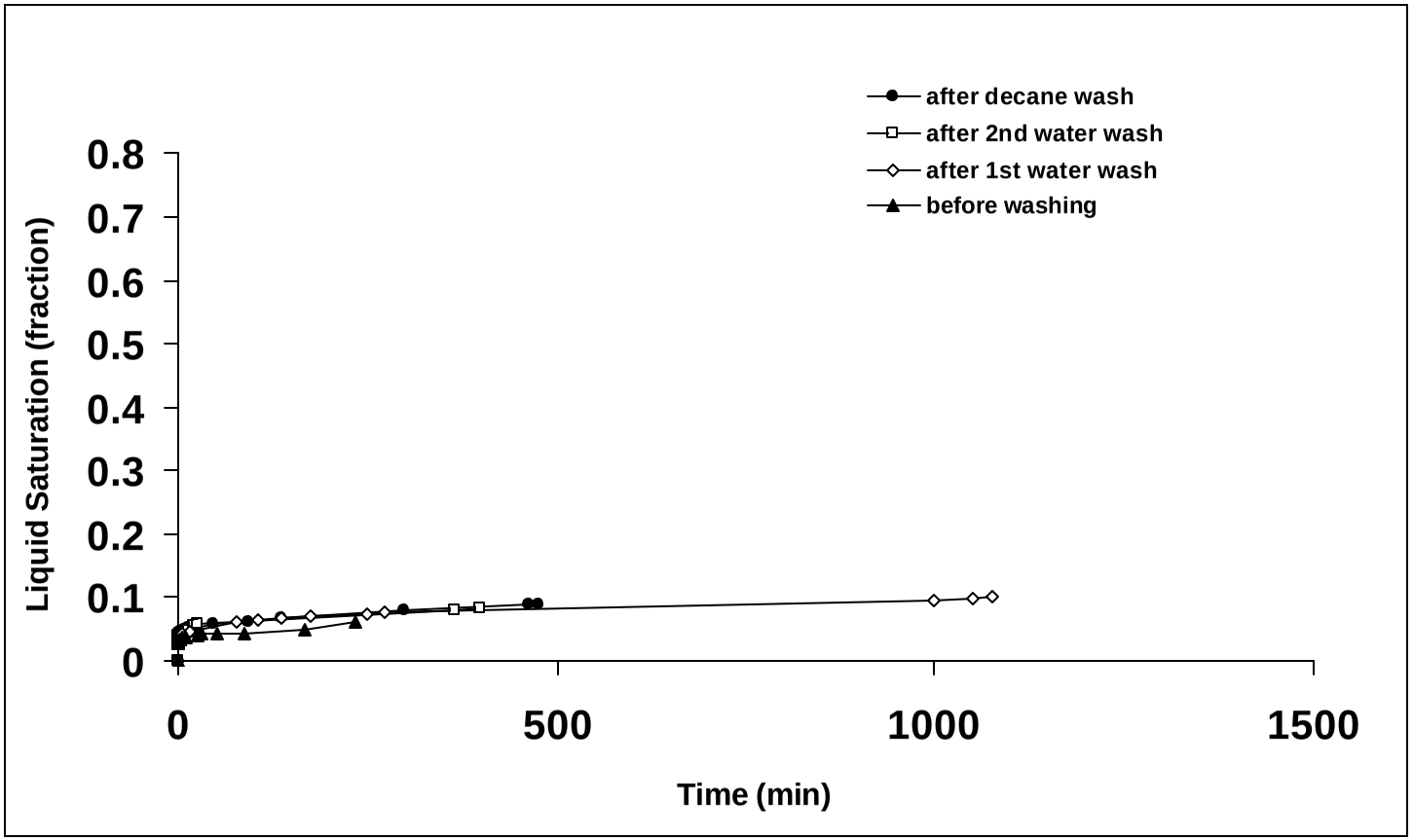

Fig. 4 - Spontaneous water imbibition at room temperature in MB1 treated with 8% FC-759 at 140°C (third treatment).

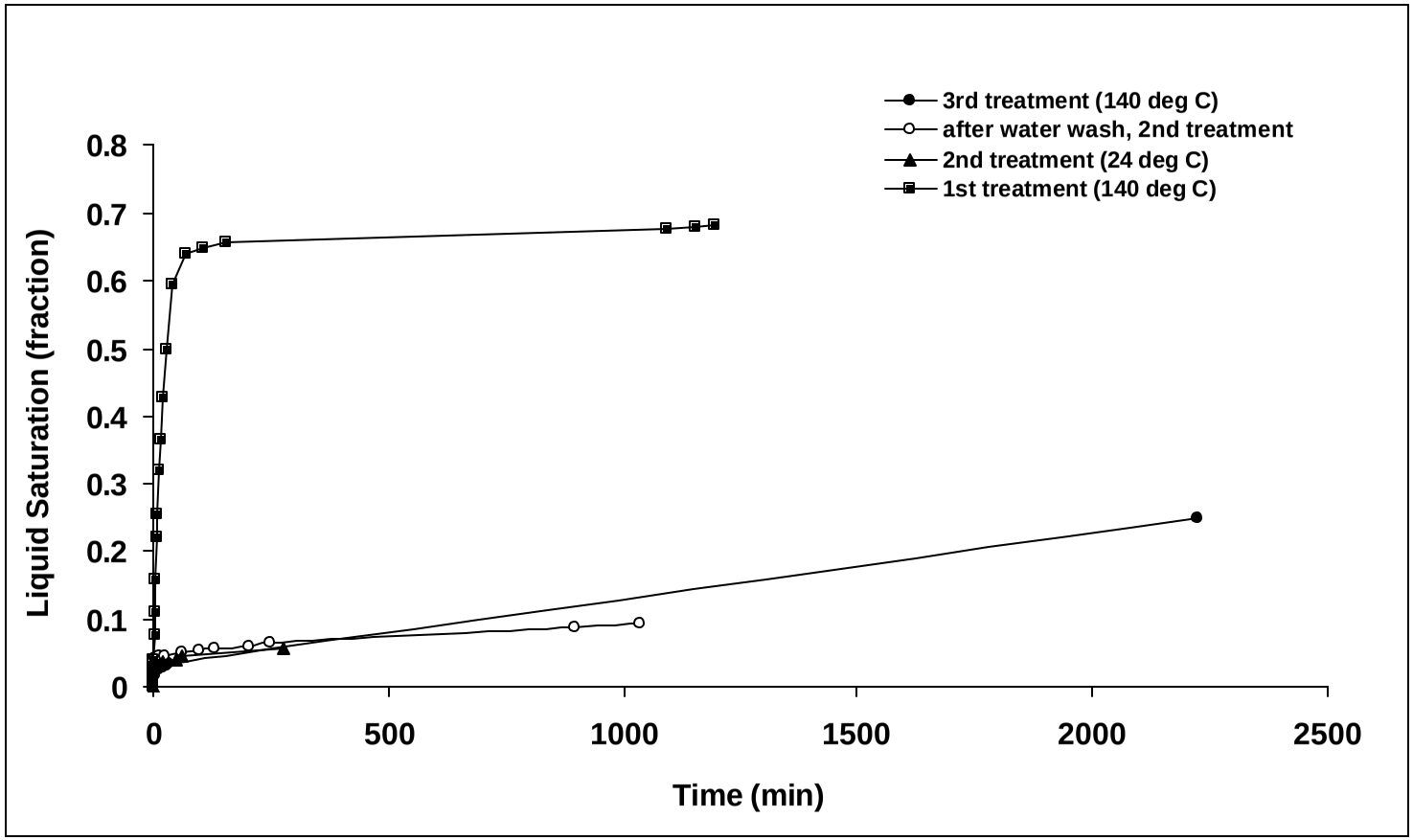

Fig. 5 - Spontaneous water imbibition at room temperature in MB3 treated with 8% D-chemical at 140°C and at room temperature.

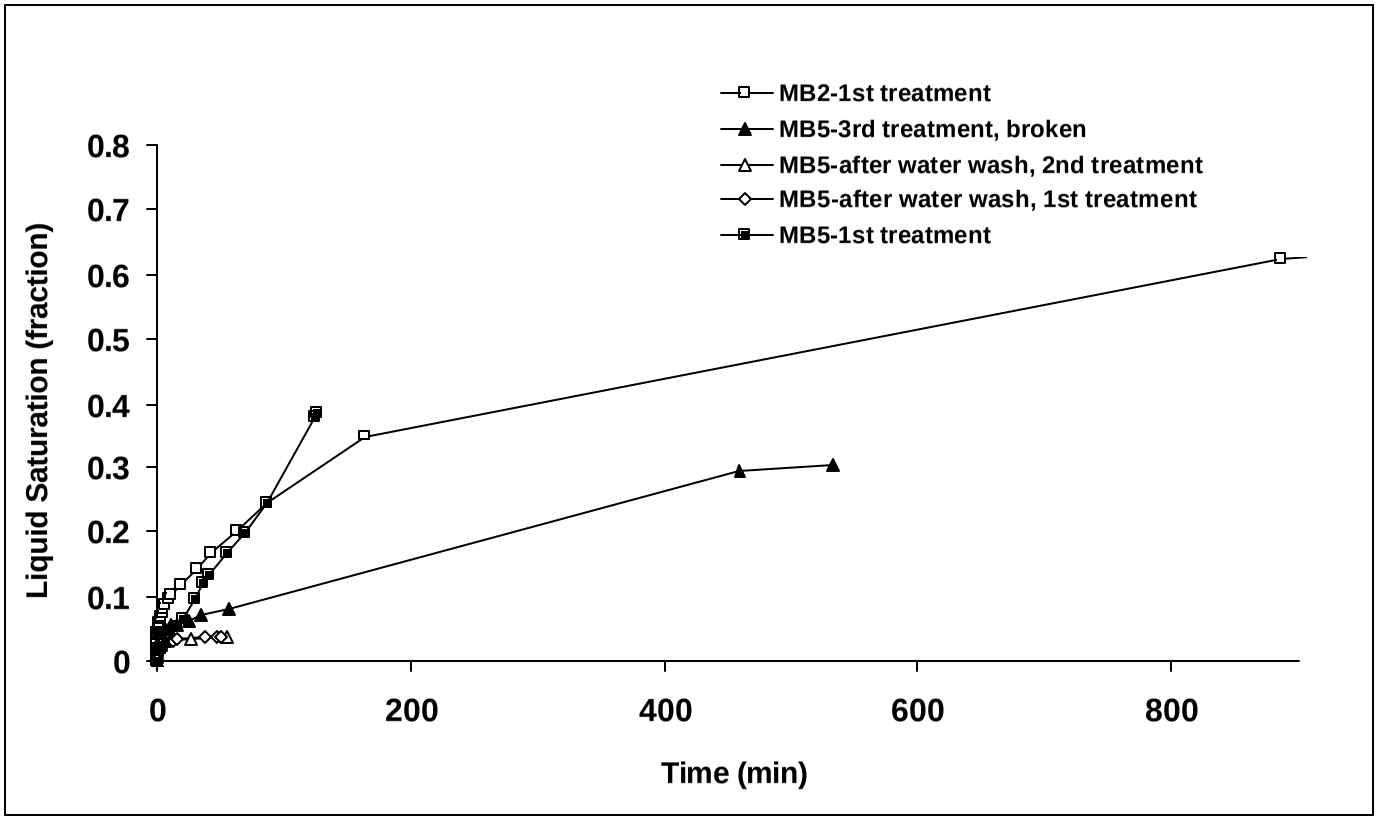

Fig. 6 - Spontaneous water imbibition at room temperature in MB2 and MB5 treated with 8% A-chemical and 8% B-chemical, respectively, at 140°C (2^{nd} treatment with B-chemical was at room temperature).

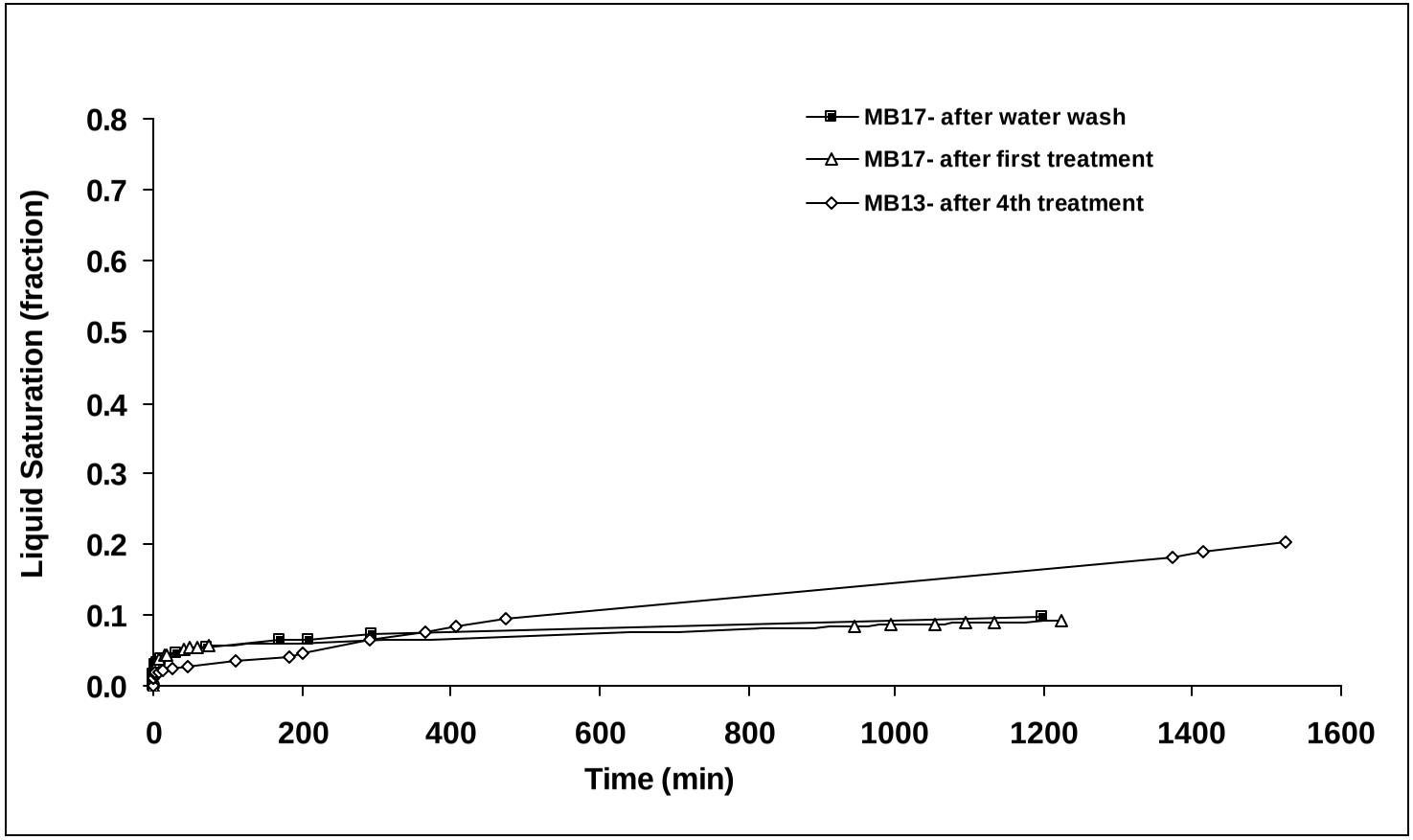

Fig. 7- Spontaneous water imbibition at room temperature in MB17 and MB13 treated with 0.4% FC722 at 140°C.

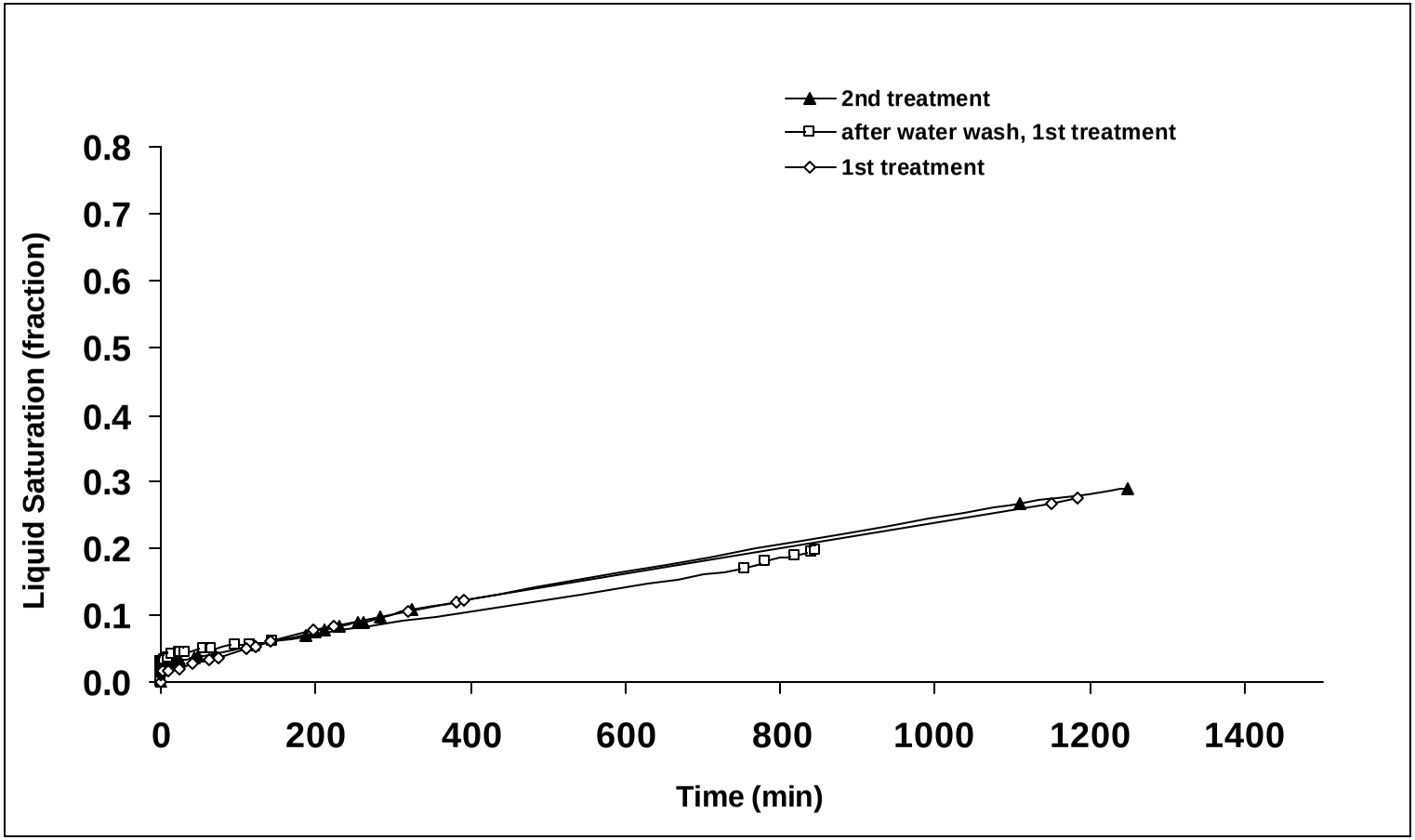

Fig. 8 - Spontaneous water imbibition at room temperature in MB21 treated with 8% L-chemical at 140°C.

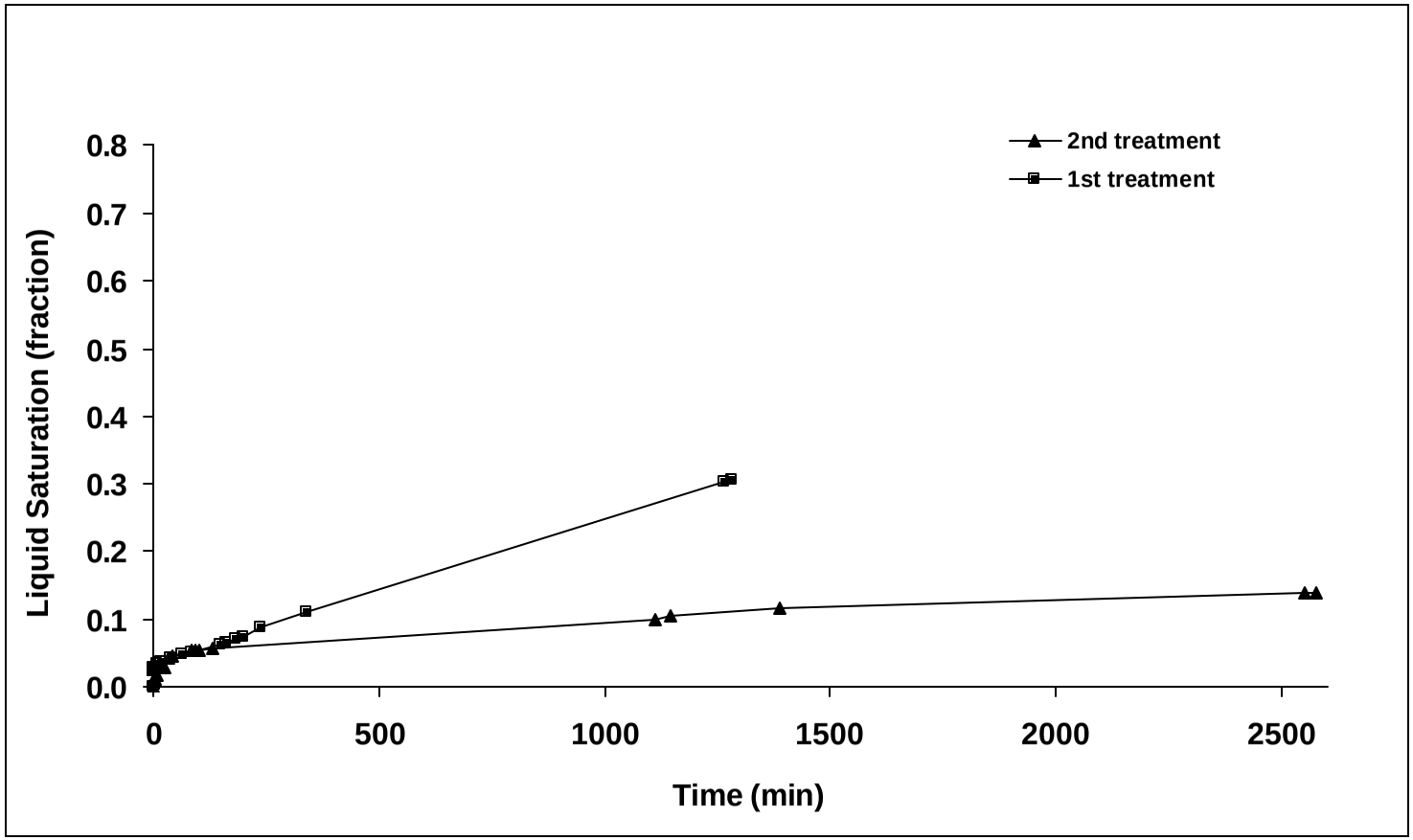

Fig. 9 - Spontaneous water imbibition at room temperature in MB23 treated with 1% EGC-1700 at 90°C.

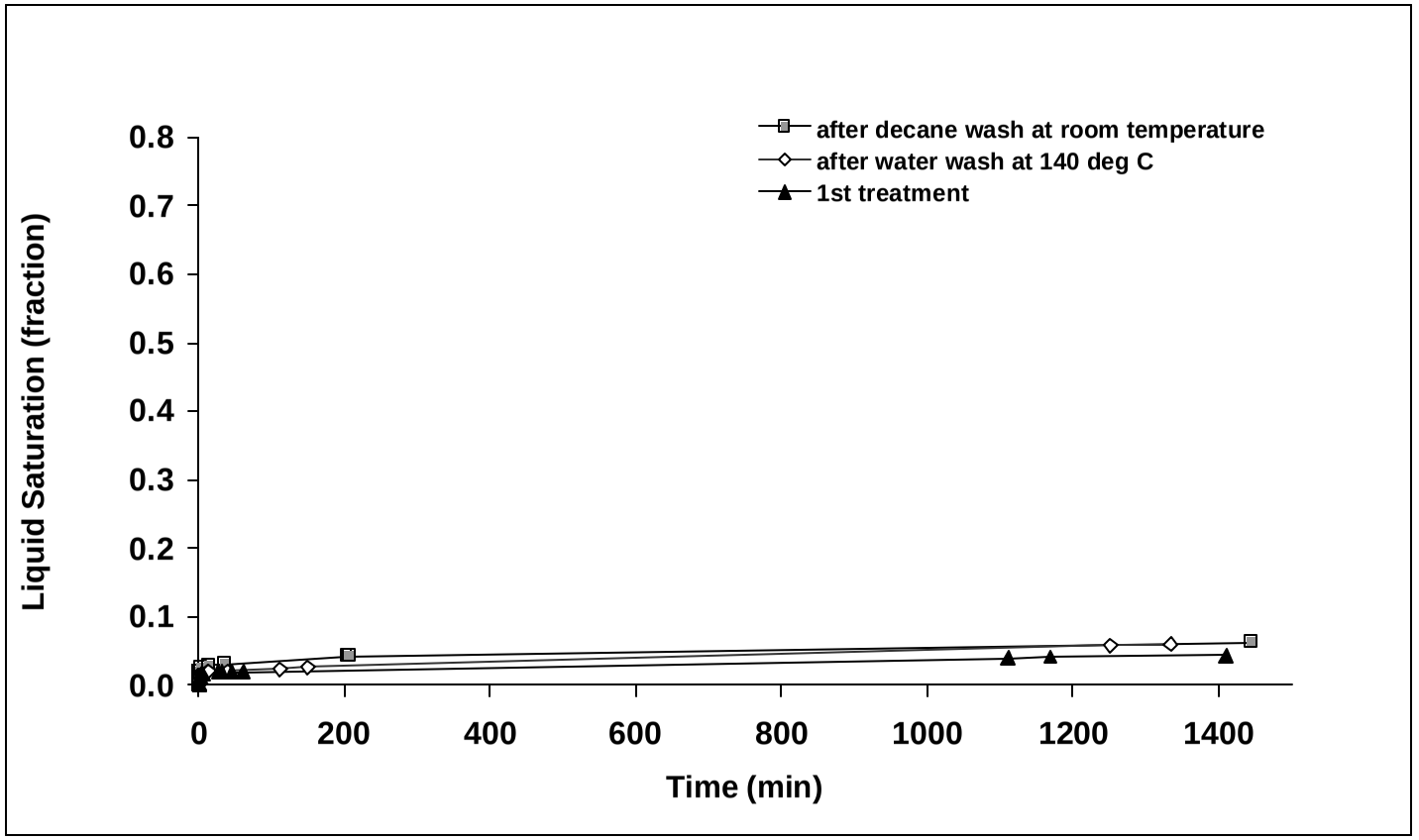

Fig. 10 - Spontaneous water imbibition at room temperature in MB27 treated once with 8% C-chemical at 140°C.

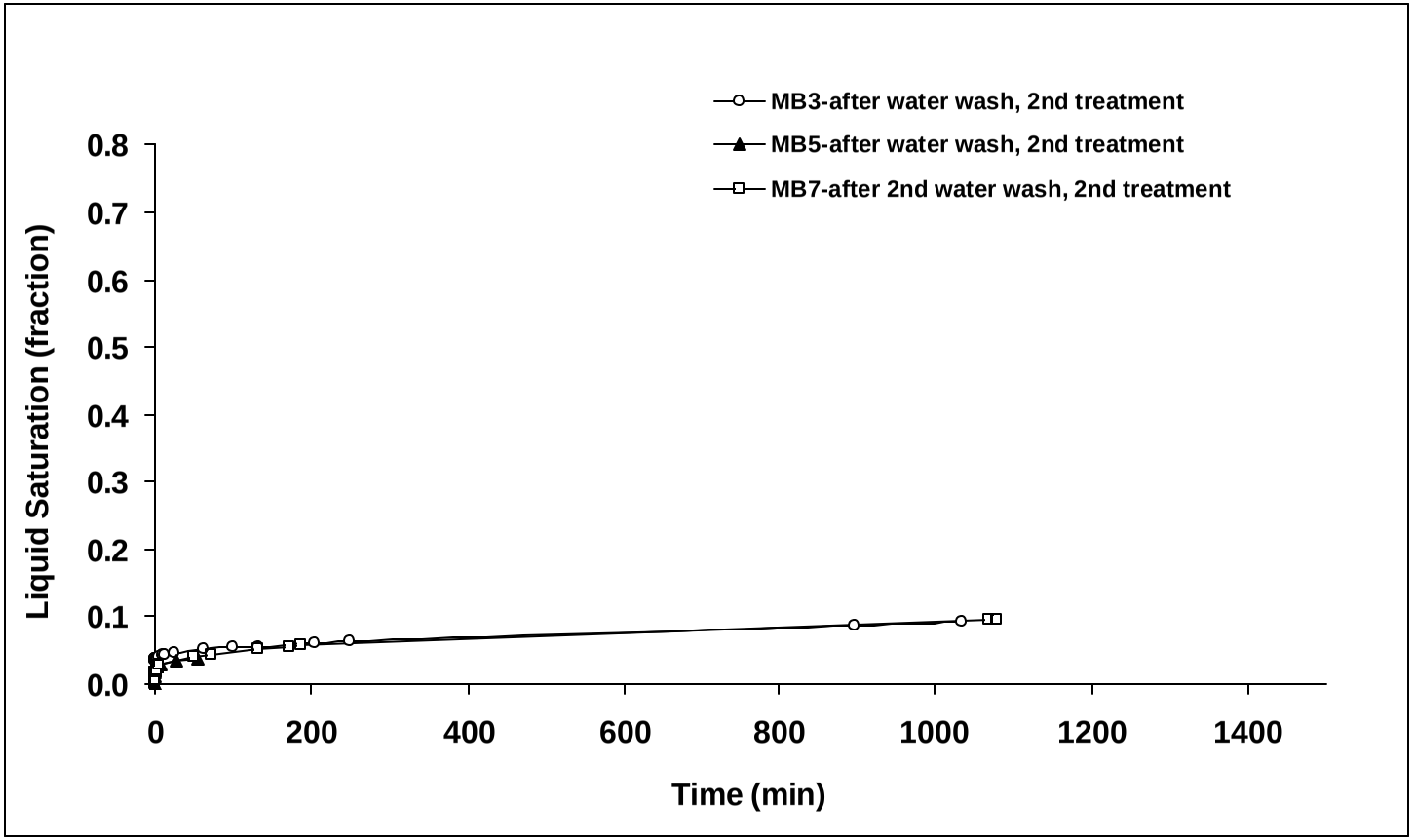

Fig. 11 - Spontaneous water imbibition at room temperature in MB3 and MB5 treated with 8% D- and B- chemicals and MB7 treated with 0.4% FC722 at room temperature.

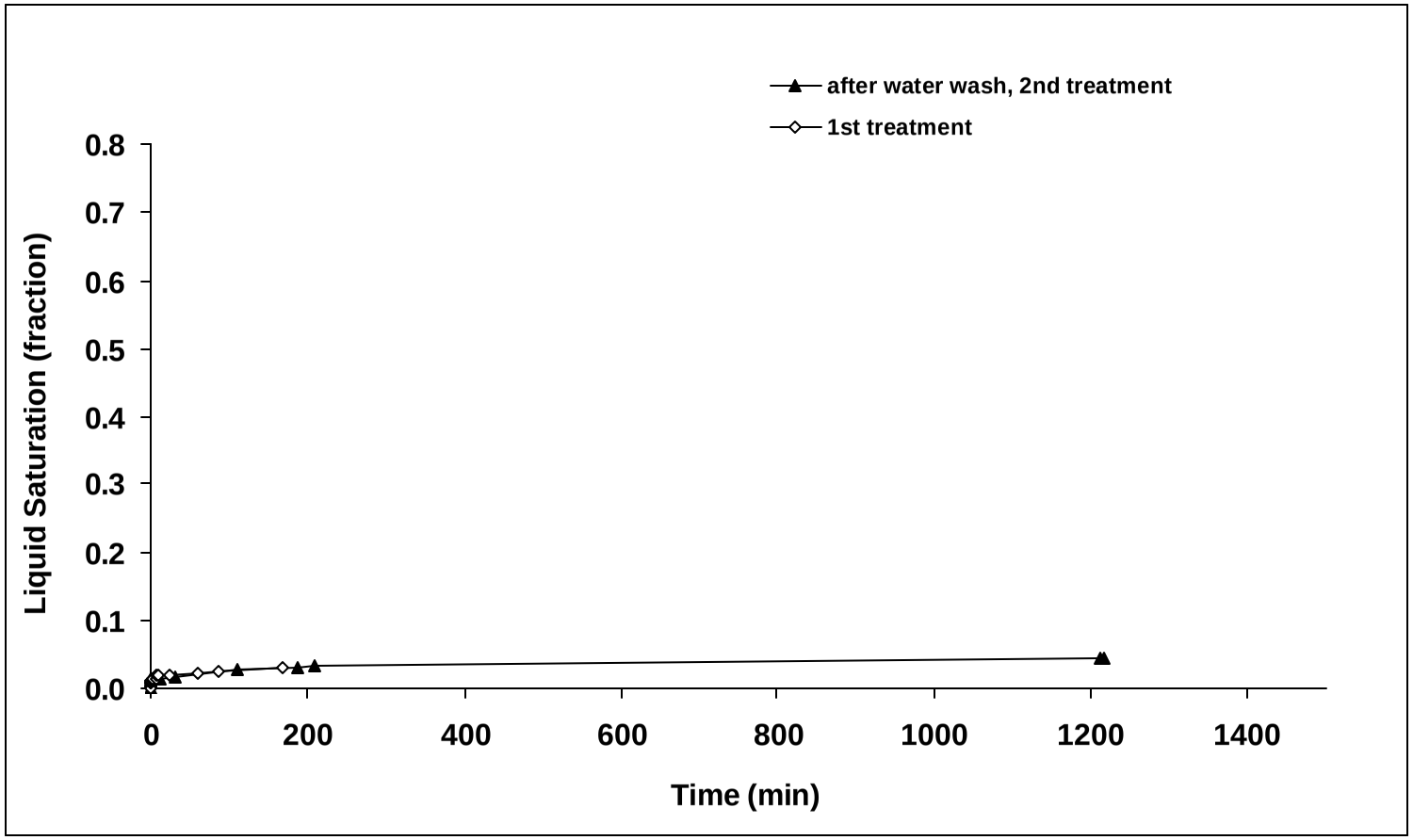

Fig. 12 - Spontaneous water imbibition at room temperature in MB11 treated with 8% L-chemical at room temperature.

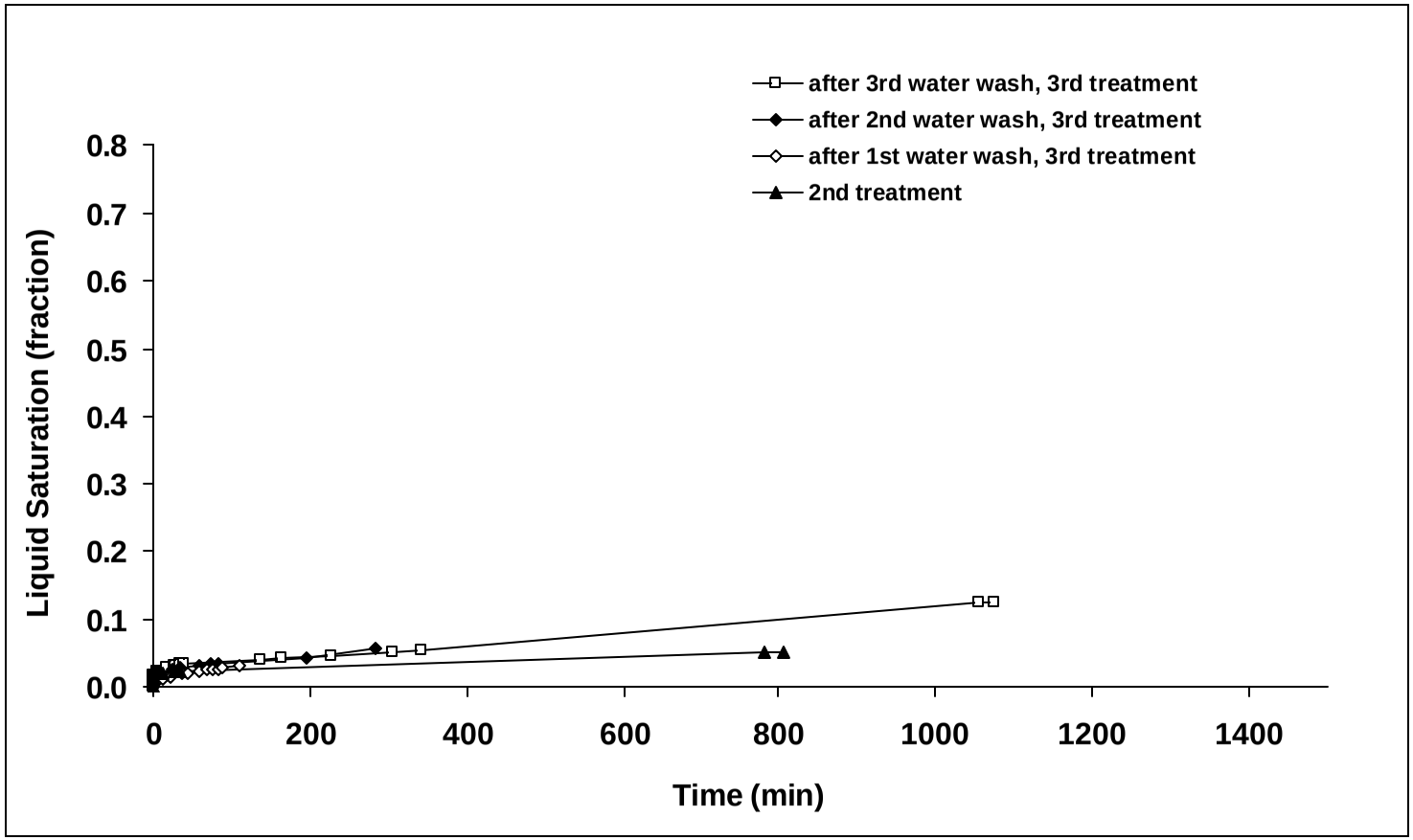

Fig. 13 - Spontaneous water imbibition at room temperature in MB19 treated with 1% and 2% EGC-1700 at room temperature.

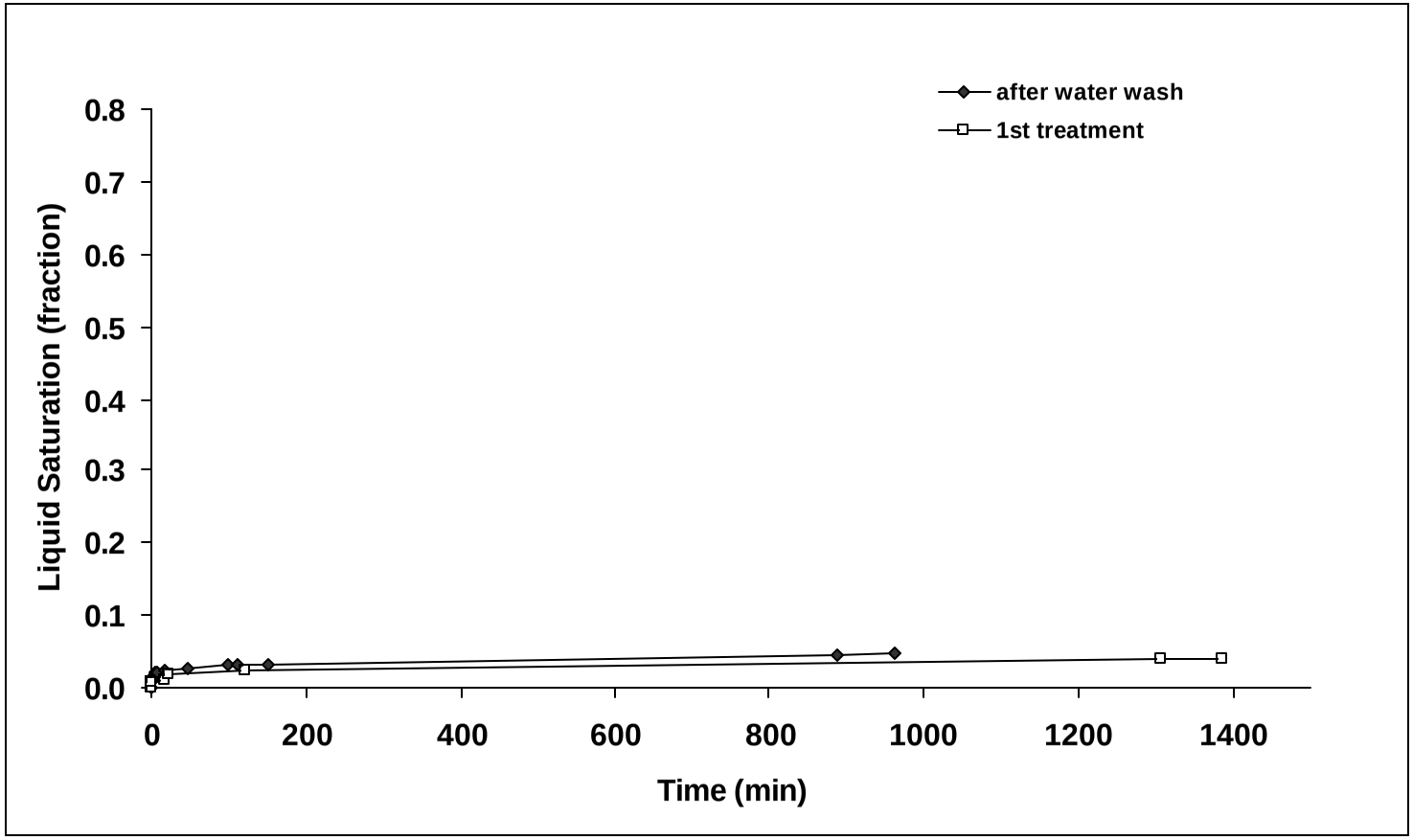

Fig. 14 - Spontaneous water imbibition at room temperature in MB25 treated with 8% C-chemical at room temperature.

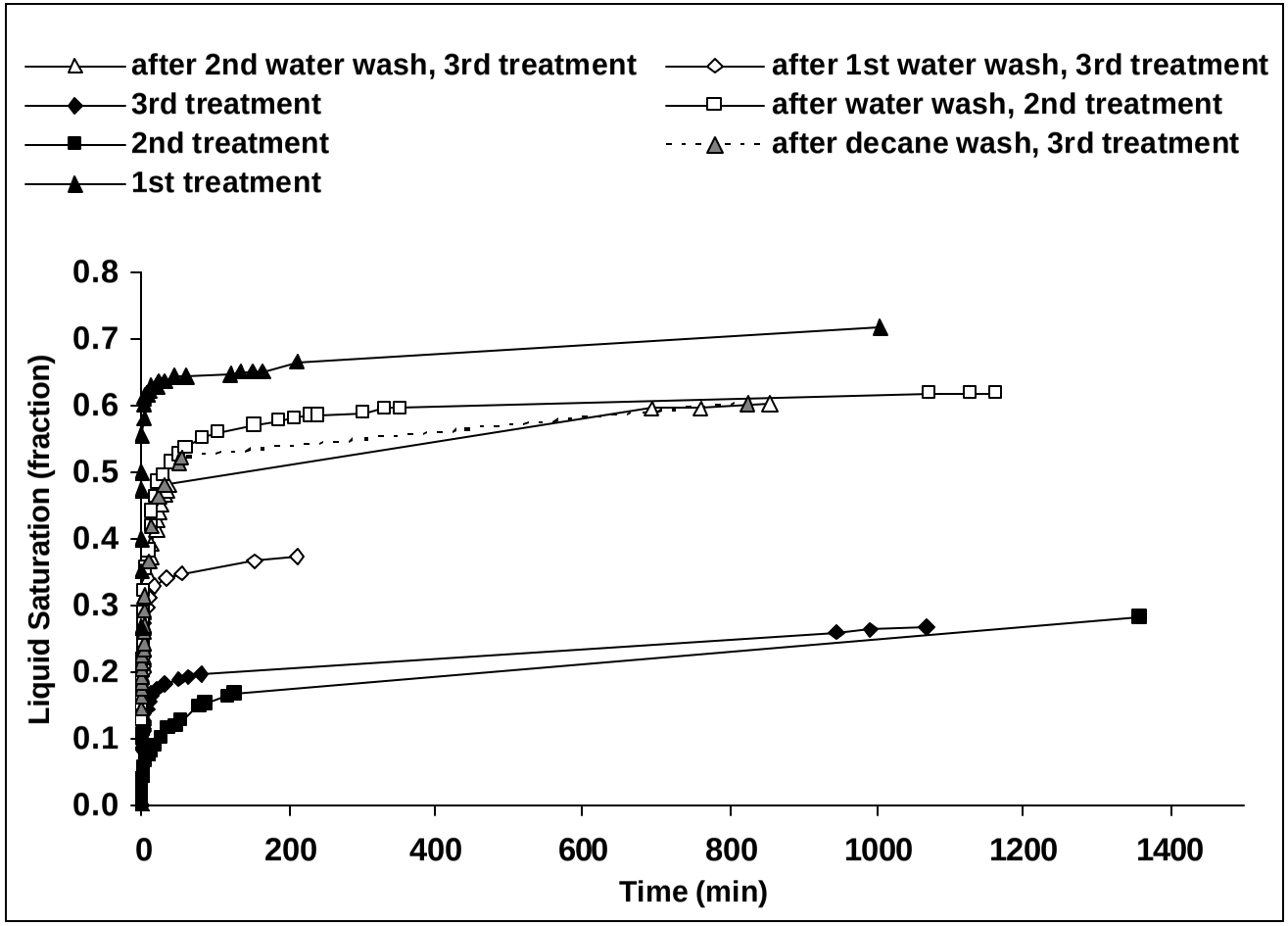

Fig. 15 - Spontaneous decane imbibition at room temperature in MB1 treated with 8% FC-759 at 140°C.

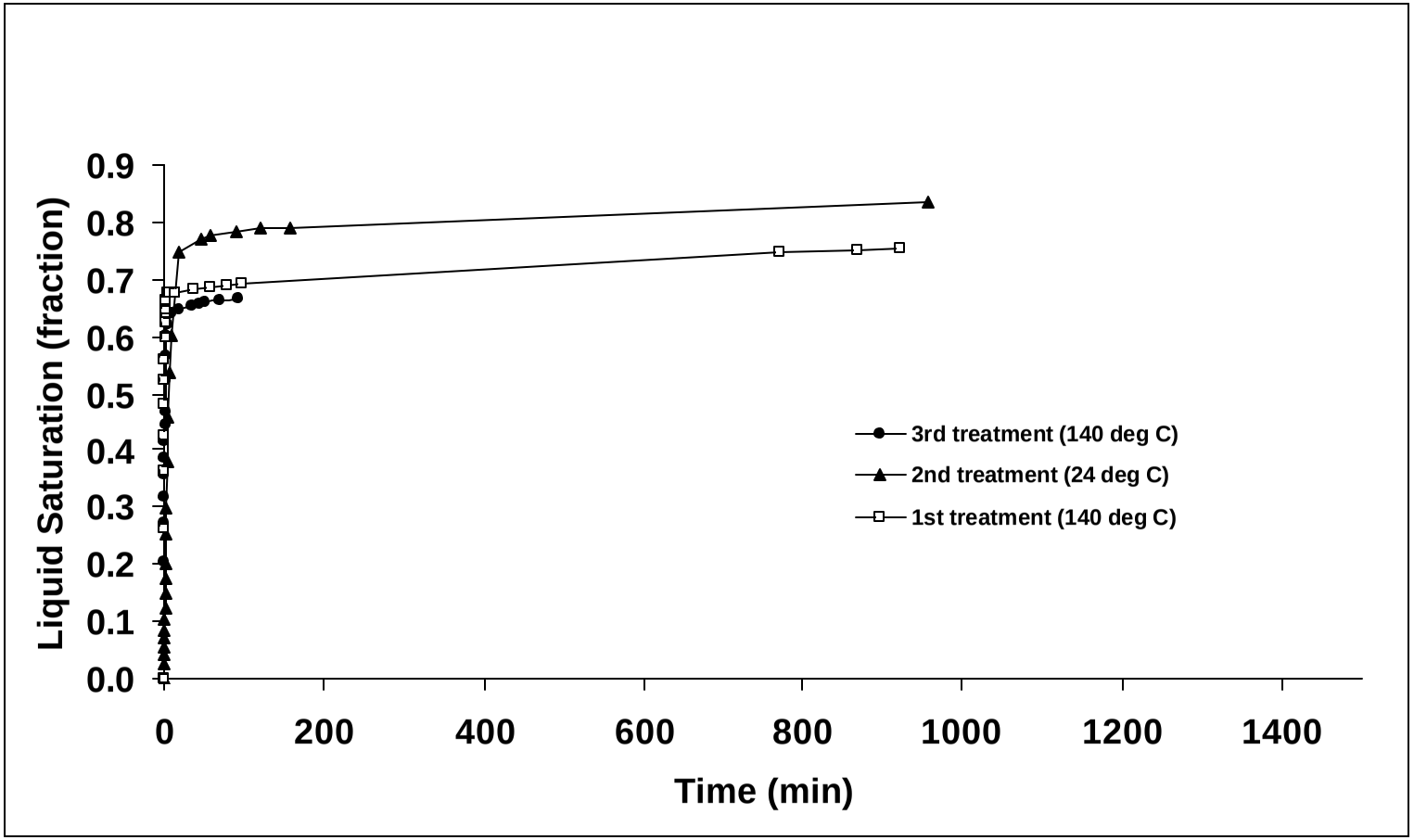

Fig. 16 - Spontaneous decane imbibition at room temperature in MB3 treated with 8% D-chemical at 140°C and at room temperature.

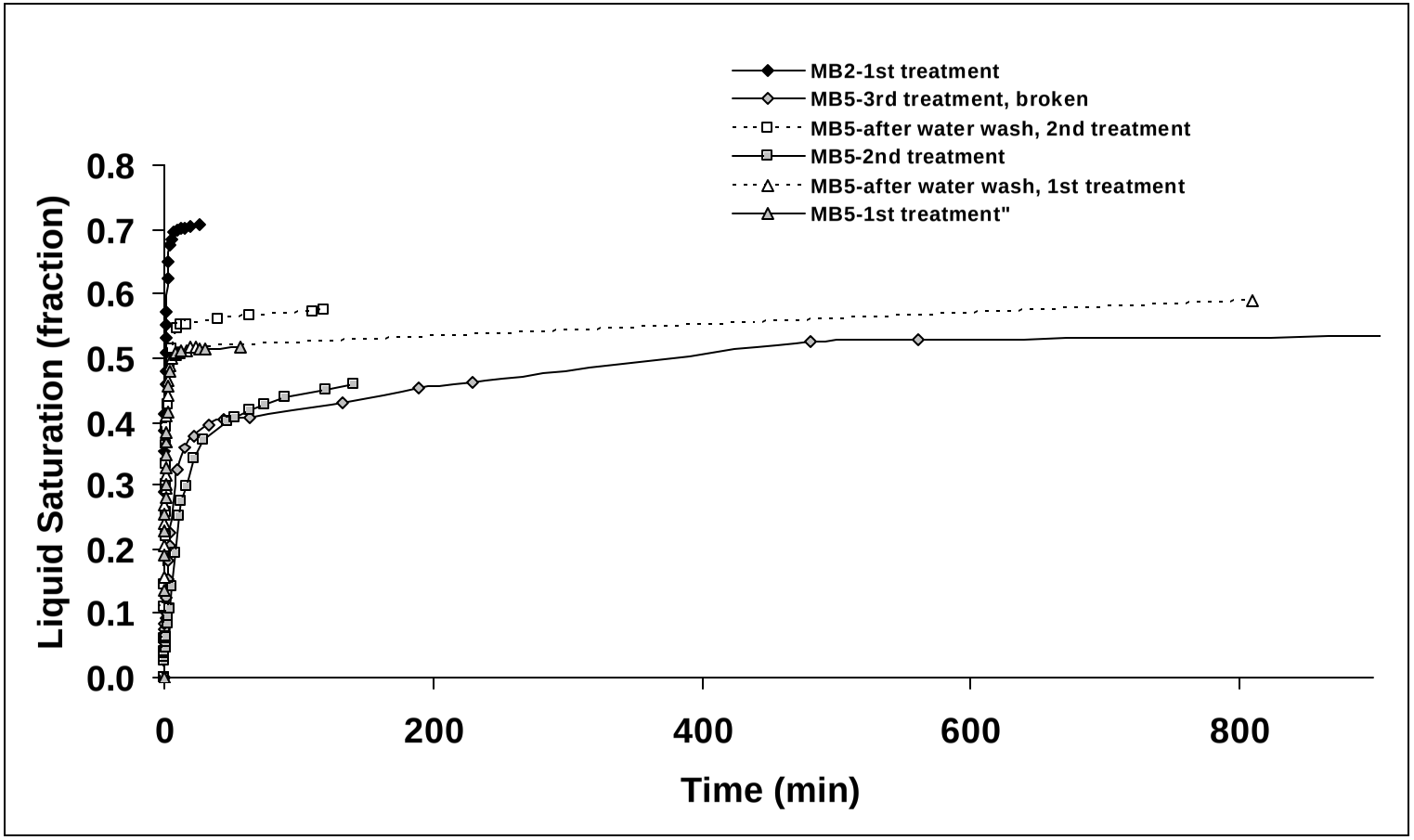

Fig. 17 - Spontaneous decane imbibition at room temperature in MB2 and MB5 treated with 8% A-chemical and 8% B-chemical, respectively, at 140°C (2^{nd} treatment with B-chemical was at room temperature)

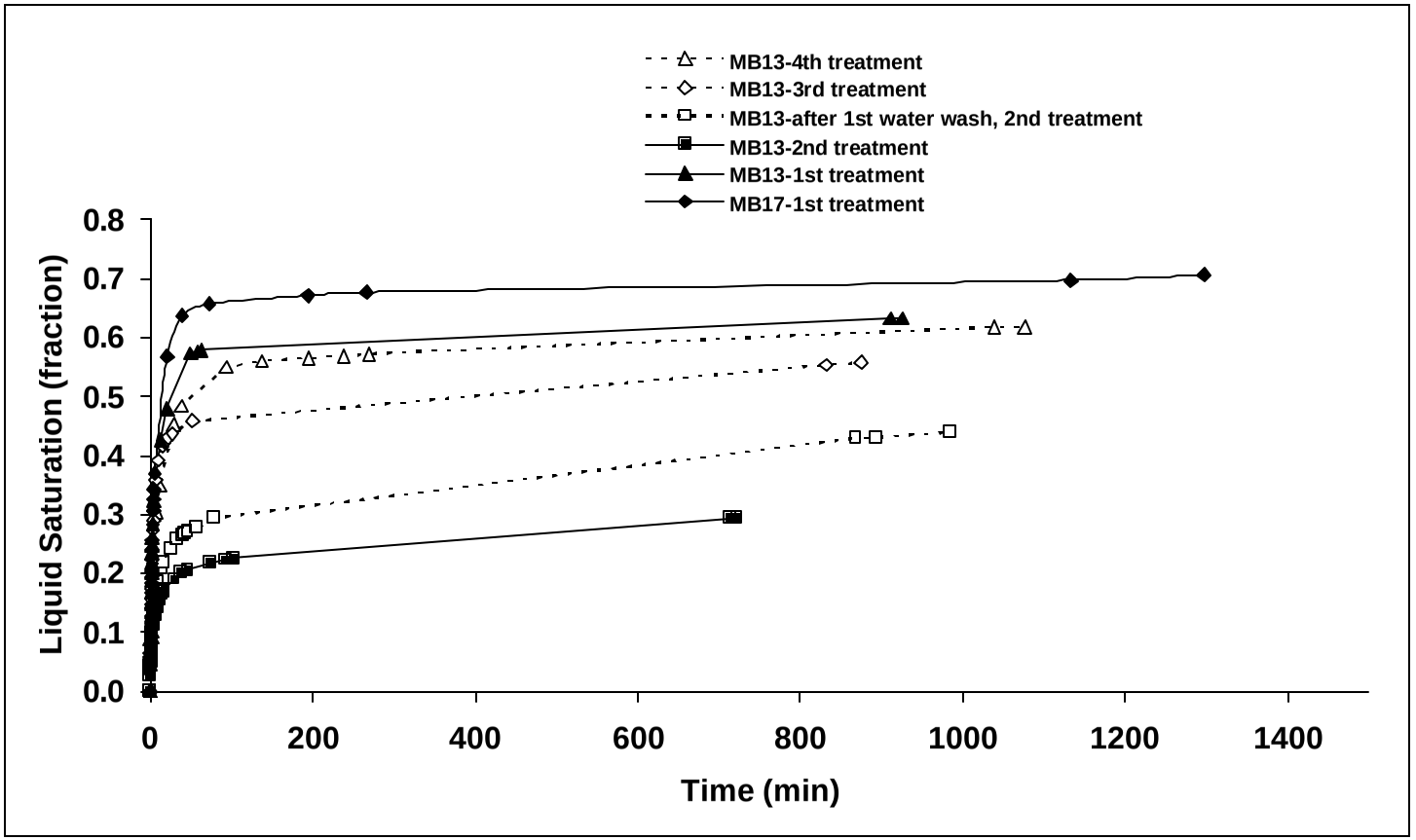

Fig. 18 - Spontaneous decane imbibition at room temperature in MB13 and MB17 treated with 0.4% FC-722 at 140°C.

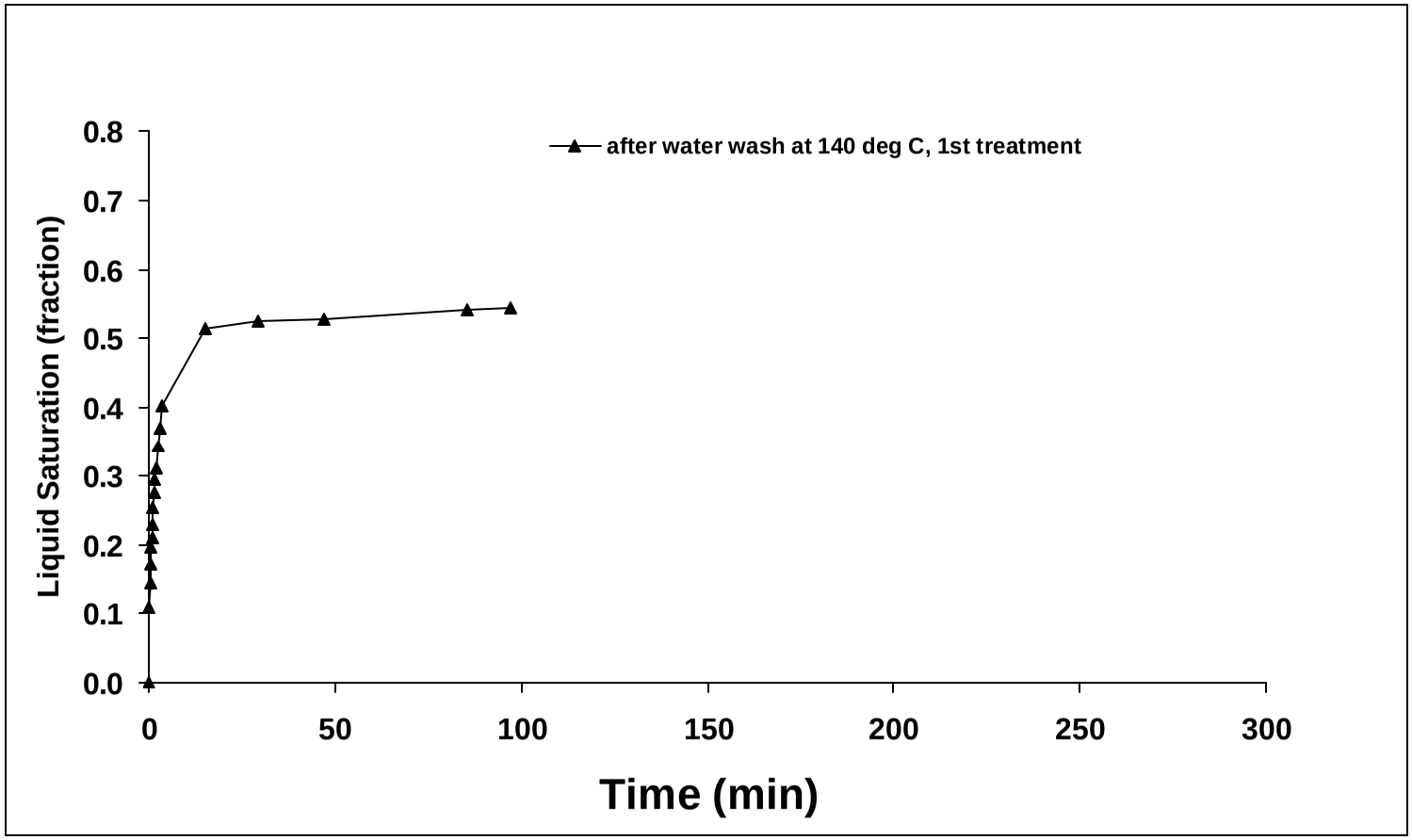

Fig. 19 - Spontaneous decane imbibition at room temperature in MB27 treated with 8% C-chemical at 140°C.

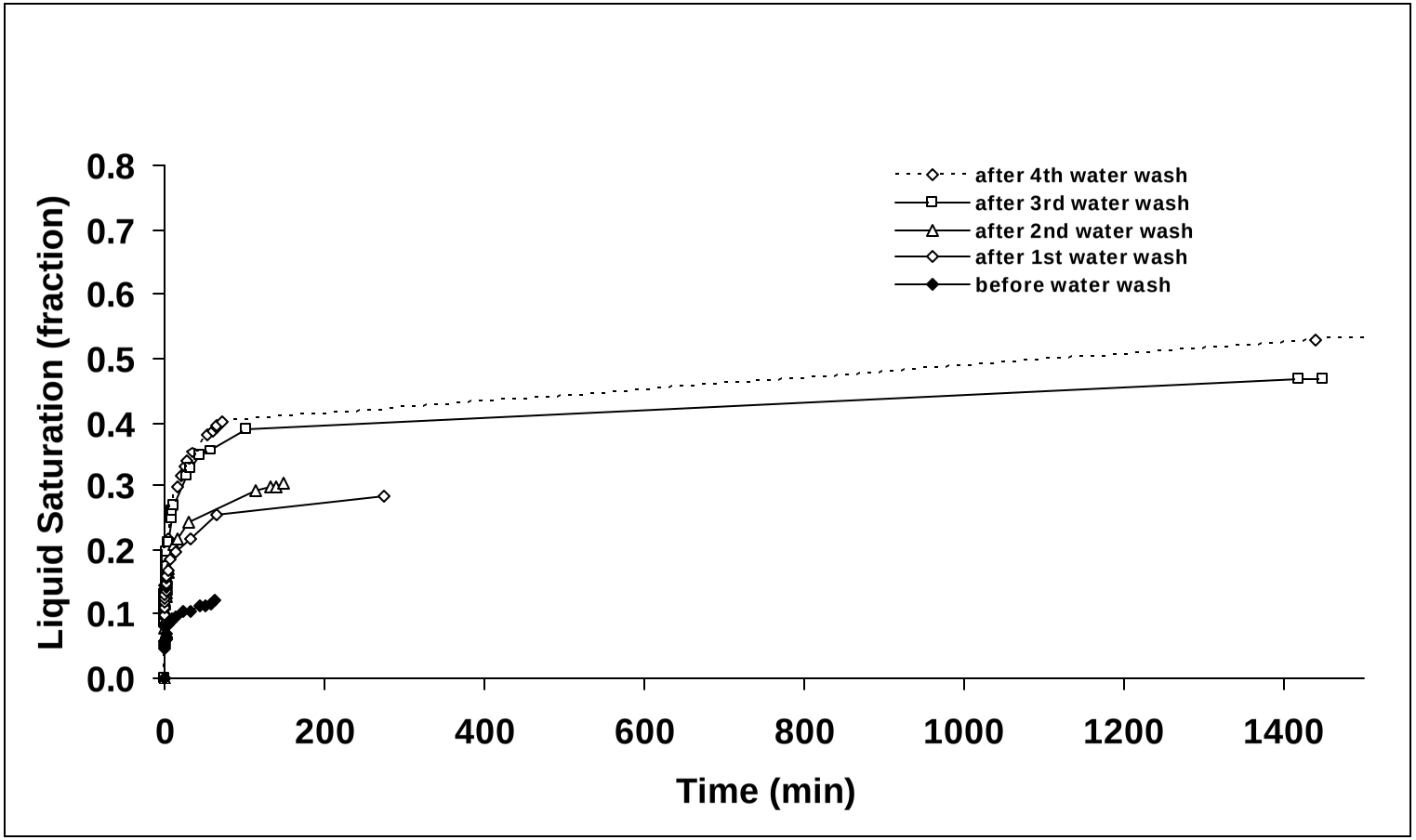

Fig. 20 - Spontaneous decane imbibition at room temperature in MB7 after the 1st treatment with 0.4% FC-722 at room temperature.

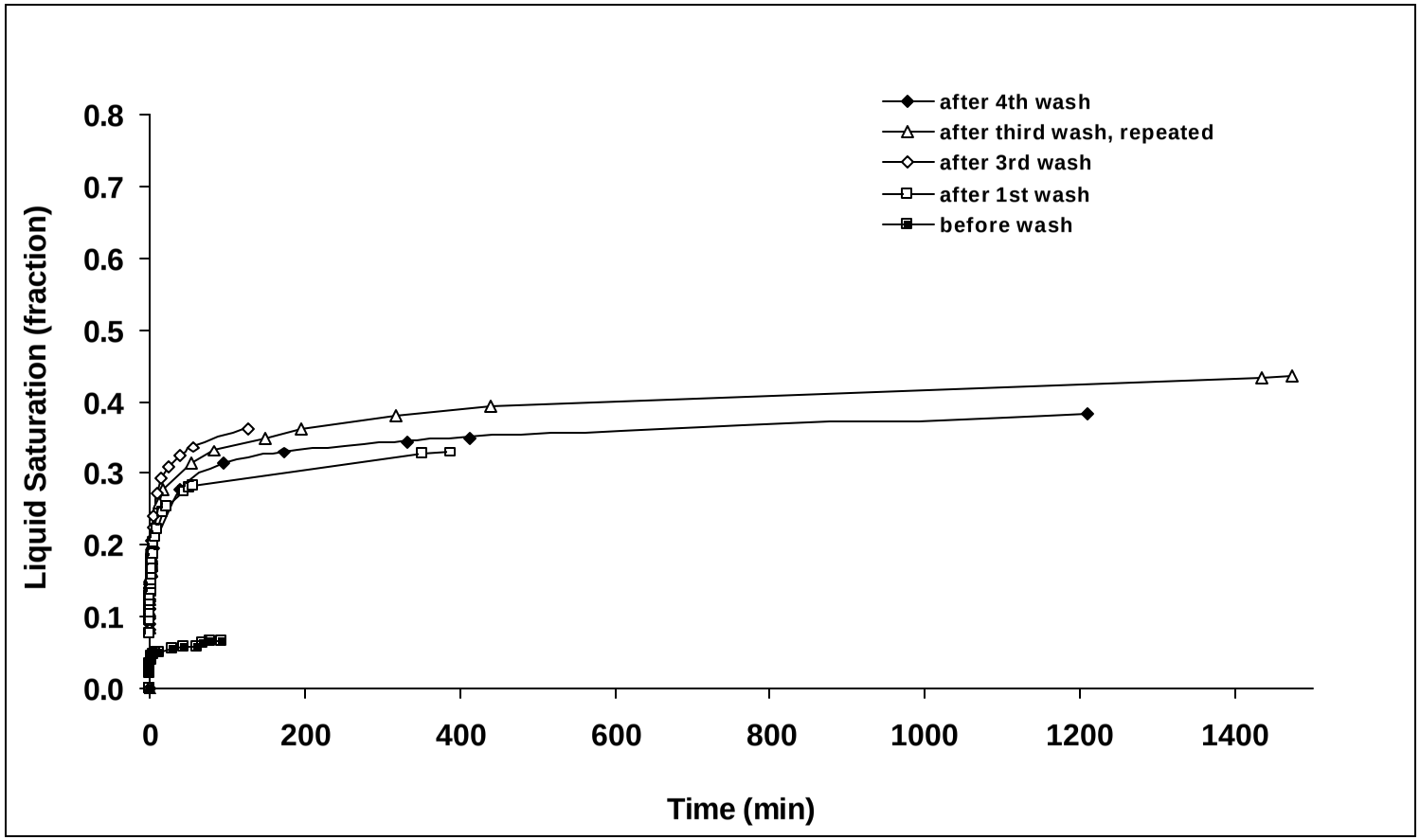

Fig. 21 - Spontaneous decane imbibition at room temperature in MB7 after the 2nd treatment with 0.4% FC722 at room temperature.

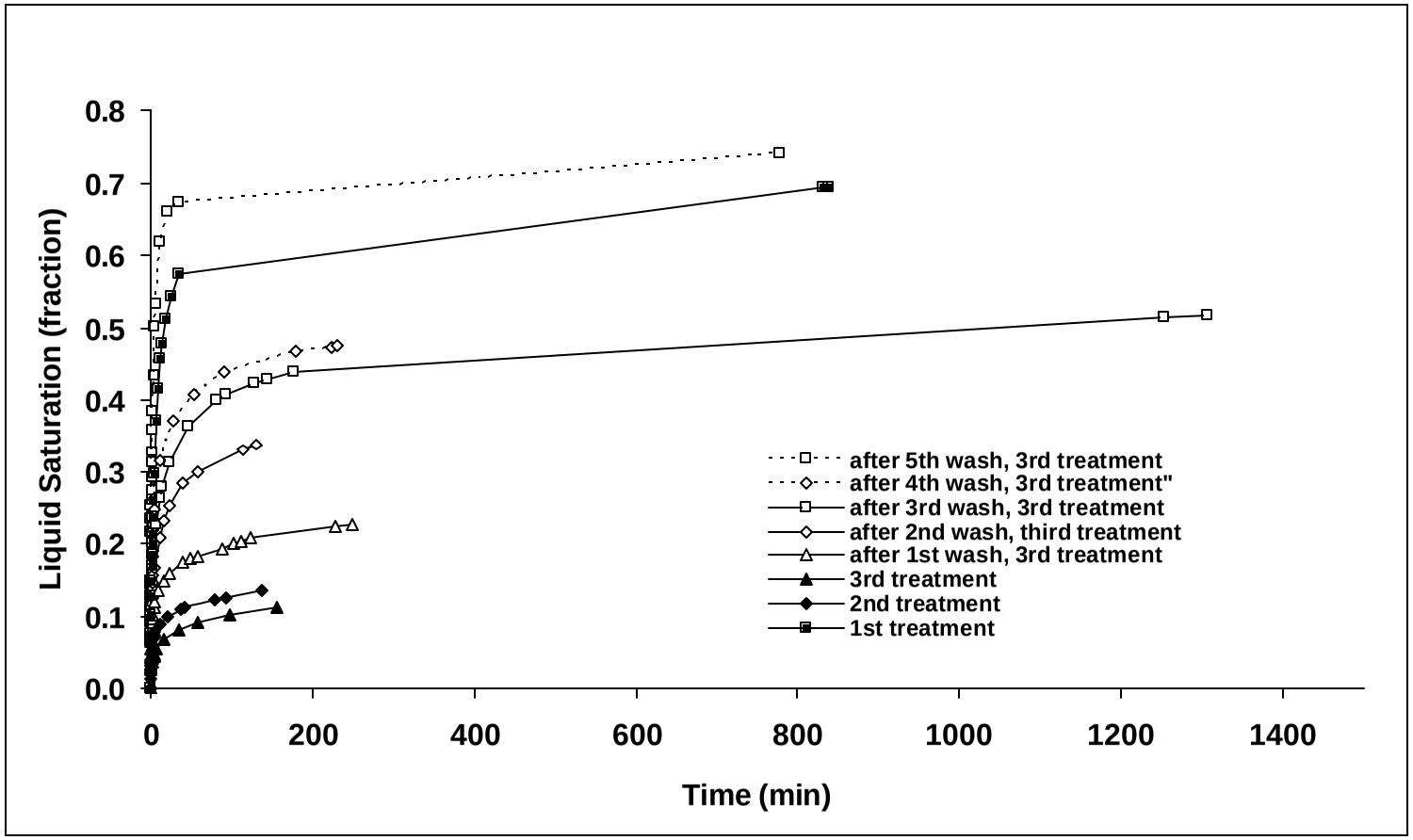

Fig. 22 - Spontaneous decane imbibition at room temperature in MB15 treated with 0.4% FC722 at room temperature.

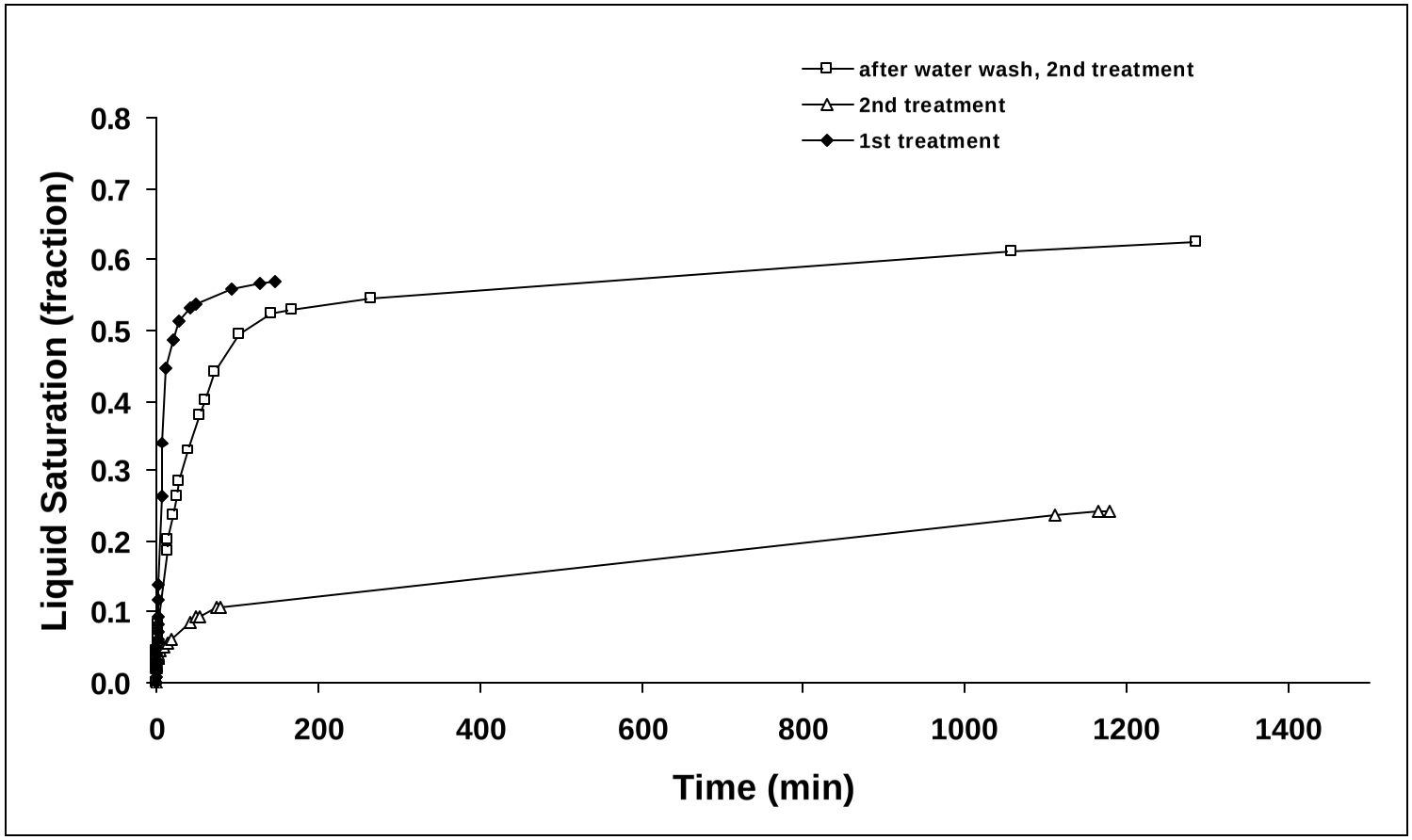

Fig. 23 - Spontaneous decane imbibition at room temperature in MB11 treated with 8% L-chemical at room temperature.

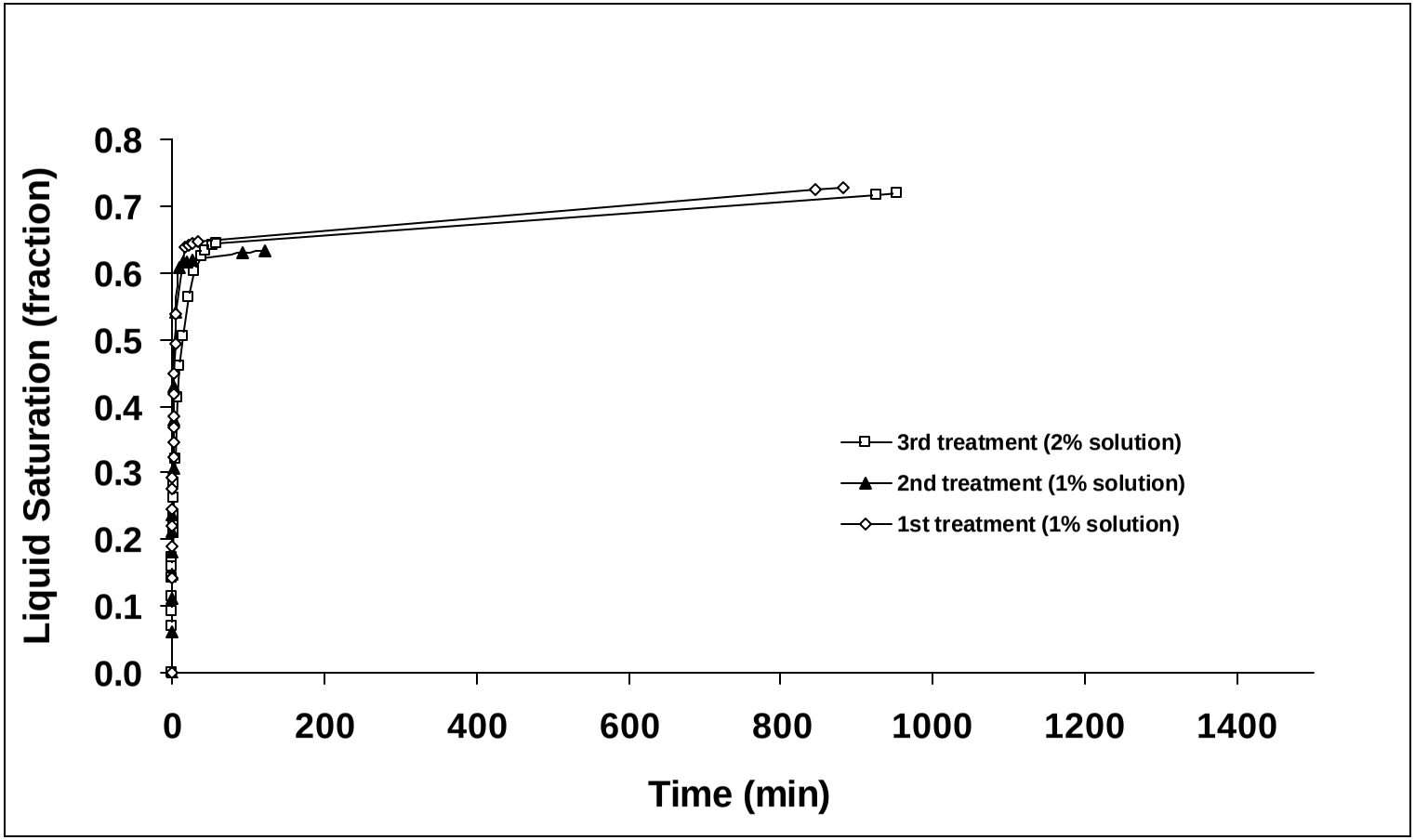

Fig. 24 - Spontaneous decane imbibition at room temperature in MB19 treated with 1% and 2% EGC-1700 at room temperature.

Table 1 - Data on core samples

Core designation	Length	Chemical	Treatment temperature	Permeability before treatment	Number of	Adsorption 1st treatment	Adsorption 2nd treatment	Adsorption 3rd treatment	Permeability after treatment
	(inch)		(°C)	(md)	treatments	(mg/g)	(mg/g)	(mg/g)	(md)
MB1	3.58	FC759	140	476	3	1.09		0.66	
MB2	3.45	A	140	795	2	1.22			
MB3	3.49	D	140 and 24	890	3	0.44		0.33	860 (3rd treatment)
MB5	3.75	B	140 and 24	395	3	3.13	2.02		370 (2nd treatment)
MB7	3.46	FC722	24	650	2	1.02	0.80		540 (2nd treatment)
MB9	3.49	FC722	140	175	1				
MB11	3.48	L	24	149	2	1.02	2.05		145 (2nd treatment)
MB13	3.53	FC722	140		4	0.94	0.57	0.57	
MB15	3.44	FC722	24	384	3	1.17	0.39	0.39	325 (3rd treatment)
MB17	3.52	FC722	140	324	1	0.94			368 (1st treatment)
MB19	3.33	EGC1700	24	380	3	1.31	0.81	1.01	296 (3rd treatment)
MB21	3.49	L	140	930	2	2.40	0.46		
MB23	3.44	EGC1700	90	800	2	1.16			
MB25	3.44	C	24	302	1	0.96			325 (1st treatment)
MB27	3.44	C	140	290	1	1.07			230 (1st treatment)

Table 2 - Properties of the chemicals used for core treatment

Chemical	Solvent	T tested	color	Solubility
FC-759	water	140	yellow	water soluble
FC-722	C6F14	140 & 25	colorless	water insoluble
A	water	140	yellow	water soluble
B	water	140 & 25	yellow	water soluble
C	water	140 & 25	yellow	water soluble
D	water	140 & 25	yellow	water soluble
L	water	140 & 25	yellow	water soluble
EGC-1700	HFE-7100	90 & 25	colorless	water soluble

Chapter 3 - Curvature Dependence of Surface Tension in Multicomponent Systems

Erik Santiso, RERI

Abbas Firoozabadi, RERI

Abstract

The effect of curvature on the surface tension of droplets and bubbles in both single and multicomponent systems is modeled using the basic equations from classical thermodynamics. The three basic expressions used in our work are the Gibbs adsorption equation for multicomponent systems, the relation between the surface tension at the surface of tension and the distance parameter d and the Macleod-Sugden equation for surface tension and its extension to multicomponent systems. The Peng-Robinson equation of state is used to describe the bulk phases. We also assume that the surface tension expression remains valid in terms of the properties of the bulk phases for both flat and curved interfaces. The results from our model reveal a decrease in surface tension with curvature in bubbles and a non-monotonic behavior in droplets for single-component systems. Our predictions are in good agreement with the literature results when the interface is described using the framework of the density functional theory by three different groups. For multicomponent systems, the results show that the surface tension in a bubble, although monotonic with curvature, can increase or decrease in a large bubble depending on the temperature and composition of the mixture. In a droplet, the surface tension can have a non-monotonic behavior similar to single component systems.

Introduction

Surface tension is a prime parameter in the basic formulation of a large number of processes including nucleation and cluster formation. The work of formation of a critical-size nucleus is proportional to the surface tension to the power three(1). The solute clustering in supersaturated solutions and concentration gradients in a vertical column of a supersaturated solution may also depend on the surface tension of nano-particles(2). In addition to applications in nucleation and solute clustering in supersaturated solutions, there is a wide interest in the important role of surface tension in determining the behavior of small droplets and bubbles including oil recovery processes. For a long time it has been recognized that when a cluster of a new phase is small (that is, has a high curvature), the surface tension is size-dependent (that is, curvature dependent).

In an early paper, Tolman derived the expression for the effect of droplet size on surface tension in a single-component system(3,4). A key parameter in Tolman's work is the parameter d, the distance between the surface of tension and the equimolecular dividing surface. For a plane surface of separation, Tolman computed d for a variety of substances, including water(3). His results show that the distance d is positive and of the order of 1 to 3.5 Å (of the order of the intermolecular distances in liquids) for pure substances over the range of conditions studied.

Since the early work of Tolman, a large number of investigators have studied the curvature dependence of surface tension and nucleation theory. There is generally consensus that the curvature dependence of surface tension may indeed result in significant variation of the work of formation of the critical nucleus(5) and the nucleation rate(6,7). However, there is widespread

confusion and controversy in the literature on the effect of curvature on the surface tension of a bubble and a droplet in single component systems. Defay and Prigogine(9) provide results for the effect of curvature on the surface tension of water at 18 ºC for both bubbles and droplets. Their results show an increase of the surface tension with increasing curvature for a bubble whereas there is a decrease of surface tension with increasing curvature for a droplet (see Table 15.7 of Defay and Prigogine(9). On the other hand, Kashchiev(9) presents results for water bubbles at 583 K and droplets at 293 K, both decreasing with increasing curvature (see Fig. 6.1 of Kashchiev(1)). Kashchiev used a positive value of d of 1 Å for water droplets and bubbles. Another example is the work of Hadjiagapiou(10), which provides results from density functional theory showing an increase of the surface tension for a droplet with increasing curvature, followed by a decrease at very high curvatures. Guermeur, Biquard and Jacolin(11) have also studied the effect of curvature on the surface tension for nitrogen bubbles and droplets. Their results show that the surface tension in the bubble decreases with increasing curvature. It has a non-monotonic behavior in the droplet. On the other hand, as was stated earlier, many authors predict that the surface tension in, for example, a droplet, should decrease rapidly with the radius (see for example Lee, Gama and Gubbins(12), and the references therein). In a different approach presented in Ref. 13, Schmelzer and Baidakov argue that the Gibbs method for determining the reference states for the description of bulk properties of the critical nucleus does not give a correct description of the bulk properties of the critical clusters at high supersaturation. They postulate that at a non-equilibrium state, the chemical potentials of the interface and the ambient phase (in their terminology, this is, the bulk phase other than the cluster bulk phase) are the same. They also make other postulations and obtain new expressions, including a new expression for the pressure difference between the cluster phase and the other

bulk phase given by $p_a - p_b = 2s / R_+ + r_a (m_a - m_b)$ where p is the pressure, r is the density, m is the chemical potential, s is the surface of tension, and R_+ is the radius of the critical cluster (or critical nucleus); a is the cluster phase, and b is the ambient phase. All pertain to a critical cluster. (We are using nomenclature from Ref. 13; later, we will use our own.) Obviously, the expression for $(p_a - p_b)$ from Ref. 13 is different from the Laplace equation given by $p_a - p_b = (2s / R_+)$. When the work from Ref. 13 is used, the surface tension both for a bubble and for a droplet decrease with curvature and approach zero at the spinodal. For a droplet, first there is a slight increase (not noticeable) followed by a decrease with curvature. The work of critical cluster also approaches zero at the spinodal. We will get back to this point later.

Most of the work on curvature dependence of the surface tension is limited to single components. Schmelzer et al.(5) have developed an empirical relation for d in multicomponent systems for a droplet. In a more recent work, Baidakov, Boltashev, and Schmelzer(14), use an approach based on Ref. 13 to study the effect of curvature on surface tension in mixtures. The results show that similar to a single component system, the surface tension vanishes at the spinodal for a two-component mixture. In this work, we present results to show that there are differences in surface tension curvature dependency of pure components and multicomponent systems.

The purpose of this work is to derive the expressions for the curvature dependence of the surface tension for bubbles and droplets in both single and multicomponent systems. The derivations are based on the general expressions from classical thermodynamics using the work of Gibbs. We

use an equation of state to describe the bulk gas and liquid phase properties. Therefore, there is no need to make assumptions regarding compressibility and compositional effects.

In the following, we first derive basic thermodynamic relations for the curvature dependence of the surface tension using a new simple approach. Then we apply the derived expressions coupled with a surface tension model to obtain the basic expressions for bubbles and droplets in single-component systems. Next, the basic expressions in multicomponent systems, also for both bubbles and droplets, are obtained. In the above two sections we provide numerical examples. At the end we make several concluding remarks.

THERMODYNAMIC RELATIONS FOR THE CURVATURE DEPENDENCE OF SURFACE TENSION

The two fundamental equations that form the basis of this work can be directly obtained from the basic postulates of thermodynamics and have been derived in Ref. 15. The first equation is the *Gibbs adsorption equation* that, for a multicomponent system with a spherical interface can be written as(15):

$$d\sigma = -s^s\, dT - \sum_{i=1}^{c} G_i\, d\mu_i^s + \left[\frac{\partial \sigma}{\partial a}\right] da \qquad (1)$$

In this expression, σ is the surface tension, s^s is the entropy per unit area of the interface (the superscript s denotes a surface property) G_i and m_i^s are, respectively, the number of moles per

unit area and chemical potential of component i in the interface, c is the number of components, a is the radius of the interface and $[\partial s/\partial a]$ represents the change in the surface tension when the mathematical diving surface between the two phases is displaced. The particular dividing surface for which $[\partial s/\partial a]=0$ is called the *surface of tension*. Throughout this work, all properties referred to the surface of tension are identified with the subscript s. The second key equation mentioned above relates the surface tension to the radius of the interface and can be written as(15):

$$\left(\frac{\partial \ln s_s}{\partial \ln a_s}\right)=2\left(\frac{d}{a_s}\right)\frac{1+(d/a_s)+(1/3)(d/a_s)^2}{1+2(d/a_s)[1+(d/a_s)+(1/3)(d/a_s)^2]} \tag{2}$$

Note that in the above equation, the derivative is taken along a path where the temperature and composition of the continuous bulk phase are held constant (we refer to the small bulk phase as the cluster phase in the work). The parameter d is the distance between two dividing surfaces: one is the surface of tension and the other is the dividing surface defined by:

$$\sum_{i=1}^{c}\Gamma_i\tilde{v}_i^a=0 \tag{3}$$

where $\tilde{v}_i^a$ is the partial molar volume of component i in the continuous bulk phase (denoted by the superscript a). Parameters and properties referred to the dividing surface defined by Eq. 3 will be identified by the subscript v. The parameter d is given by:

$$d = a_v - a_s \tag{4}$$

One of the most challenging tasks in the past has been the estimation of d. Some authors have made calculations to show that d for a flat interface is positive, some others suggest that it is negative, and there is a third group who estimate d to be zero for a flat interface. The implication for d being zero for a flat interface is that there is no adsorption at the interface. The d parameter for a flat interface may also have different signs in a bubble and in a droplet (see Ref. 16 and references therein). Our goal in this work is to find a suitable approach in predicting this parameter. To achieve this goal, we need to find a clearer relation between d and other properties of the system.

The total volume of the two-phase system based on the dividing surface defined by Eq. 3 can be expressed as:

$$V = V_v^a + V_v^b = \sum_{i=1}^{c} N_{i,v}^a \tilde{v}_i^a + \sum_{i=1}^{c} N_{i,v}^b \tilde{v}_i^b \tag{5}$$

where N_i is the number of moles of component i. We have introduced the superscript b to identify the cluster phase. Using the mass balance of component i to eliminate $N_{i,v}^a$ from Eq. 5 we obtain:

$$V = \sum_{i=1}^{c} N_i \tilde{v}_i^a + \sum_{i=1}^{c} N_{i,v}^b \left(\tilde{v}_i^b - \tilde{v}_i^a \right) \tag{6}$$

In Eq. 6 we have used Eq. 3 to eliminate the amounts of adsorption at the interface. The total volume of the two-phase system based on the surface of tension leads to:

$$V = \sum_{i=1}^{c} N_i \tilde{v}_i^a + \sum_{i=1}^{c} N_{i,s}^b \left(\tilde{v}_i^b - \tilde{v}_i^a \right) - A_s \sum_{i=1}^{c} G_{i,s} \tilde{v}_i^a \tag{7}$$

In Eq. 7 A_s is the surface area of the interface. Equating the right-hand sides of Eqs. 6 and 7 and simplifying we obtain:

$$V_v^b - \sum_{i=1}^{c} N_{i,v}^b \tilde{v}_i^a = V_s^b - \sum_{i=1}^{c} N_{i,s}^b \tilde{v}_i^a - A_s \sum_{i=1}^{c} G_{i,s} \tilde{v}_i^a \tag{8}$$

Introducing the molar concentrations c_i and rearranging we obtain:

$$V_v^b = V_s^b - \frac{A_s \sum_{i=1}^{c} G_{i,s} \tilde{v}_i^a}{1 - \sum_{i=1}^{c} c_i^b \tilde{v}_i^a} \tag{9}$$

The equation above provides a relationship between the sizes of the cluster calculated for the two dividing surfaces. It can be written in terms of the radii as:

$$a_v = a_s^{2/3}\left(a_s - \frac{3\sum_{i=1}^{c} G_{i,s}\tilde{v}_i^a}{1-\sum_{i=1}^{c} c_i^b \tilde{v}_i^a} \right)^{1/3} \tag{10}$$

Combining Eqs. 4 and 10 we obtain:

$$\frac{d}{\mathrm{a_s}} = \left(1 - \frac{3}{a_s}\frac{\sum_{i=1}^{c} G_{i,s}\tilde{v}_i^a}{1-\sum_{i=1}^{c} c_i^b \tilde{v}_i^a} \right)^{1/3} - 1 \tag{11}$$

which provides d. For studying the curvature dependence of the surface tension, one may rearrange Eq. 11 to:

$$d\left[\frac{1}{3}\left(\frac{d}{\mathrm{a_s}} \right)^2 + \frac{d}{a_s} + 1 \right] = \frac{-\sum_{i=1}^{c} G_{i,s}\tilde{v}_i^a}{1-\sum_{i=1}^{c} c_i^b \tilde{v}_i^a} \tag{12}$$

Equation 12 relates d to the properties of the two-bulk phases and the interface for a multicomponent system. For a single-component system, Eq.12 simplifies to:

$$d\left[\frac{1}{3}\left(\frac{d}{\mathrm{a_s}} \right)^2 + \frac{d}{a_s} + 1 \right] = \frac{G_s}{?^{ß} - ?^a} \tag{13}$$

where r is the molar density. Tolman(4) derived Eq. 13 using an integral approach; we use the relationships from classical thermodynamics in our derivation. Note that one may not use Eq. 13 to generalize it to multicomponent mixtures without certain assumptions (5). Substituting Eq. 12 into Eq. 2 we find an equation for the curvature dependence of the surface tension that does not include d:

$$\left(\frac{\partial \ln s_s}{\partial \ln a_s}\right) = \frac{2\sum_{i=1}^{c} G_{i,s}\tilde{v}_i^a}{2\sum_{i=1}^{c}\Gamma_{i,s}\tilde{v}_i^a - a_s\left(1-\sum_{i=1}^{c} c_i^b\,\tilde{v}_i^a\right)} \tag{14}$$

Note that in the above equation the problem has shifted from obtaining the parameter d to obtaining the amounts of adsorption of the components at the interface. To proceed further, we relate the surface tension to the properties of both phases to obtain the sum that includes the amounts of adsorption.

The sum in Eq. 14 that contains the amounts of adsorption can be related to the surface tension by combining Gibbs adsorption equation and the chemical equilibrium conditions. Writing Eq. 1 for the surface of tension and replacing the surface chemical potentials by the chemical potentials in the bulk continuous phase we obtain:

$$ds_s = -s_s^s\,dT - \sum_{i=1}^{c} G_{s,i}\,d\mu_i^a \tag{15}$$

The differential of the chemical potentials of the continuous bulk phase can be expressed as:

$$d\mu_i^a = -\tilde{s}_i^a\, dT + \tilde{v}_i^a\, dP^a + \sum_{j=1}^{c-1}\left(\frac{\partial \mu_i^a}{\partial x_j^a}\right)_{T,P^a,x_{k\neq j,c}^a} dx_j^a \qquad i = 1,..,c \tag{16}$$

where x represents the mole fraction. Substituting Eq. 16 into Eq. 15 we find:

$$ds_s = \left(-s_s^s + \sum_{i=1}^{c} G_{i,s}\tilde{s}_i^a\right)dT - \left(\sum_{i=1}^{c} G_{i,s}\tilde{v}_i^a\right)dP^a - \sum_{j=1}^{c-1}\left[\sum_{i=1}^{c} G_{i,s}\left(\frac{\partial \mu_i^a}{\partial x_j^a}\right)_{T,P^a,x_{k\neq j,c}^a}\right]dx_j^a \tag{17}$$

Which leads to:

$$\left(\frac{\partial s_s}{\partial P^a}\right)_{T,x_i^a} = -\sum_{i=1}^{c} G_{i,s}\tilde{v}_i^a \tag{18}$$

Equation 18 is the sought relationship. Providing a model for the surface tension as a function of the properties of both phases, Eqs. 14 and 18 can be combined to evaluate the curvature dependence of the surface tension. In the following two sections we will present the methodology first for single-component and then for multicomponent systems.

SINGLE-COMPONENT SYSTEMS

For a single-component system Eq. 14 simplifies to:

$$\left(\frac{\partial \ln s_s}{\partial \ln a_s}\right) = \frac{2G_s}{2G_s - a_s\left(?^{a} - ?^{ß}\right)} \tag{19}$$

Also, Eq. 18 becomes:

$$\left(\frac{\partial s_s}{\partial P^{a}}\right)_T = \frac{-G_s}{?_s} \tag{20}$$

To proceed further we desire an equation for the equilibrium surface tension. For a single-component system, the well-known Macleod-Sugden equation for the surface tension of a flat interface(17-19) can be used:

$$s_{\infty}^{1/4} = ?\left(?^{L} - ?^{V}\right) \tag{21}$$

In Eq. 21, s_{∞} is the surface tension of the flat interface, $?$ is the parachor and the superscripts L and V denote liquid and vapor, respectively. Equation 21 provides the surface tension of non-polar fluids with a remarkable accuracy over a wide range of temperature conditions(20) and although it was introduced empirically(17,18), it was later derived theoretically(19). In what follows we will use two different approaches: we assume that Eq. 21, 1) is valid for large values of the interface radius and obtain the limiting dependence of d for a flat interface (that is, d_{∞}); then assume that d is constant to obtain the curvature dependence of the surface tension, and 2) applies to a surface with a curved interface, which implies that d can change with curvature.

The assumptions have to be examined for their validity. Let us use the terms "d_∞ model" and "$?$ model" to refer to the two methods.

It turns out that in either approach it will be necessary to obtain d as a function of curvature assuming that Eq. 21 is valid for a curved interface. For the d_∞ model we will take the limit as the interface radius tends to infinity. Thus, we will replace s_∞ by s_s in Eq.21. Let us first consider a bubble in a continuous bulk liquid phase and replace L and V in Eq. 21 by a and b, respectively. The expression for surface tension will take the form:

$$s_s^{1/4} = ?\left(r^a - r^b\right) \tag{22}$$

The droplet in a continuous bulk vapor phase will be considered later. Substituting Eq.22 into Eq. 20 we obtain:

$$G_s = 4?\,?^a s_s^{3/4}\left[\left(\frac{\partial r^b}{\partial P^a}\right)_T - \left(\frac{\partial r^a}{\partial P^a}\right)_T\right] \tag{23}$$

The second derivative in the square bracket in Eq. 23 is given by:

$$\left(\frac{\partial r^a}{\partial P^a}\right)_T = r^a C_T^a \tag{24}$$

where C_T^a is the isothermal compressibility of phase a, which can be readily obtained from an equation of state. Next we find an expression for the first derivative in Eq. 23. From the chain rule we write:

$$\left(\frac{\partial r^b}{\partial P^a}\right)_T = \left(\frac{\partial r^b}{\partial P^b}\right)_T \left(\frac{\partial P^b}{\partial P^a}\right)_T = r^b C_T^b \left(\frac{\partial P^b}{\partial P^a}\right)_T \tag{25}$$

The derivatives in Eq. 25 are taken along an equilibrium path. Therefore we can write:

$$\left(\frac{\partial m^a}{\partial P^a}\right)_T = \left(\frac{\partial m^b}{\partial P^a}\right)_T = \left(\frac{\partial m^b}{\partial P^b}\right)_T \left(\frac{\partial P^b}{\partial P^a}\right)_T \tag{26}$$

Replacing the derivatives of the chemical potentials with respect to the pressure of their respective phases by the inverse of the molar densities, we obtain:

$$\left(\frac{\partial P^b}{\partial P^a}\right)_T = \left(\frac{r^b}{r^a}\right) \tag{27}$$

Combining Eqs. 23, 24, 25 and 27 we get:

$$G_s = 4?\, s_s^{3/4} \left[(r^b)^2 C_T^b - (r^a)^2 C_T^a \right] \tag{28}$$

Equations 22 and 28, together with an equation of state, allow the calculation of the amount of adsorption at the surface of tension. For the d_∞ model, we will use Eq. 28 to obtain the limiting value of d as the radius of the interface goes to infinity. Substituting Eq. 28 into Eq. 13 and taking the limit as $a_s \to \infty$ we obtain:

$$\left(\frac{\partial \ln s_s}{\partial \ln a_s}\right) = \frac{8? s_s^{3/4}\left[\left(?^{ß}\right)^2 C_T^{ß} - \left(?^{a}\right)^2 C_T^{a}\right]}{8? s_s^{3/4}\left[\left(?^{ß}\right)^2 C_T^{ß} - \left(?^{a}\right)^2 C_T^{a}\right] - a_s\left(?^{a} - ?^{ß}\right)} \tag{30}$$

Equation 30 can be integrated numerically to compute the curvature dependence of the surface tension. In Figure 1 we show the surface tension s_s as a function of the radius of the surface of tension for a bubble of n-pentane at 310.9 K using the two models. The Peng-Robinson equation of state(21) and the standard 4-th order Runge-Kutta method were employed for calculations in Figure 1 and similar calculations to be presented later. The parachor of n-pentane was taken as 230. From this graph we note that: 1) the surface tension is constant down to $a_s \approx 100$ nm , and 2) the $?$ model predicts a sharper variation of the surface tension with curvature for $a_s < 10$ nm ; the difference between the two models increases as the radius decreases. Figure 2 shows the variation of d with curvature as predicted by the $?$ model. In this figure, it is clear too that there is almost no difference between the two models for sizes down to $a_s \approx 10$ nm , but as the radius decreases further, d grows sharply, which accounts for the steeper variation of the surface tension predicted by this model at larger curvatures. This change in d can be explained by the fact that the pressure, and thus the densities, starts changing much faster at these large

curvatures. Ref. 22 provides results similar to Figure 2 based on the semi-empirical van der Waals/Cahn-Hilliard theory. Note that d vs. the radius is positive in Figure 2.

For a droplet in a continuous vapor phase, it is necessary to exchange the superscripts a and b in Eq. 22. Repeating the procedure we used for a bubble we obtain, for the limiting value of d for a flat interface:

$$d_\infty = 4?\, s_\infty^{3/4} \frac{\left(r^a\right)^2 C_T^a - \left(r^b\right)^2 C_T^b}{r^b - r^a} \tag{31}$$

Note that the above expression for d_∞ in a droplet is different from the expression derived in Ref. 16. There is no need to assume that density or volume can be expanded linearly with pressure. There is also no need for other assumptions except a need for a general expression for s_∞. According to Eq. 31, even when $C_T^a = 0$, d_∞ may not be zero. Substituting d_∞ from Eq. 31 into Eq. 2 and integrating we obtain the variation of s_s with curvature for the d_∞ model. For the constant-$?$ model, we obtain:

$$\left(\frac{\partial \ln s_s}{\partial \ln a_s}\right) = \frac{8?\, s_s^{3/4}\left[\left(?^a\right)^2 C_T^a - \left(?^ß\right)^2 C_T^b\right]}{8?\, s_s^{3/4}\left[\left(?^a\right)^2 C_T^a - \left(?^ß\right)^2 C_T^b\right] - a_s\left(?^a - ?^ß\right)} \tag{32}$$

Figure 3 shows the variation of the surface tension with the radius of the surface of tension using the two models for a droplet of n-pentane at 310.9 K. For a droplet the difference between the

d_∞ model and the ? model is more pronounced: for the d_∞ model, the surface tension increases monotonically with decreasing radius whereas the ? model predicts that the surface tension will go through a maximum at an approximate radius of 1.1 nm and then decreases rapidly with decreasing radius. Hadjiagapiou(10) and Guermeur et al.(11) have predicted a similar non-monotonic behavior. Figure 4 shows the variation of d with curvature as predicted by the ? model, where the variation of d with curvature is similar to that of the bubble, being almost constant at small curvatures and then growing fast as the radius decreases. However, d_∞ is negative for the droplet and d changes sign and causes the surface tension to go through a maximum. A negative value for d_∞ in a droplet has been presented in Refs. 16 and 22 using different approaches. In Ref. 16, d_∞ is approximated by $-C_T^a s_\infty / 3$ based on a number of assumptions. Based on another set of assumptions(6) $d_\infty \approx -C_T^a s_\infty$. Ref. 22 also discusses the difference between the density function (DF) approach in predicting a negative d_∞ and the molecular dynamics (MD) simulations which predicts a position d_∞ for a droplet.

Note that, for a single-component system, the dividing surface defined by Eq. 3 is the same regardless of which phase is selected to be phase a. Thus, the absolute value of d_∞ obtained as the limit for the bubble will be the same as that obtained for the droplet, only with opposite sign. The change in sign is due to the fact that in the bubble the distances are measured from the gas side and in a droplet they are measured from the liquid side (see Eq. 29). However, for a multicomponent system, this is not the case because the dividing surface defined by Eq. 3 is different for different choices of the phase a since the two phases have different partial molar volumes (to be shown later). Thus, the limiting value d_∞ obtained using the equations for a

bubble may be different from that obtained with the equations for a droplet not only in sign, but also in magnitude. To avoid ambiguity, in the discussion for multicomponent systems we will use the symbols d_{∞}^{b} for the former and d_{∞}^{d} for the latter.

The results shown above for the curvature dependency of surface tension in bubbles and droplets have similar trends to those of Guermeur et al.(11) and Hadjiagapiou(10). Figure 5 shows a comparison between the results of Guermeur et al. for bubbles of nitrogen at 77.3 K and the results for the same system obtained with our ? model (nitrogen parachor of 52 was used in our calculations based on surface tension data for nitrogen). Figure 6 shows the same comparison for a droplet of nitrogen at the same temperature. In both figures we observe that the trends predicted by our model and the work of Guermeur et al. are the same, although the two models are very different. Guermeur et al. describe the inhomogeneous fluid in the interface using a stress tensor in the frame of gradient theory, and predict a sharper variation of the surface tension with curvature for the bubbles and a smaller variation for the droplets. Although they also obtain a maximum in the surface tension plot for the droplet, the maximum is at a smaller curvature and the corresponding surface tension is also smaller. The results for our d_{∞} model (not shown) are farther from their results in both cases.

In order to compare with Hadjiagapiou's results, we computed the surface tension as a function of curvature for a droplet of Argon at a reduced temperature of 0.8 (argon parachor of 52 was used in our calculations). Argon was chosen for comparison because it is a substance well suited for Hadjiagapiou's treatment of thermodynamic properties. The results, in terms of the reduced variables defined in his work, are shown in Figure 7. In this case, our ? model predicts a

smaller variation of the surface tension with curvature than Hadjiagapiou's model, however our ? model predicts a smaller droplet radius for the maximum surface tension. In view of the simplicity of our model, it is interesting to note that its predictions are close to those of Hadjiagapiou, which is based on density functional theory.

Before proceeding to multicomponent system, we would like to point out a deficiency in regard to the work of critical cluster formation at the spinodal (that is, at the limit of stability). The work of critical cluster formation is expected to vanish as we approach the spinodal. In the classical theory of nucleation, the barrier height approaches a finite value at the spinodal, which is not correct[23]. When one accounts for the effect of curvature on the surface tension, the work of critical cluster formation at the spinodal reduces, but may not vanish. This is to be expected because of extremely small size of the clusters, comprised of say some 40 atoms, at the spinodal. Instead of using classical thermodynamics, one may use statistical or molecular thermodynamics for very small clusters (that is, at very high supersaturation) to account for non-classical effects[23]. In our approach, similar to Guermeur et al.(11), the surface tension for a droplet is greater than the flat interface for large droplets but becomes smaller for smaller droplets. For bubbles, the surface tension remains less than s_∞. These results are consistent with work of Ref. 23, that classical and non-classical barrier heights cross from droplet formation but do not for bubble formation.

Schmelzer and coworkers, in a different approach, as we stated earlier, use certain postulations which lead to a vanishing of the critical cluster formation at the spinodal, as well as the vanishing of the surface tension (Ref. 13 and references within).

Figure 8 shows the plot for the work of critical cluster formation (in dimensionless units) vs. a_s in a bubble of n-pentane at 310.9 K. Note that as the spinodal is approached, W/kT decreases. Despite a small W of about 1.5 kT, it does not vanish at the spinodal. The droplet has also a similar behavior. The work of critical cluster formation for the Argone bubble at the spinodal (for $T_r = 0.8$) is about 2.5 kT, which is not far from kT.

MULTICOMPONENT SYSTEMS

For multicomponent systems we follow an approach similar to that of single-component systems. Weinaugh and Katz have extended Eq. 21 to multicomponent systems(24,25):

$$s_{\infty}^{1/4} = \sum_{i=1}^{c} ?_i \left(c_i^L - c_i^V \right) \tag{33}$$

The above equation provides good predictions in non-polar multicomponent hydrocarbon mixtures(18,20,21). In order to apply Eq. 33 to obtain the curvature dependence of the surface tension, we will follow an approach similar to the one used in the previous section. Again, we will explore two options: 1) assume that Eq. 33 is valid for curved interfaces with a very large radius, use it to obtain the limiting value d_{∞} for the flat interface and then use d_{∞} to integrate Eq. 2, and 2) assume that Eq. 33 is valid for a curved interface, thus allowing for d to vary with curvature. To keep the terminology used in section III, we will call the first approach the "d_{∞} model" and the second the "$?$ model".

Similar to a single-component system, we need to find an expression for d as a function of curvature assuming that Eq. 33 is valid for a curved interface. For the d_∞ model we will take the flat interface limit in the resulting expression. Thus, we will replace s_∞ by s_s in Eq. 33. First we will consider a bubble in a continuous bulk liquid phase and replace L and V in Eq. 21 by a and b, respectively. With the altered notation, Eq. 33 takes the form:

$$s_s^{1/4} = \sum_{i=1}^{c} ?_i \left(c_i^a - c_i^{ß} \right) \tag{34}$$

Substituting Eq. 34 into Eq. 18 leads to:

$$\sum_{i=1}^{c} G_{i,s} \tilde{v}_i^a = 4 s_s^{3/4} \sum_{i=1}^{c} ?_i \left[\left(\frac{\partial c_i^{ß}}{\partial P^a} \right)_{T,x_j^a} - \left(\frac{\partial c_i^a}{\partial P^a} \right)_{T,x_j^a} \right] \tag{35}$$

As in Eq. 23, the second derivative inside the square bracket in Eq. 35 can be readily obtained from an equation of state:

$$\left(\frac{\partial c_i^a}{\partial P^a} \right)_{T,x_j^a} = C_T^b c_i^a \quad i = 1, \cdots, c \tag{36}$$

The first derivative, however, is more complicated to evaluate. Let us first write the differential of the variable c_i^b in two different ways: first as a function of the variables of phase b and then as a function of the variables of phase a :

$$dc_i^b = \left(\frac{\partial c_i^b}{\partial T}\right)_{P^b, x_j^b} dT + \left(\frac{\partial c_i^b}{\partial P^b}\right)_{T, x_j^b} dP^b + \sum_{j=1}^{c-1} \left(\frac{\partial c_i^b}{\partial x_j^b}\right)_{T, P^b, x_{k\neq j,c}^b} dx_j^b \quad i = 1, \cdots, c \tag{37}$$

$$dc_i^b = \left(\frac{\partial c_i^b}{\partial T}\right)_{P^a, x_j^a} dT + \left(\frac{\partial c_i^a}{\partial P^a}\right)_{T, x_j^a} dP^a + \sum_{j=1}^{c-1} \left(\frac{\partial c_i^b}{\partial x_j^a}\right)_{T, P^a, x_{k\neq j,c}^a} dx_j^a \quad i = 1, \cdots, c \tag{38}$$

Considering a process at constant temperature and composition of the phase a , which are the conditions for which Eq. 2 holds, and equating Eqs. 37 and 38 we obtain:

$$\left(\frac{\partial c_i^b}{\partial P^a}\right)_{T, x_j^a} dP^a = \left(\frac{\partial c_i^b}{\partial P^b}\right)_{T, x_j^b} dP^b + \sum_{j=1}^{c-1} \left(\frac{\partial c_i^b}{\partial x_j^b}\right)_{T, P^b, x_{k\neq j,c}^b} dx_j^b \quad i = 1, \cdots, c \tag{39}$$

Or, in terms of derivatives with respect to P^a :

$$\left(\frac{\partial c_i^b}{\partial P^a}\right)_{T, x_j^a} = \left(\frac{\partial c_i^b}{\partial P^b}\right)_{T, x_j^b} \left(\frac{\partial P^b}{\partial P^a}\right)_{T, x_j^a} + \sum_{j=1}^{c-1} \left(\frac{\partial x_j^b}{\partial P^a}\right)_{T, x_j^a} \left(\frac{\partial c_i^b}{\partial x_j^b}\right)_{T, P^b, x_{k\neq j,c}^b} \quad i = 1, \cdots, c \tag{40}$$

Half of the derivatives in the right-hand side of Eq. 40 can be directly obtained from an equation of state:

$$\left(\frac{\partial c_i^b}{\partial P^b}\right)_{T,x_j^b} = C_T^b c_i^b \quad i=1,\cdots,c \tag{41}$$

$$\left(\frac{\partial c_i^b}{\partial x_j^b}\right)_{T,P^b,x_{k\neq j,c}^b} = r^b\left[d_{ij} - d_{ic} + c_i^b\left(\tilde{v}_j^b - \tilde{v}_c^b\right)\right] \qquad i=1\cdots,c; \quad j=1,\cdots,c-1 \tag{42}$$

Equation 42 is obtained from the definition of $c_i^b = x_i^b r^b$ and the Gibbs-Duhem equation in terms of partial molar volumes (see problem 1.5 of Chapter I in Ref. 26). The symbol d in Eq. 42 is the Kronecker delta. Substituting Eqs. 41 and 42 into Eq. 40 we obtain:

$$\left(\frac{\partial c_i^b}{\partial P^a}\right)_{T,x_j^a} = (C_T)^b c_i^b\left(\frac{\partial P^b}{\partial P^a}\right)_{T,x_j^a} + r^b\left(\frac{\partial x_i^b}{\partial P^a}\right)_{T,x_i^a} + r^b c_i^b\sum_{j=1}^{c-1}\left(\tilde{v}_c^b - \tilde{v}_j^b\right)\left(\frac{\partial x_j^b}{\partial P^a}\right)_{T,x_j^a} \tag{43}$$

$$i=1,\cdots,c-1$$

And, for $i=c$:

$$\left(\frac{\partial c_i^b}{\partial P^a}\right)_{T,x_j^a} = b^b c_i^b\left(\frac{\partial P^b}{\partial P^a}\right)_{T,x_j^a} - r^b\sum_{j=1}^{c-1}\left(\frac{\partial x_j^b}{\partial P^a}\right)_{T,x_j^a} + r^b c_i^b\sum_{j=1}^{c-1}\left(\tilde{v}_c^b - \tilde{v}_j^b\right)\left(\frac{\partial x_j^b}{\partial P^a}\right)_{T,x_j^a} \tag{44}$$

However, from the sum condition of phase b:

$$\sum_{j=1}^{c-1}\left(\frac{\partial x_j^b}{\partial P^a}\right)_{T,x_j^a} = -\left(\frac{\partial x_c^b}{\partial P^a}\right)_{T,x_j^a} \tag{45}$$

Substituting Eq. 45 into Eq. 44 we obtain Eq. 43 with $i = c$. Thus, we can regard Eq. 43 as valid for all $i = 1, \cdots, c$. In order to use Eq. 43 we need to find the derivatives of the pressure and composition of phase b with respect to the pressure of phase a. We use an approach similar to the one used for the single-component system. Since the derivatives appearing in Eq.43 are taken in an equilibrium path, we use:

$$m_i^a = m_i^b \quad i = 1, \cdots, c \tag{46}$$

Differentiating Eq. 46 with respect to the pressure of phase a at constant temperature and composition of phase a we obtain:

$$\left(\frac{\partial m_i^a}{\partial P^a}\right)_{T,x_j^a} = \left(\frac{\partial m_i^b}{\partial P^a}\right)_{T,x_j^a} \quad i = 1, \cdots, c \tag{47}$$

The derivative on the left-hand side of Eq. 47 is the partial molar volume of component i in phase a. For the derivative in the right hand-side, one can write:

$$\left(\frac{\partial m_i^b}{\partial P^a}\right)_{T,x_j^a} = \left(\frac{\partial m_i^b}{\partial P^b}\right)_{T,x_j^b}\left(\frac{\partial P^b}{\partial P^a}\right)_{T,x_j^a} + \sum_{j=1}^{c-1}\left(\frac{\partial x_j^b}{\partial P^a}\right)_{T,x_j^a}\left(\frac{\partial m_i^b}{\partial x_j^b}\right)_{T,P^b,x_{k\neq j,c}^b} \quad i = 1, \cdots, c \tag{48}$$

The first derivative on the right-hand side is the partial molar volume of component i in phase b. Substituting Eq.48 into Eq. 47 we obtain:

$$\tilde{v}_i^{\,a} = \tilde{v}_i^{\,b}\left(\frac{\partial P^b}{\partial P^a}\right)_{T,x_j^a} + \sum_{j=1}^{c-1}\left(\frac{\partial x_j^b}{\partial P^a}\right)_{T,x_j^a}\left(\frac{\partial m_i^b}{\partial x_j^b}\right)_{T,P^b,x_{k\neq j,c}^b} \qquad i=1,\cdots,c \tag{49}$$

Multiplying Eq. 49 by x_j^b and taking the sum we find:

$$\sum_{j=1}^{c} x_j^b \tilde{v}_j^{\,a} = v^b\left(\frac{\partial P^b}{\partial P^a}\right)_{T,x_l^a} + \sum_{k=1}^{c-1}\left(\frac{\partial x_k^b}{\partial P^a}\right)_{T,x_l^a}\sum_{j=1}^{c} x_j^b\left(\frac{\partial m_j^b}{\partial x_k^b}\right)_{T,P^b,x_{l\neq k,c}^b} \tag{50}$$

where v is the molar volume. From the Gibbs-Duhem equation for phase b:

$$\sum_{j=1}^{c} x_j^b\left(\frac{\partial m_j^b}{\partial x_k^b}\right)_{T,P^b,x_{l\neq k,c}^b} = 0 \tag{51}$$

Combining Eqs.50 and 51 provides:

$$\left(\frac{\partial P^b}{\partial P^a}\right)_{T,x_j^a} = r^b\sum_{i=1}^{c} x_i^b\tilde{v}_i^{\,a} = \sum_{i=1}^{c} c_i^b\tilde{v}_i^{\,a} \tag{52}$$

Substituting Eq. 52 into Eq.49 leads to:

$$\sum_{j=1}^{c-1}\left(\frac{\partial x_j^b}{\partial P^a}\right)_{T,x_j^a}\left(\frac{\partial m_i^b}{\partial x_j^b}\right)_{T,P^b,x_{k\neq j,c}^b} = \tilde{v}_i^a - \tilde{v}_i^b \sum_{j=1}^{c} c_j^b \tilde{v}_j^a \quad i=1,\cdots,c \tag{53}$$

Note that, although Eq. 53 is valid for $i=1,\cdots,c$, only (c-1) of the equations are independent because we already used their sum to obtain Eq.52. The first (c-1) equations in Eq.53 can be used to obtain the derivatives of the compositions of phase b with respect to the pressure of phase a, provided we use an equation of state to obtain the derivatives of the chemical potentials with respect to the compositions in phase b.

Substituting Eqs. 36, 43 and 52 into Eq. 35:

$$\sum_{i=1}^{c} G_{i,s}\tilde{v}_i^a = -4s_s^{3/4}\sum_{i=1}^{c} ?_i\left[C_T^a c_i^a - C_T^b c_i^b \sum_{j=1}^{c} c_j^b \tilde{v}_j^a - r^b\left(\frac{\partial x_i^b}{\partial P^a}\right)_{T,x_i^a}\right. \tag{54}$$

$$\left. + r^b c_i^b \sum_{j=1}^{c} \tilde{v}_j^b \left(\frac{\partial x_j^b}{\partial P^a}\right)_{T,x_j^a}\right]$$

where the derivatives of the composition of phase b are obtained by solving the system of Eq. 53. For the d_∞ model we will substitute Eq.54 into Eq.12 and take the limit as $a_s \to \infty$ to obtain:

$$d_{\infty}^{b} = \frac{-4s_{\infty}^{3/4}\sum_{i=1}^{c} P_i \left[C_T^b c_i^b \sum_{j=1}^{c} c_j^b \tilde{v}_j^a + r^b \left(\frac{\partial x_i^b}{\partial P^a} \right)_{T,x_i^a} - r^b c_i^b \sum_{j=1}^{c} \tilde{v}_j^b \left(\frac{\partial x_j^b}{\partial P^a} \right)_{T,x_j^a} - C_T^a c_i^a \right]}{1 - \sum_{i=1}^{c} c_i^b \tilde{v}_i^a} \qquad (55)$$

Note that the superscript b indicates the limiting value for the bubble, as explained at the end of the previous section. For this model, d_{∞} will be regarded as independent of curvature. Substituting Eq. 55 into Eq .2 and integrating we can calculate the curvature dependence of the surface tension. For the ? model, Eq. 54 is substituted into Eq. 14 and the resulting equation is integrated numerically.

Figure 9 shows the variation of surface tension with the radius of the bubble in an equimolar liquid mixture of propane and n-octane at 300 K, using the d_{∞} and the ? models. The parachors in the surface tension model are: C_3, 150; nC_4, 200; nC_6; 300; nC_8, 400. The binary interaction parameters in the Peng-Robinson equation of state were taken as zero. The behavior shown is similar to that obtained for the single-component system. The variation in surface tension is only important for bubble sizes of less than 10 nm. The overall change in surface tension in the two-component system considered is smaller than in the single-component system. The variation of d with curvature for the ? model is shown in Figure 10, which is consistent with the variation of the surface tension.

The equations for a droplet in a continuous bulk vapor phase can be obtained by exchanging the a and b superscripts in Eq. 34 and repeating the above procedure. In the following equations a will refer to the vapor phase and b to the liquid phase:

$$\sum_{i=1}^{c} G_{i,s}\tilde{\nu}_i^a = 4s_s^{3/4}\sum_{i=1}^{c} ?_i\left[ß^a c_i^a - ß^ß c_i^ß \sum_{j=1}^{c} c_j^ß \tilde{\nu}_j^a - ?^ß\left(\frac{\partial x_i^ß}{\partial P^a}\right)_{T,x_i^a} + ?^ß c_i^ß \sum_{j=1}^{c}\tilde{\nu}_j^ß\left(\frac{\partial x_j^ß}{\partial P^a}\right)_{T,x_j^a}\right] \qquad (56)$$

The derivatives of the composition in Eq. 56 will be found by solving the system of Eq. 53. For the limiting value of d in a droplet:

$$d_\infty^d = \frac{4s_\infty^{3/4}\sum_{i=1}^{c} P_i\left[C_T^b c_i^b \sum_{j=1}^{c} c_j^b \tilde{\nu}_j^a + r^b\left(\frac{\partial x_i^b}{\partial P^a}\right)_{T,x_i^a} - r^b c_i^b \sum_{j=1}^{c}\tilde{\nu}_j^b\left(\frac{\partial x_j^b}{\partial P^a}\right)_{T,x_j^a} - C_T^a c_i^a\right]}{1-\sum_{i=1}^{c} c_i^b \tilde{\nu}_i^a} \qquad (57)$$

Comparison of Eqs. 55 and 57 reveals the sign difference as well as the phase identity differences. For the d_∞ model, we will substitute Eq. 57 into Eq. 2 and integrate to calculate the curvature dependence of the surface tension. For the $?$ model, Eq. 56 is substituted into Eq.14 and the result is integrated numerically.

Figure 11 shows the variation of the surface tension with the radius of the droplet in an equimolar gaseous mixture of propane and n-octane at 400 K. The same model as that of the bubble example was used. The behavior of the droplet in the multicomponent system is similar to

that of the single-component droplet. Figure 12, showing the variation of d as a function of curvature, indicates a stronger increase of d towards the high curvature region.

Figure 14 shows the behavior of the parameter d_{∞}^{b} (taking the liquid as the continuous bulk phase) as a function of temperature for an equimolar liquid mixture of propane and n-octane. The behavior is somewhat different from that observed in the single-component system; d_{∞}^{b} becomes negative at temperatures closer to the critical point. This is an important new result, showing that the surface tension for the bubble can either increase or decrease with curvature depending on the temperature; this may be the case for a large bubble. In Figure 13 we show the effect of composition at different temperatures on the parameter d_{∞}^{b}. At low temperatures and pressures, where the system can be regarded as ideal, d_{∞}^{b} increases monotonically with composition of propane, growing from the value for pure n-octane to the value for pure propane. At higher temperatures, the curve first decreases and then increases with composition. As the temperature increases towards the critical point, the curve becomes monotonically decreasing and d_{∞}^{b} for higher compositions of propane becomes negative. This shows that the surface tension increase or decrease with curvature depends not only on the temperature but also on the composition of the mixture – the increase for a large bubble. As the system approaches the limit of stability (that is, the spinodal), the behavior changes.

We have carried out some calculations for ternary systems; the behavior found is similar to that shown in figures 9-14. Since the features are similar to what we obtained for the binaries, we have not included the results for the sake of brevity.

CONCLUDING REMARKS

A rigorous thermodynamic model is presented for the effect of curvature on the surface tension in bubbles and droplets for both single and multicomponent systems. The results for the nonpolar hydrocarbon systems that we have studied reveal that:

(1) There is generally a decrease of surface tension in bubbles with increasing curvatures in single component systems. The distance parameter d for these systems is positive.

(2) For a droplet, if the distance parameter d is assumed constant and equal to the value for the flat interface, there is an increase in the surface tension with increasing curvature in single component systems. The distance parameter of the flat interface is generally negative. With a variable distance parameter model, the behavior of the surface tension is non-monotonic; the surface tension increases with curvature first and then decreases. The predicted results from our thermodynamic model with a variable distance parameter are in qualitative agreement with the work of Guermeur et al.(11) and the work of Hadjiagapiou(10) based on density functional theory. It is also in line with the work of Oxtoby and Evans(23).

(3) In multicomponent systems the distance parameter of the flat interface for a bubble may be either positive or negative depending on the temperature and composition. The surface tension may thus increase or decrease with curvature at different conditions for a large bubble.

(4) In both a bubble and in a droplet the surface of tension decreases for a small cluster from the $?$ model presented in the work. This is another evidence in support of the validity of the results from our $?$ model.

Acknowledgments

The work was supported by DOE DE-FC26-00BC15306, and member companies of Reservoir Engineering Research Institute.

References

(1) D. Kashchiev, *Nucleation*: *Basic Theory with Applications*, Butterworth Heinemann, Oxford, 2000.

(2) M.A. Larson and J. Garside, J. of Crystal Growth **76**, 88 (1986).

(3) R.C. Tolman, J. Chem. Phys. **17**, No. 2, 118 (1949a).

(4) R.C. Tolman, J. Chem. Phys. 333 (1949b).

(5) J.W.P. Schmelzer, I. Gutzow, and J. Schmelzer Jr., J. of Colloid and Interface Science **178**, 657 (1996).

(6) A. Laaksonen and R. McGraw, Europhys Letters **35**, No. 5, 367 (1996).

(7) R. McGraw and A. Laaksonen, J. Chem. Phys. **106**, No. 12, 5284 (March 1997).

(8) V. Baidakov, A. Kaverin, and G. Boltachev, J. Phys. Chem. B. **106**, No. 1, 167 (2002).

(9) R. Defay and J. Prigogine, *Surface Tension and Adsorption* ,Longman, London, 1966.

(10) I. Hadjiagapiou, J. Physics: Condens. Matter, **6**, 5303 (1994).

(11) R. Guermeur, F. Biquard, and C. Jacolin, J. of Chem. Phys. **82**, No. 4, 2040 (Feb. 1985).

(12) D.J. Lee, M.M. Telo da Gama, and K.E. Gubbins, J. Chem. Phys. **85**, No. 1, 490 (July 1986).

(13) J.W.P. Schmelzer and V.G. Baidakov, J. Phys. Chem. B., **105**, 11595 (2001).

(14) V.G. Baidakov, G. Sh. Boltashev, and J.W.P. Schmelzer, J. Coll. Int. Sciences, **231**, 312 (2000).

(15) Ono and Kondo, Encyclopedia of Physics, edited by S. Flugge **10**, 134 ,Springer, Berlin, 1960.

(16) L.S. Bartell, J. Phys. Chem. B, **105**, 11615 (2001).

(17) D.B. Macleod, Trans Faraday Soc. **19**, 38 (1923).

(18) S. Sugden, Ind. & Eng. Chem. **35**, 239 (Feb. 1943).

(19) R.H. Fowler, Proc. Royal Soc. of London, Series A, 229 (1937).

(20) B.E. Poling, J.M. Prausnitz, and J.P. O'Connell, *The Properties of Gases and Liquids* McGraw-Hill, 5th Ed., New York, 2001.

(21) D.Y. Peng and Robinson, Ind. Eng. Chem. Found. **15**, 59 (1976).

(22) L. Granasy, J. Chem. Phys., **109**, 22, 9660 (1998).

(23) D.W. Oxtoby and R. Evans, J. Chem Phys., **89**, 12, 7521 (Dec. 1988).

(24) C.F. Weinaugh and D.L. Katz, Ind. & Eng. Chem. **35**, 239 (Feb. 1943).

(25) A. Firoozabadi, D.L. Katz, H. Soroosh, and V.A. Sajjadian, SPE Reservoir Engineering, 265 (Feb. 1988).

(26) A. Firoozabadi, *Thermodynamics of Hydrocarbon Reservoirs*, McGraw-Hill, New York, 1999.

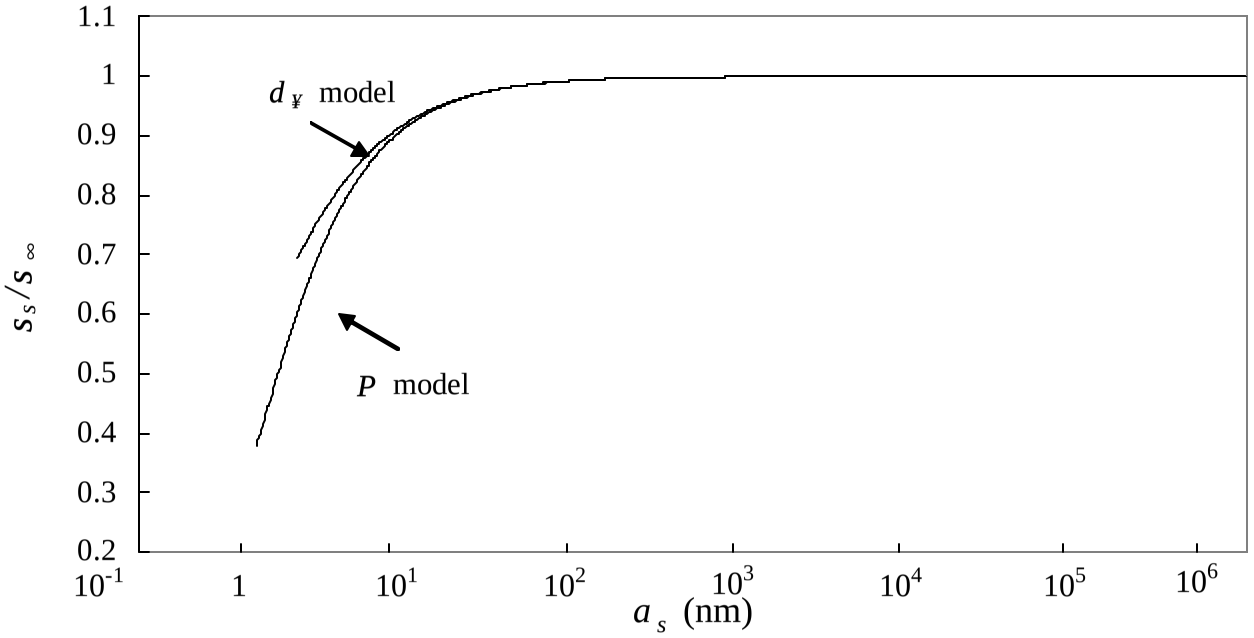

Fig. 1 Curvature dependence of the surface tension for a bubble of n-pentane at 310.9 K from the d_∞ and the ? models

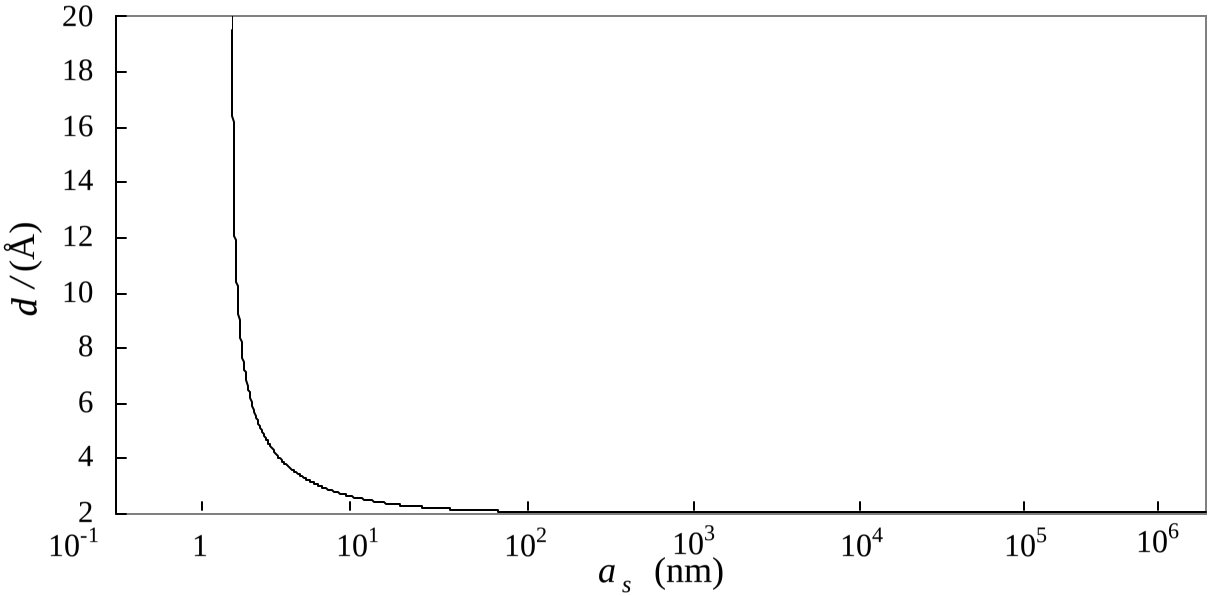

Fig. 2 Curvature dependence of the parameter *d* for the ? model in the n-pentane bubble example (*T*=310.9 K)

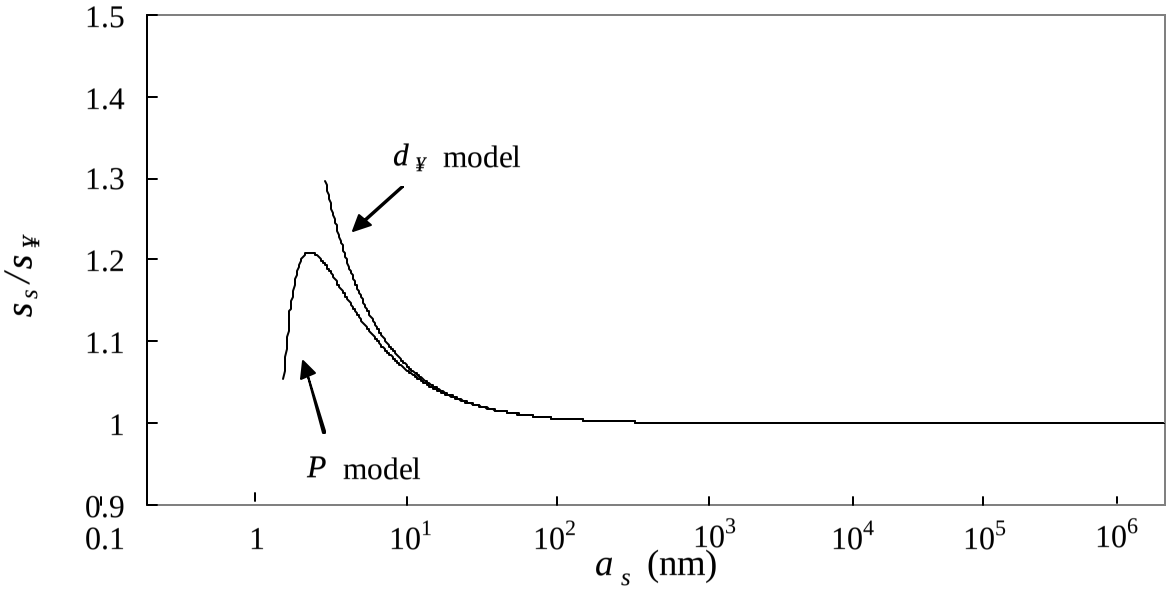

Fig. 3 Curvature dependence of the surface tension for a droplet of n-pentane at 310.9 K from the d_∞ and the ? models

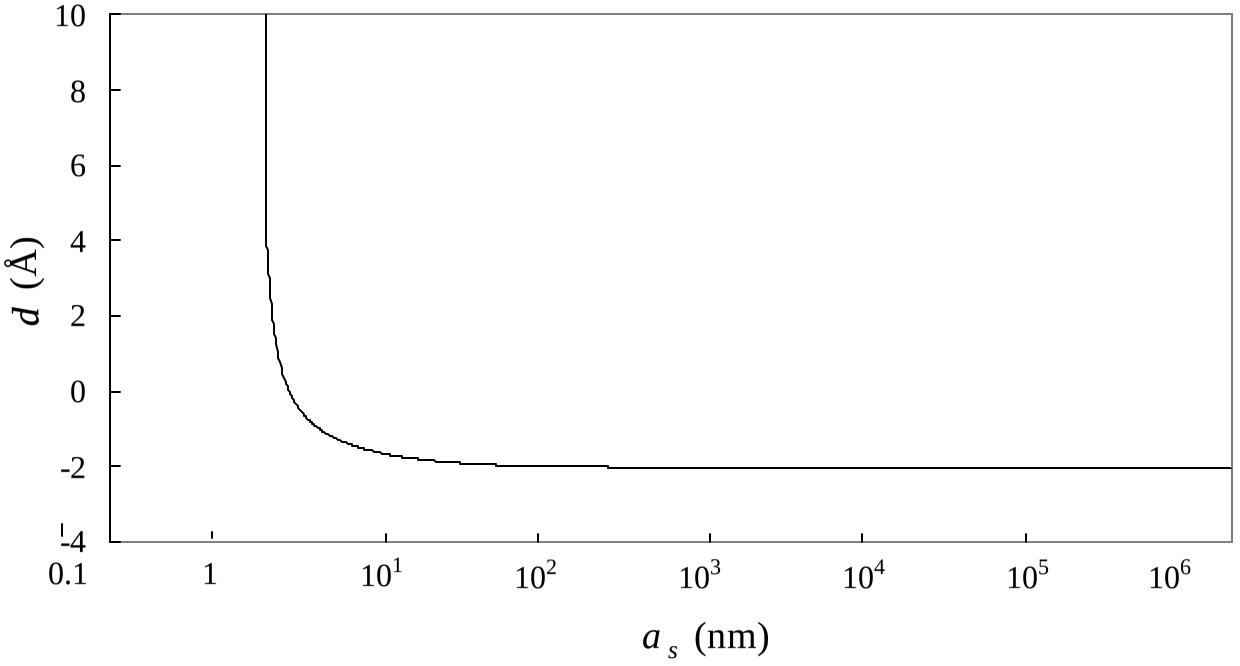

Fig. 4 Curvature dependence of the parameter d for the ? model in the n-pentane droplet example (T=310.9 K)

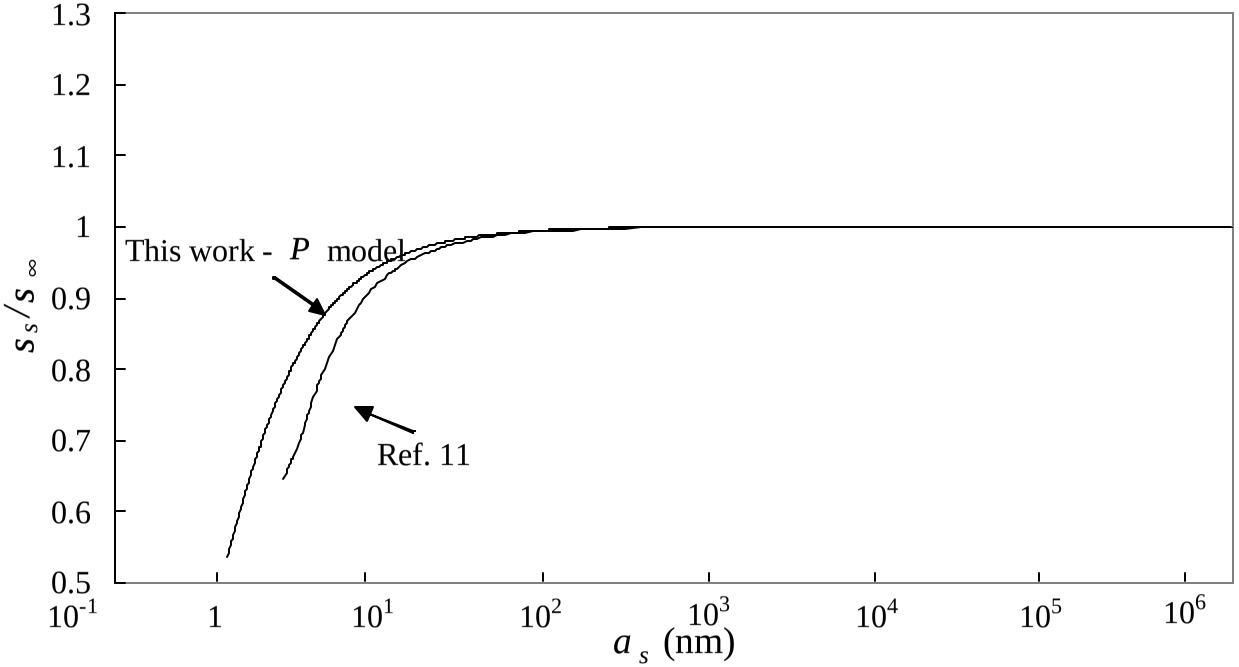

Fig. 5 Curvature dependence of the surface tension predicted by the ? model and the results from Ref. 11 for a nitrogen bubble at 77.3 K

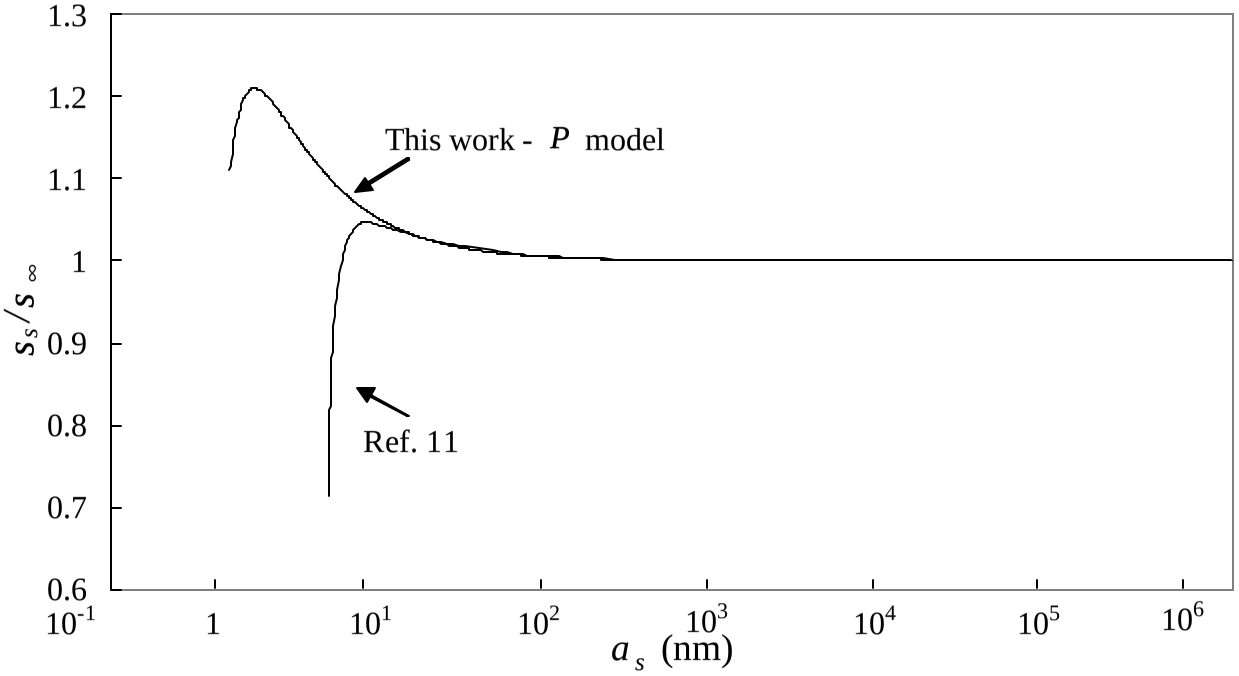

Fig. 6 Comparison between the curvature dependence of the surface tension predicted by the ? model and the results from Ref. 11 for a nitrogen droplet at 77.3 K

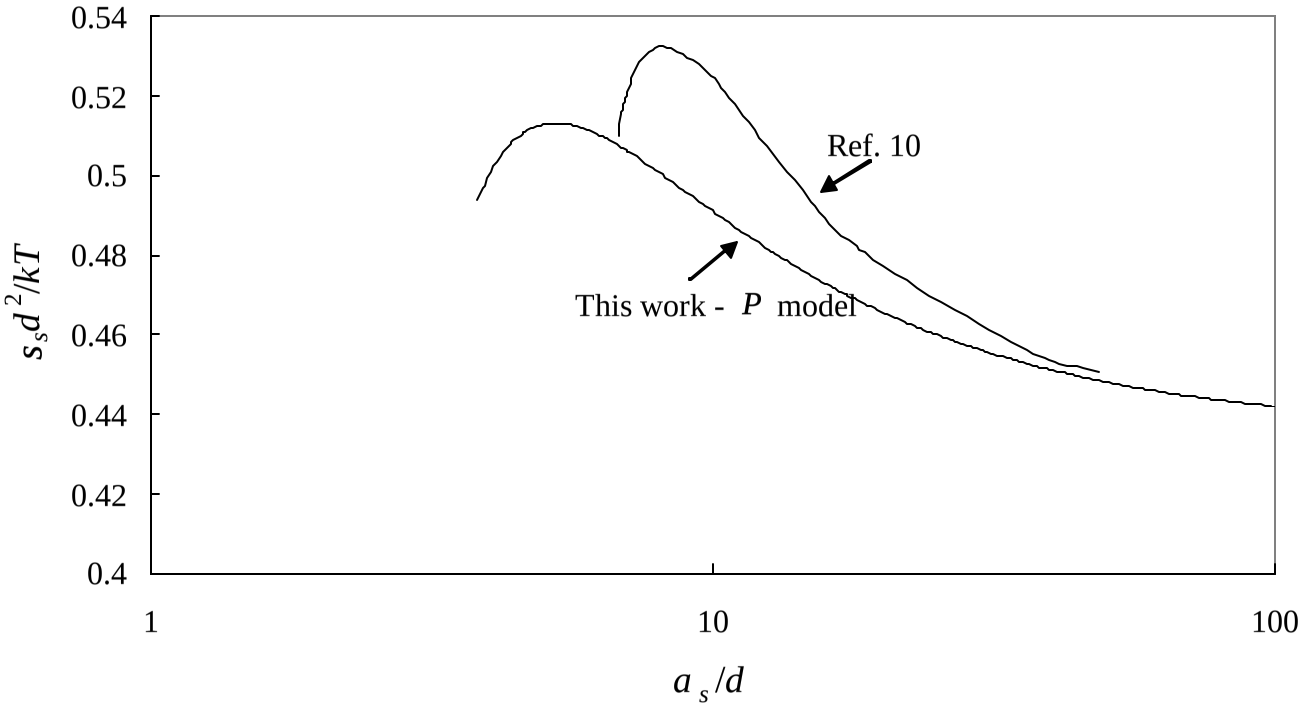

Fig. 7 Curvature dependence of the surface tension predicted by the ? model for Argon at a reduced temperature of 0.8 and the results from Ref. 11. The new variables appearing in the dimensionless groups plotted are *d* (molecular diameter) and *k* (Boltzmann's constant).

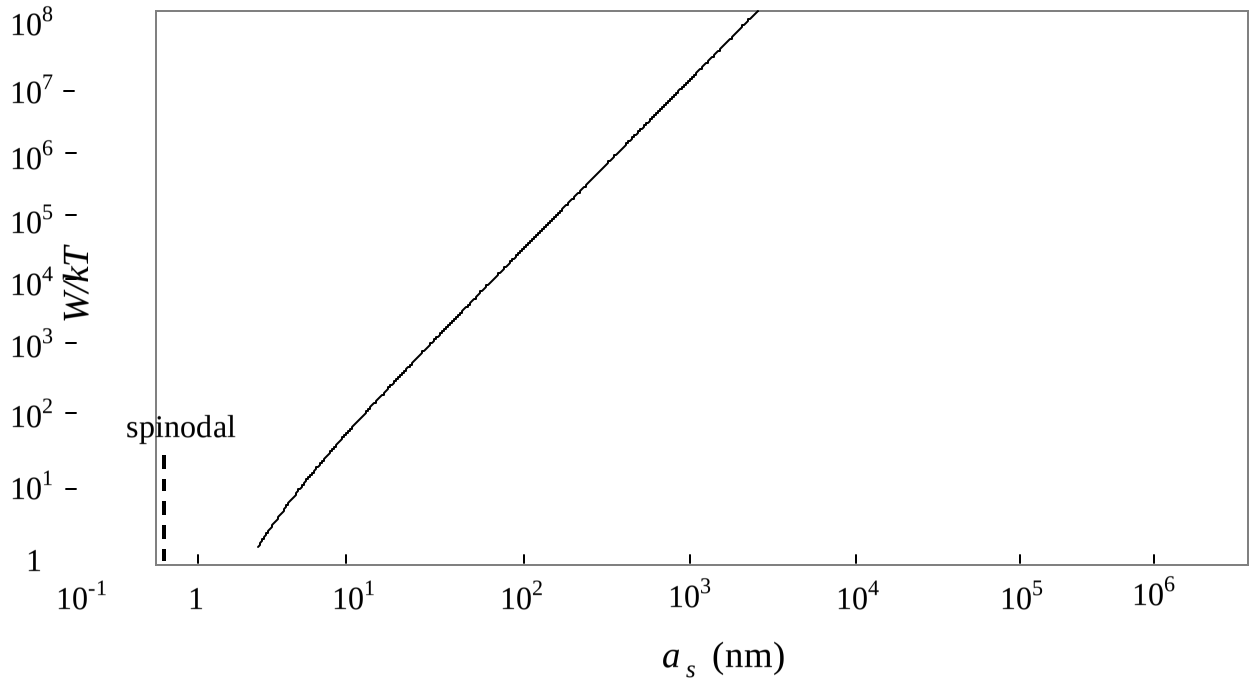

Fig. 8 Work of cluster formation (critical) vs. radius of the surface of tension in the n-pentane bubble at T = 310.9 K

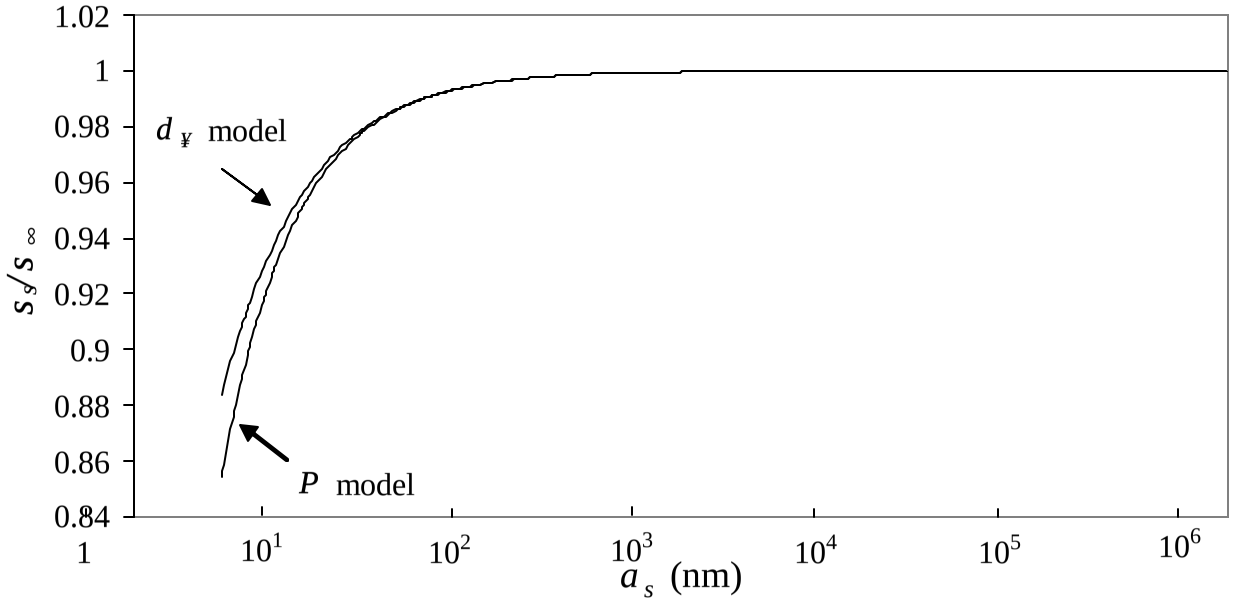

Fig. 9 Curvature dependence of the surface tension for a bubble in an equimolar liquid mixture of propane and n-octane at 300 K from the d_∞ and the ? models

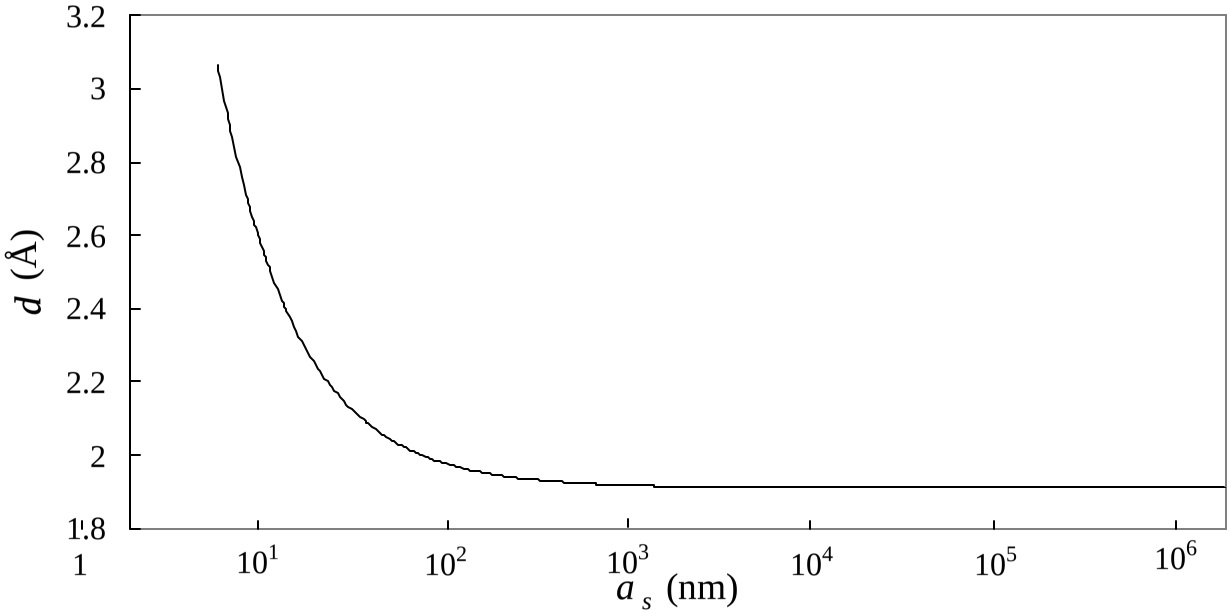

Fig. 10 Curvature dependence of the parameter d for the ? model in the binary-bubble example (equimolar liquid mixture of propane and n-octane at 300 K)

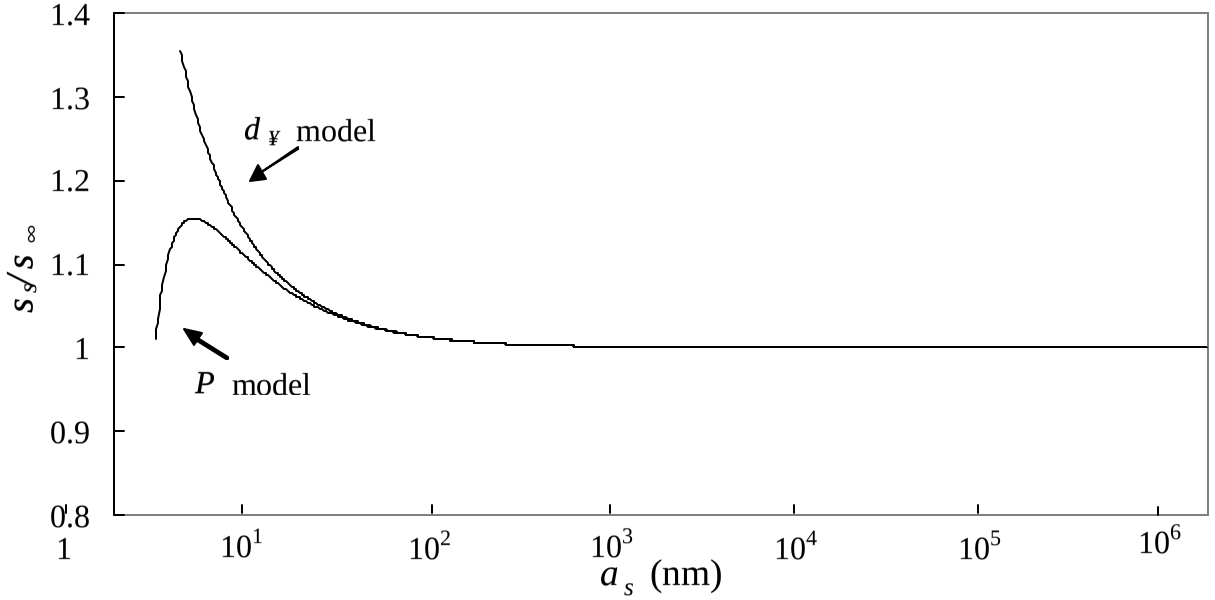

Fig. 11 Curvature dependence of the surface tension for a droplet in an equimolar gaseous mixture of propane and n-octane at 400 K from the d_∞ and the ? models

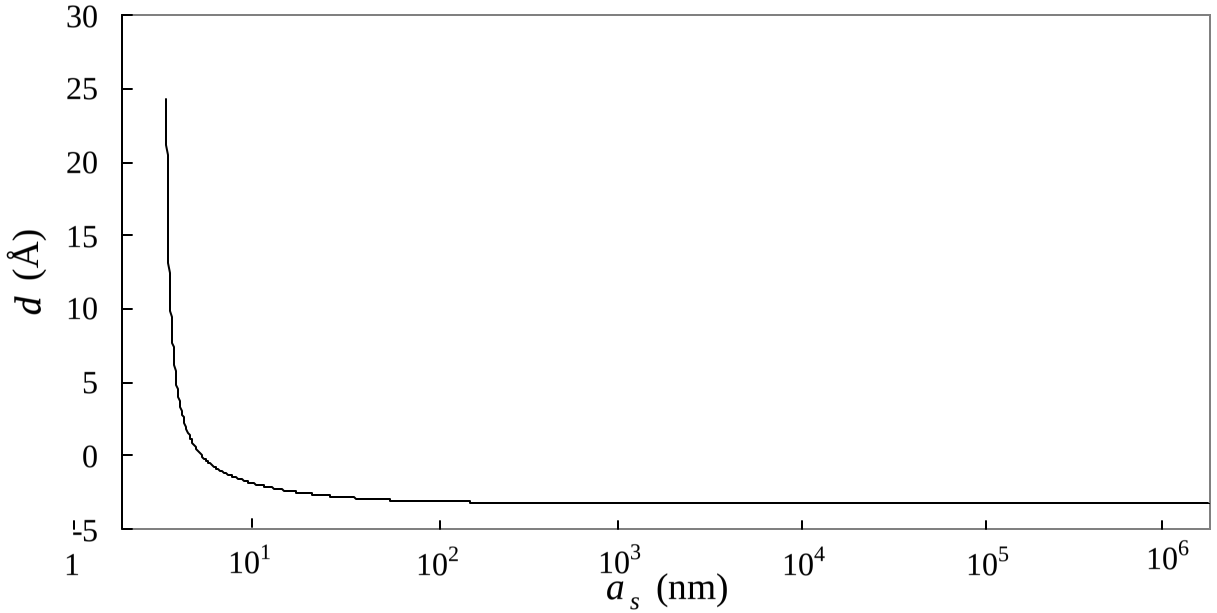

Fig. 12 Curvature dependence of the parameter d from the ? model in the binary droplet example (equimolar gaseous mixture of propane and n-octane at 400 K).

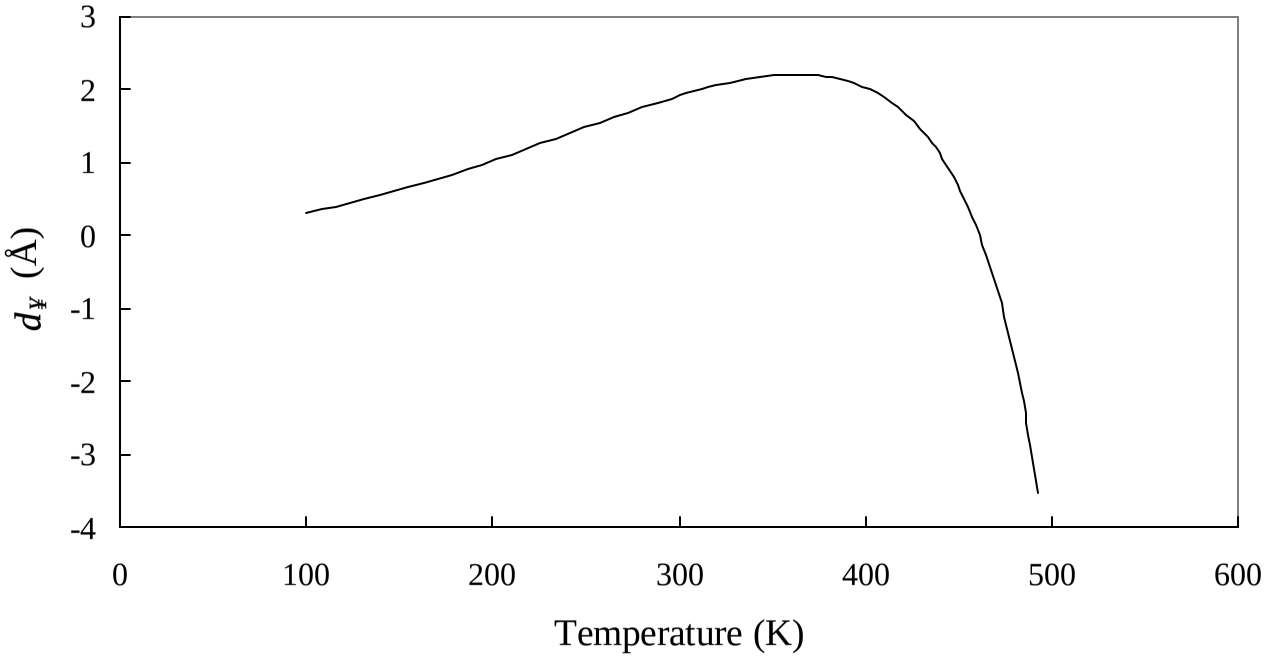

Fig. 13 The parameter d_{∞}^{b} vs. temperature for a bubble in an equimolar mixture of propane and n-octane

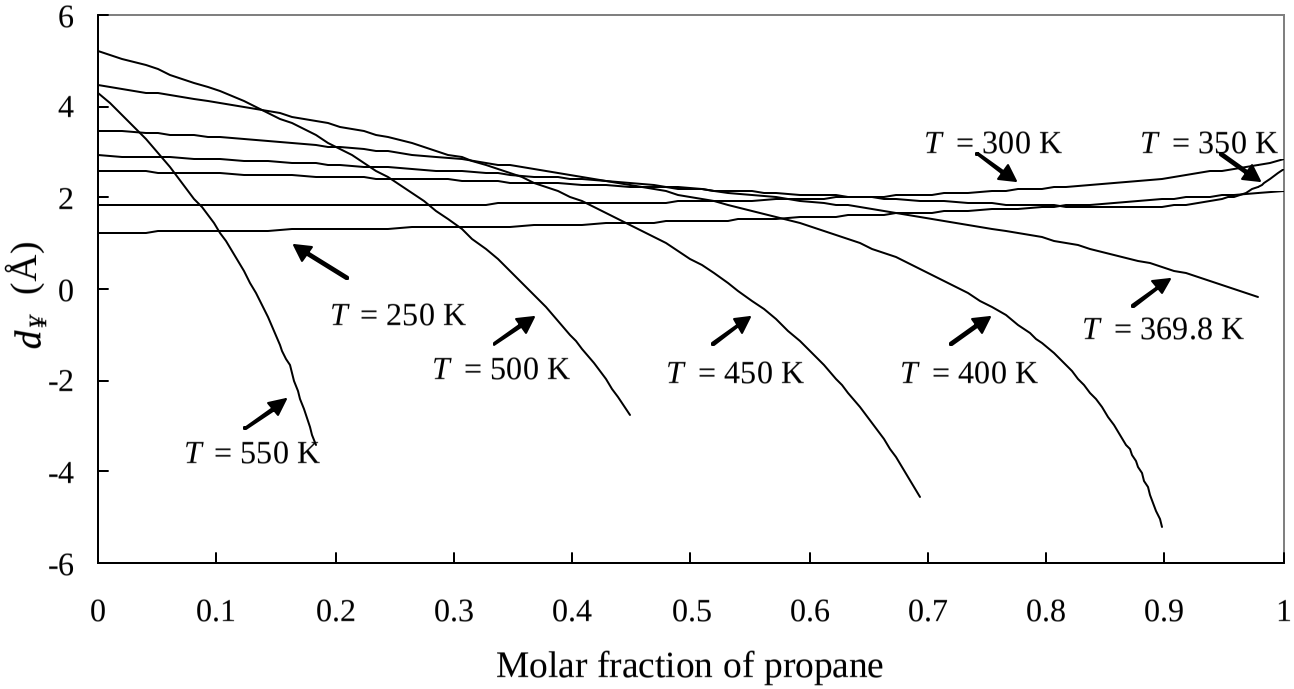

Fig. 14 The parameter d_{∞}^{b} vs. composition for a bubble in a liquid mixture of propane and n-octane at different temperatures

Chapter 4 - Adsorption, Surface Energy, and Surface Entropy in Multicomponent Systems

Erik Santiso and Abbas Firoozabadi, Reservoir Engineering Research Institute

Abstract

In a multicomponent two-phase mixture, the amount of adsorption at the interface (that is, the interface composition) plays a key role. As an example, in a two-phase gas-liquid system, when a surfactant is added to a bulk liquid phase, it mostly moves to the interface between the gas and liquid bulk phases; the result can be a large reduction of the interfacial tension. In a solid-liquid system, there may be a similar process which can result in the change of wettability. In this study, we provide a formulation for the calculation of the amount of the adsorption in the gas-liquid multicomponent systems. As a first step, the fluid mixture is assumed to consist of non-polar species. This would then allow the use of the simple equations of state such as the Peng-Robinson EOS for the description of bulk phase properties.

Introduction

A large number of processes in petroleum reservoirs and production and in other disciplines are affected by the composition and the energy of the interface between the phases. When a component is added to a phase in a gas-liquid system, it is often distributed in the two bulk phases and the interface. Sometimes when a small amount of a component is added to a two-phase system, most of it may end up at the interface between the phases. It is because of high adsorption at the interface that the surface

tension can be lowered significantly by a small amount of a surfactant. Another important phenomenon is the surface wetting, which is related to composition and surface energy. In our work on wettability alteration (Tang and Firoozabadi, 2002a and b), it is because of the adsorption of polymers onto the rock substrate that the surface energy is lowered. The result is change in wettability. Our goal is to model the process of adsorption at the interface between gas and liquid, liquid-solid, and gas-solid systems in order to examine the effect of temperature among other factors.

This work is our second report on interfacial thermodynamics which addresses the issues related to interface adsorption and interface energy. The first report was focused on the effect of curvature on interfacial tension (Santiso and Firoozabadi, 2002). In this work, we provide a formulation for the calculation of interface composition (or sufrace composition), as well as surface energy and entropy. The objective is to estimate the amount of adsorption for all the components in the mixture. In our approach, there is no need to assign zero value of adsorption for one of the components. The conventional approach in the literature is to compute the relative adsorption (Defay and Prigogine, 1966).

This report is structured along the following lines. We first provide thermodynamic relations for the calculation of the amount of adsorption at the interface for a gas-liquid system at equilibrium. Several numerical examples provide the amount of adsorption at the interface for a binary mixture and a ternary mixture. We then provide expressions for surface entropy and surface energy.

Thermodynamic relations for the amounts of adsorption at the interface.

The surface tension s, the amount of adsorption of component i, G_i, the chemical potential of component i at the interface m_i^s for the spherical interface with radius a are related by

$$ds = -s^s\, dT - \sum_{i=1}^{c} G_i dm_i^s + \left[\frac{\partial s}{\partial a}\right] da \qquad (1)$$

where s^s is the entropy per unit area of the interface (the superscript s denotes a surface property), c is the number of components, and $[\partial s / \partial a]$ represents the change in the interfacial tension when the mathematical dividing surface between the two phases is displaced. The above equation was used by Santiso and Firoozabadi (2002) to study the effect of curvature on s.

We can consider the flat interface just as the limit when the radius goes to infinity. If we choose the surface of tension as our dividing surface, (1) becomes:

$$ds_s = -s_s^s\, dT - \sum_{i=1}^{c} G_{i,s} dm_{i,s}^s \qquad (2)$$

The properties referring to the surface of tension are identified with subscript s.Since the system under consideration is in phase equilibrium we can replace the surface chemical potentials in (2) by the chemical potentials of bulk phase a:

$$ds_s = -s_s^s\, dT - \sum_{i=1}^{c} G_{i,s}\, dm_i^a \qquad (3)$$

The chemical potential of bulk phase a can be written in terms of independent variables temperature *T*, pressure of phase a , P^a , and composition of component *j* in phase a x_j^a :

$$dm_i^a = -\tilde{s}_i^a\, dT + \tilde{v}_i^a\, dP^a + \sum_{j=1}^{c-1} \left(\frac{\partial m_i^a}{\partial x_j^a} \right)_{T,P^a,x_{k\neq j,c}^a} dx_j^a \qquad (4)$$

where $\tilde{s}_i^a$ and $\tilde{v}_i^a$ are the partial molar entropy and partial molar volume, respectively. Substituting (4) into (3) we obtain

$$ds_s = \left(-s_s^s + \sum_{i=1}^{c} G_{i,s} \tilde{s}_i^a \right) dT - \left(\sum_{i=1}^{c} G_{i,s} \tilde{v}_i^a \right) dP^a - \sum_{j=1}^{c-1} \left[\sum_{i=1}^{c} G_{i,s} \left(\frac{\partial m_i^a}{\partial x_j^a} \right)_{T,P^a,x_{k\neq j,c}^a} \right] dx_j^a \qquad (5)$$

which is equation (17) in Ref. 3. There, we only developed relations involving the second term of the equation. However, the other two terms contain also valuable information. The first will provide an expression for the surface entropy and the third will provide expressions for the surface adsorptions. In particular, (5) implies that:

$$\left(\frac{\partial s_s}{\partial x_j^a} \right)_{T,P^a,x_{k\neq j,c}^a} = -\sum_{i=1}^{c} G_{i,s} \left(\frac{\partial m_i^a}{\partial x_j^a} \right)_{T,P^a,x_{k\neq j,c}^a} \qquad j = 1,\cdots,c-1 \qquad (6)$$

An expression for the surface tension allows us to calculate the derivatives in the left-hand side of (6) together with an equation of state for the bulk phases (note that (6) would also be valid if we replaced a by b), then (6) is a system of $(c-1)$ equations with c unknowns (the amounts of adsorption). However, we have another equation that also comes from (5):

$$\left(\frac{\partial s_s}{\partial P^a}\right)_{T,x_j^a} = -\sum_{i=1}^{c} G_{i,s}\tilde{v}_i^a \qquad (7)$$

We used this equation in our previous work (Ref. 3) to obtain the size dependence of the surface tension. Equations (6) and (7) complete a system of c equations for the c unknown amounts of adsorption. In the next section, we will proceed with further formulation

Amounts of adsorption for a multicomponent gas-liquid system in equilibrium

In order to solve the system of equations (6)-(7), we need an expression for the surface tension. As we have done in our previous work, we use the Weinaugh-Katz equation (Weinaugh and Katz, 1943) in order to establish the solution procedure.

Let us write the Weinaugh-Katz equation as:

$$s_s^{1/4} = \sum_{i=1}^{c} P_i \left(c_i^b - c_i^a \right) \tag{8}$$

Here we assign the superscript b to the liquid phase and the superscript a to the vapor phase. We also assume that the equation will be valid for a curved interface; for the flat interface we take the limit as the curvature tends to zero. These are the same assumptions made in our previous work.

The Weinaugh-Katz equation will provide the left-hand side terms in equations (6)-(7). From equation (6)-(7) we have:

$$\sum_{i=1}^{c} G_{i,s} \tilde{v}_i^a = -4 s_s^{3/4} \sum_{i=1}^{c} P_i \left[c_T^a - c_T^b \sum_{j=1}^{c} c_j^b \tilde{v}_j^a - r^b \left(\frac{\partial x_i^b}{\partial P^a} \right)_{T, x_i^a} + r^b c_i^b \right] \tag{9}$$

which is (54) in Santiso and Firoozabadi (2002). The derivatives of the compositions of phase b with respect to the pressure of phase a are obtained by solving the system of equations:

$$\sum_{j=1}^{c-1}\left(\frac{\partial x_j^b}{\partial P^a}\right)_{T,x_j^a}\left(\frac{\partial m_i^b}{\partial x_j^b}\right)_{T,P^b,x_{k\neq j,c}^b} = \tilde{v}_i^a - \tilde{v}_i^b \sum_{j=1}^{c} c_j^b \tilde{v}_j^a \qquad i=1,\cdots,c \tag{10}$$

The above equation is the same as (53) in Santiso and Firoozabadi (2002). Now we need the derivatives of the surface tension with respect to the compositions of phase a from equation (6). The procedure to obtain these derivatives is similar to the one we used for the derivative with respect to the pressure, but it is somewhat more involved. We start by differentiating (8) with respect to the composition of component j in phase a and combine the result with (6):

$$\left(\frac{\partial s_s}{\partial x_j^a}\right)_{T,P^a,x_{k\neq j,c}^a} = 4s_s^{3/4}\sum_{i=1}^{c} P_i\left[\left(\frac{\partial c_i^a}{\partial x_j^a}\right)_{T,P^a,x_{k\neq j,c}^a} - \left(\frac{\partial c_i^b}{\partial x_j^a}\right)_{T,P^a,x_{k\neq j,c}^a}\right] \qquad j=1,\cdots,c-1 \tag{11}$$

The first derivative in the square bracket can be readily obtained from an equation of state:

$$\left(\frac{\partial c_i^a}{\partial x_j^a}\right)_{T,P^a,x_{k\neq j,c}^a} = r^a\left[c_i^a\left(\tilde{v}_c^a - \tilde{v}_j^a\right) + d_{ij} - d_{ic}\right] \qquad i=1,\cdots,c \text{ and } j=1,\cdots,c-1 \tag{12}$$

where d_{ij} is the Kronecker delta.

The second derivative is, however, more complicated. In order to get an expression for it, we first write the differential of the concentrations in phase b as a function of the properties of both phase a and phase b:

$$dc_i^b = \left(\frac{\partial c_i^b}{\partial T}\right)_{P^b, x_j^b} dT + \left(\frac{\partial c_i^b}{\partial P^b}\right)_{T, x_j^b} dP^b + \sum_{j=1}^{c-1} \left(\frac{\partial c_i^b}{\partial x_j^b}\right)_{T, P^b, x_{k\neq j,c}^b} dx_j^b \quad i = 1, \cdots, c \qquad (13)$$

$$dc_i^b = \left(\frac{\partial c_i^b}{\partial T}\right)_{P^a, x_j^a} dT + \left(\frac{\partial c_i^b}{\partial P^a}\right)_{T, x_j^a} dP^a + \sum_{j=1}^{c-1} \left(\frac{\partial c_i^b}{\partial x_j^a}\right)_{T, P^a, x_{k\neq j,c}^a} dx_j^a \quad i = 1, \cdots, c \qquad (14)$$

Considering now a process where the temperature, the pressure of phase a and the compositions of all components in phase a except for components j and c are held constant and equating (13) and (14) we obtain:

$$\left(\frac{\partial c_i^b}{\partial x_j^a}\right)_{T, P^a, x_{k\neq j,c}^a} = \left(\frac{\partial c_i^b}{\partial P^b}\right)_{T, x_j^b} \left(\frac{\partial P^b}{\partial x_j^a}\right)_{T, P^a, x_{k\neq j,c}^a}$$

$$+\sum_{k=1}^{c-1}\left(\frac{\partial c_i^b}{\partial x_k^b}\right)_{T,P^b,x^b_{m\neq k,c}}\left(\frac{\partial x_k^b}{\partial x_j^a}\right)_{T,P^a,x^a_{m\neq j,c}} \qquad i=1,\cdots,c \text{ and } j=1,\cdots,c-1 \quad (15)$$

There are four types of derivatives in the right-hand side of (15). The first one can be directly obtained from an equation of state:

$$\left(\frac{\partial c_i^b}{\partial P^b}\right)_{T,x_j^b} = c_i^b C_T^b \qquad i=1,\cdots,c \qquad (16)$$

where C_T is the isothermal compressibility. The third set of derivatives in (15) is similar to the one in (12):

$$\left(\frac{\partial c_i^b}{\partial x_k^b}\right)_{T,P^b,x^b_{m\neq k,c}} = r^b\left[c_i^b\left(\tilde{v}_c^b-\tilde{v}_k^b\right)+d_{ik}-d_{ic}\right] \quad i=1,\cdots,c\,,\ k=1,\cdots,c-1 \qquad (17)$$

Now we need expressions for the second and the fourth set of derivatives in (15). These can be obtained from the chemical equilibrium condition:

$$m_i^a = m_i^b \Rightarrow \left(\frac{\partial m_i^a}{\partial x_j^a}\right)_{T,P^a,x^a_{k\neq j,c}} = \left(\frac{\partial m_i^b}{\partial x_j^a}\right)_{T,P^a,x^a_{k\neq j,c}} \qquad i=1,\cdots,c\,;\ \ k=1,\cdots,c-1 \qquad (18)$$

The left-hand side in (18) can be directly obtained from an equation of state. In order to calculate the right-hand side, we follow a procedure similar to that of equations (13)-(15) for the chemical potentials of phase b, obtaining:

$$\left(\frac{\partial m_i^b}{\partial x_j^a}\right)_{T,P^a,x^a_{k\neq j,c}} = \left(\frac{\partial m_i^b}{\partial P^b}\right)_{T,x_j^b}\left(\frac{\partial P^b}{\partial x_j^a}\right)_{T,P^a,x^a_{k\neq j,c}} + \sum_{k=1}^{c-1}\left(\frac{\partial m_i^b}{\partial x_k^b}\right)_{T,P^b,x^b_{m\neq k,c}}\left(\frac{\partial x_k^b}{\partial x_j^a}\right)_{T,P^a,x^a_{m\neq j,c}} \qquad (19)$$

$$i = 1,\cdots,c \text{ and } j = 1,\cdots,c-1$$

The first derivative on the right-hand side of (19) is the partial molar volume of component i in phase b. Substituting (19) into (18) we obtain:

$$\left(\frac{\partial m_i^a}{\partial x_j^a}\right)_{T,P^a,x^a_{k\neq j,c}} = \tilde{v}_i^b\left(\frac{\partial P^b}{\partial x_j^a}\right)_{T,P^a,x^a_{k\neq j,c}} + \sum_{k=1}^{c-1}\left(\frac{\partial m_i^b}{\partial x_k^b}\right)_{T,P^b,x^b_{m\neq k,c}}\left(\frac{\partial x_k^b}{\partial x_j^a}\right)_{T,P^a,x^a_{m\neq j,c}} \qquad (20)$$

$$i = 1,\cdots,c\,;\ j = 1,\cdots,c-1$$

Multiplying (20) by x_i^b and summing over $i = 1,\cdots,c$ we get:

$$\sum_{i=1}^{c} x_i^b\left(\frac{\partial m_i^a}{\partial x_j^a}\right)_{T,P^a,x^a_{k\neq j,c}} = v^b\left(\frac{\partial P^b}{\partial x_j^a}\right)_{T,P^a,x^a_{k\neq j,c}} + \sum_{k=1}^{c-1}\left(\frac{\partial x_k^b}{\partial x_j^a}\right)_{T,P^a,x^a_{m\neq j,c}}\sum_{i=1}^{c} x_i^b\left(\frac{\partial m_i^b}{\partial x_k^b}\right)_{T,P^b,x^b_{m\neq k,c}}$$

$$j = 1,\cdots,c-1 \qquad (21)$$

From the Gibbs-Duhem equation for phase b we have:

$$\sum_{i=1}^{c} x_i^b \left(\frac{\partial m_i^b}{\partial x_k^b} \right)_{T,P^b,x_{m\neq k,c}^b} = 0 \qquad (22)$$

Substituting (22) into (21) we obtain:

$$\left(\frac{\partial P^b}{\partial x_j^a} \right)_{T,P^a,x_{k\neq j,c}^a} = r^b \sum_{i=1}^{c} x_i^b \left(\frac{\partial m_i^a}{\partial x_j^a} \right)_{T,P^a,x_{k\neq j,c}^a} = \sum_{i=1}^{c} c_i^b \left(\frac{\partial m_i^a}{\partial x_j^a} \right)_{T,P^a,x_{k\neq j,c}^a} \qquad j = 1,\cdots,c-1 \quad (23)$$

This is the second derivative in the right-hand side of (15). Substituting (23) into (20) we obtain:

$$\sum_{k=1}^{c-1} \left(\frac{\partial m_i^b}{\partial x_k^b} \right)_{T,P^b,x_{m\neq k,c}^b} \left(\frac{\partial x_k^b}{\partial x_j^a} \right)_{T,P^a,x_{m\neq j,c}^a} = \left(\frac{\partial m_i^a}{\partial x_j^a} \right)_{T,P^a,x_{k\neq j,c}^a} - \tilde{v}_i^b \sum_{k=1}^{c} c_k^b \left(\frac{\partial m_k^a}{\partial x_j^a} \right)_{T,P^a,x_{k\neq j,c}^a}$$

$$i = 1,\cdots,c\,;\ j = 1,\cdots,c \qquad (24)$$

Equations (24), for each value of $j = 1,\cdots,c-1$, are a system of c equations that can be used to obtain the derivatives of the composition of all components in phase b with respect to the composition of component j of phase a. Note that one of these c equations is dependent because we used their sum to obtain the derivative of the pressure in (23). These systems of equations provide us with the last set of derivatives in (18), thus

completing the information needed to calculate the derivatives of the surface tension with respect to the compositions. Substituting (16), (17), (23) into (15) we obtain:

$$\left(\frac{\partial c_i^b}{\partial x_j^a}\right)_{T,P^a,x^a_{k\neq j,c}} = c_i^b\, C_T^b \sum_{k=1}^{c} c_k^b \left(\frac{\partial m_k^a}{\partial x_j^a}\right)_{T,P^a,x^a_{m\neq j,c}} + r^b \left(\frac{\partial x_i^b}{\partial x_j^a}\right)_{T,P^a,x^a_{m\neq j,c}}$$

$$+ \sum_{k=1}^{c-1} r^b c_i^b \left(\tilde{v}_c^b - \tilde{v}_k^b\right)\left(\frac{\partial x_k^b}{\partial x_j^a}\right)_{T,P^a,x^a_{m\neq j,c}} \qquad i=1,\cdots,c\,;\ j=1,\cdots,c-1 \qquad (25)$$

It is necessary to use the sum condition of phase b to obtain the equation for $i=c$. Finally, substituting (12) and (25) into (11):

$$\left(\frac{\partial s_s}{\partial x_j^a}\right)_{T,P^a,x^a_{k\neq j,c}} = 4s_s^{3/4} \sum_{i=1}^{c} P_i \left\{ c_i^b\, b^b \sum_{k=1}^{c} c_k^b \left(\frac{\partial m_k^a}{\partial x_j^a}\right)_{T,P^a,x^a_{m\neq j,c}} + r^b \left(\frac{\partial x_i^b}{\partial x_j^a}\right)_{T,P^a,x^a_{m\neq j,c}} \right.$$

$$\left. + \sum_{k=1}^{c-1} r^b c_i^b \left(\tilde{v}_c^b - \tilde{v}_k^b\right)\left(\frac{\partial x_k^b}{\partial x_j^a}\right)_{T,P^a,x^a_{m\neq j,c}} - r^a \left[c_i^a \left(\tilde{v}_c^a - \tilde{v}_j^a\right) + d_{ij} - d_{ic}\right] \right\} \quad j=1,\cdots,c-1 \quad (26)$$

Equations (9) and (26) can be combined with (10) and (24) to provide a system of equations for the amounts of adsorption at the interface.

Figures 1 to 8 present the results for the amount of adsorption at the interface for the system propane-normal octane at various temperatures and composition of the liquid phase. These calculations are made for a flat interface. The same type of calculations can be performed for a curved interface.

Figures 1 to 7 reveal that propane (that is, the lighter component) is selectively adsorbed at the interface except at high concentrations of propane in the bulk liquid phase. It is also interesting to note that for the temperatures considered, there is at least one extremum in the amount of adsorption with a secondary extremum when the temperature approaches the critical temperature of propane from below (see Fig. 4). Fig. 8 shows that the temperature variation may not have strong effect on adsorption when the liquid composition is fixed to be equimolar value.

Fig. 9 shows the adsorption at the interface vs. normal fraction of C_1 and C_3 in the ternary mixture of $C_1/C_3/nC_8$ at 250 K. Note that methane adsorption is positive for the whole range of composition. Propane exhibits both positive and negative adsorption, and a clear increasing and decreasing trend. The adsorption of n-octane is negative and its behavior is in the opposite direction to propane.

Surface entropy and surface energy

So far, we considered the consequence of looking closely at the second and third terms of equation (5). Let us look now at the first one. The process will be pretty much the same as we have used for the other two. From equation (5) we can directly infer that:

$$\left(\frac{\partial s_s}{\partial T}\right)_{P^a, x_i^a} = -s_s^s + \sum_{i=1}^{c} G_{i,s}\tilde{s}_i^a \qquad (27)$$

This can again be combined with an equation for the surface tension to obtain the surface entropy.

In order to illustrate the use and the results that can be obtained from (27), we use again equation (8). Differentiating (8) with respect to temperature keeping constant the pressure and composition of phase a leads to:

$$\left(\frac{\partial s_s}{\partial T}\right)_{P^a,x_i^a} = 4s_s^{3/4}\sum_{i=1}^{c} P_i\left[\left(\frac{\partial c_i^b}{\partial T}\right)_{P^a,x_j^a} - \left(\frac{\partial c_i^a}{\partial T}\right)_{P^a,x_j^a}\right] \tag{28}$$

The second derivative term in the brackets can be readily obtained from an equation of state:

$$\left(\frac{\partial c_i^a}{\partial T}\right)_{P^a,x_j^a} = x_i^a\left(\frac{\partial r^a}{\partial T}\right)_{P^a,x_j^a} = -r^a x_i^a k^a = -c_i^a k^a \quad i=1,\cdots,c \tag{29}$$

where k is the isobaric expansion coefficient. To obtain the first derivative in (28) we need to use equation (13) to obtain:

$$\left(\frac{\partial c_i^b}{\partial T}\right)_{P^a,x_j^a} = \left(\frac{\partial c_i^b}{\partial T}\right)_{P^b,x_j^b} + \left(\frac{\partial c_i^b}{\partial P^b}\right)_{T,x_j^b}\left(\frac{\partial P^b}{\partial T}\right)_{P^a,x_j^a}$$

$$+\sum_{j=1}^{c-1}\left(\frac{\partial x_j^b}{\partial T}\right)_{P^a,x_k^a}\left(\frac{\partial c_i^b}{\partial x_j^b}\right)_{T,P^b,x_{k\neq j,c}^b} \quad i=1,\cdots,c \tag{30}$$

The first derivative on the right-hand side of (30) is similar to the one in (29):

$$\left(\frac{\partial c_i^{\,b}}{\partial T}\right)_{P^b,x_j^b} = -c_i^{\,b}\,k^{\,b} \qquad i = 1,\cdots,c \tag{31}$$

The derivatives of the concentration with respect to pressure in phase b can be obtained from (16), and the derivatives of the concentration with respect to mole fractions can be obtained from (17).

We need an expression for the two remaining derivatives; we differentiate the chemical equilibrium condition with respect to the temperature:

$$m_i^a = m_i^b \;\Rightarrow\; \left(\frac{\partial m_i^a}{\partial T}\right)_{P^a,x_j^a} = \left(\frac{\partial m_i^b}{\partial T}\right)_{P^a,x_j^a} \qquad i = 1,\cdots,c \tag{32}$$

The left-hand side is the partial molar entropy of component i in phase a; $(\partial m_i^a/\partial T)_{p^a,x_j^a} = \tilde{s}_i^a$. For the right-hand side we repeat the procedure used for the concentrations in equation (30) to get:

$$\left(\frac{\partial m_i^b}{\partial T}\right)_{P^a,x_j^a} = \left(\frac{\partial m_i^b}{\partial T}\right)_{P^b,x_j^b} + \left(\frac{\partial m_i^b}{\partial P^b}\right)_{T,x_j^b}\left(\frac{\partial P^b}{\partial T}\right)_{P^a,x_j^a} + \sum_{j=1}^{c-1}\left(\frac{\partial x_j^b}{\partial T}\right)_{P^a,x_k^a}\left(\frac{\partial m_i^b}{\partial x_j^b}\right)_{T,P^b,x_{k\neq j,c}^b}$$

$$i = 1,\cdots,c \qquad (33)$$

Substituting (33) into (32) and recognizing the partial molar entropies and volumes we get:

$$\tilde{s}_i^a = \tilde{s}_i^b + \tilde{v}_i^b\left(\frac{\partial P^b}{\partial T}\right)_{P^a,x_j^a} + \sum_{j=1}^{c-1}\left(\frac{\partial x_j^b}{\partial T}\right)_{P^a,x_k^a}\left(\frac{\partial m_i^b}{\partial x_j^b}\right)_{T,P^b,x_{k\neq j,c}^b} \qquad i = 1,\cdots,c \qquad (34)$$

Multiplying (34) by x_i^b and summing over $i = 1,\cdots,c$:

$$\sum_{i=1}^{c} x_i^b \tilde{s}_i^a = s^b + v^b\left(\frac{\partial P^b}{\partial T}\right)_{P^a,x_j^a} + \sum_{j=1}^{c-1}\left(\frac{\partial x_j^b}{\partial T}\right)_{P^a,x_k^a}\sum_{i=1}^{c} x_i^b\left(\frac{\partial m_i^b}{\partial x_j^b}\right)_{T,P^b,x_{k\neq j,c}^b} \qquad (35)$$

The last term vanishes due to the Gibbs-Duhem equation for phase b. Thus, we obtain:

$$\left(\frac{\partial P^b}{\partial T}\right)_{P^a,x_j^a} = r^b\left(-s^b + \sum_{i=1}^{c} x_i^b \tilde{s}_i^a\right) \qquad (36)$$

Substituting (36) into (34) and rearranging leads to:

$$\sum_{j=1}^{c-1}\left(\frac{\partial x_j^b}{\partial T}\right)_{P^a,x_k^a}\left(\frac{\partial m_i^b}{\partial x_j^b}\right)_{T,P^b,x_{k\neq j,c}^b} = \tilde{s}_i^a - \tilde{s}_i^b - \tilde{v}_i^b \rho^b\left(-s^b + \sum_{i=1}^{c} x_i^b \tilde{s}_i^a\right) \quad i=1,\cdots,c \tag{37}$$

Equations (37) form a system of c equations (one of which is dependent) that can be solved to obtain the $(c-1)$ derivatives of the composition of phase b with respect to temperature. The last one can be obtained from the sum condition. Substituting (16), (17), (31), (36) into (30) leads to:

$$\left(\frac{\partial c_i^b}{\partial T}\right)_{P^a,x_j^a} = -c_i^b \kappa^b + c_i^b \rho^b \beta^b\left(-s^b + \sum_{i=1}^{c} x_i^b \tilde{s}_i^a\right) + \rho^b\left(\frac{\partial x_i^b}{\partial T}\right)_{P^a,x_k^a}$$
$$+ \sum_{j=1}^{c-1} \rho^b c_i^b\left(\tilde{v}_c^b - \tilde{v}_j^b\right)\left(\frac{\partial x_j^b}{\partial T}\right)_{P^a,x_k^a} \qquad i=1,\cdots,c \tag{38}$$

And finally, substituting (29) and (37) into (28):

$$\left(\frac{\partial s_s}{\partial T}\right)_{P^a,x_i^a} = 4s_s^{3/4}\sum_{i=1}^{c} P_i\left\{-c_i^b \kappa^b + c_i^b \rho^b \beta^b\left(-s^b + \sum_{i=1}^{c} x_i^b \tilde{s}_i^a\right) + \rho^b\left(\frac{\partial x_i^b}{\partial T}\right)_{P^a,x_k^a}\right.$$
$$\left. + \sum_{j=1}^{c-1} \rho^b c_i^b\left(\tilde{v}_c^b - \tilde{v}_j^b\right)\left(\frac{\partial x_j^b}{\partial T}\right)_{P^a,x_k^a} + c_i^a \kappa^a\right\} \tag{39}$$

Equation (39), combined with (27), can be used to obtain the surface entropy. The surface energy can then be readily obtained from:

$$u_s^s = s_s + Ts_s^s + \sum_{i=1}^{c} G_i m_i^s \qquad (40)$$

Conclusions

We have derived the expression for the calculation of adsorption at the gas-liquid interface in multicomponent systems. The expressions for the interface entropy and energy are also derived for gas-liquid systems for multicomponents.

Numerical results show that the adsorption of one of the components in a binary mixture can increase and then decrease when the concentration of the same component increases. Numerical results for the same binary mixtures reveal that these may be two extremums of adsorption when the concentration of the same component is varied.

References

1. Tang, T. and Firoozabadi, A.: "Relative Permeability Modification in Gas-Liquid Systems through Wettability Alteration to Intermediate Gas-Wetting," SPE Reservoir and Engineering (Dec. 2002), also SPE 62934.
2. Tang, T. and Firoozabadi, A.: "Wettability Alteration to Intermediate Gas-Wetting in Porous Media at Elevated Temperature," Transport in Porous Media (Nov. 2002).

3. Santiso, E. and Firoozabadi, A.: “Curvature Dependency of Surface Tension in Multicomponent System,” Chapter III
4. Defay, R. and Prigogine, J.: “Surface Tension and Adsorption,” Longman (1966) London.
5. Weinaugh, C.F. and Katz, D.G.: “Surface Tension of Methane-Propane Mixtures,” Industrial & Eng. Chem. 35, 239 (Feb. 1943).

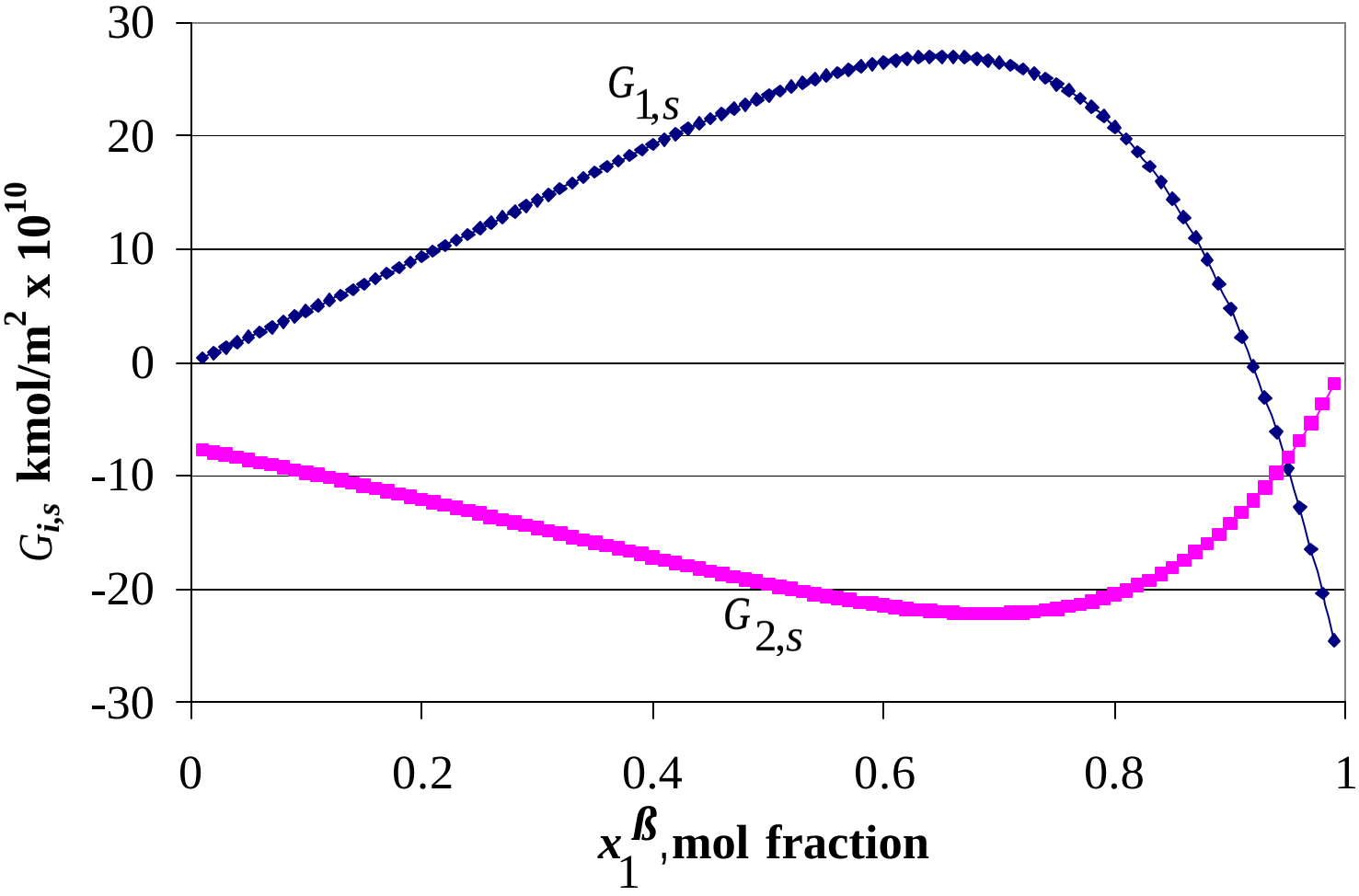

Fig. 1 – Adsorption at the Gas-Liquid Interface for Propane (1) and Normal Octane (2) Mixture vs. Mol Fraction of Propane in Liquid Phase: T = 250 K.

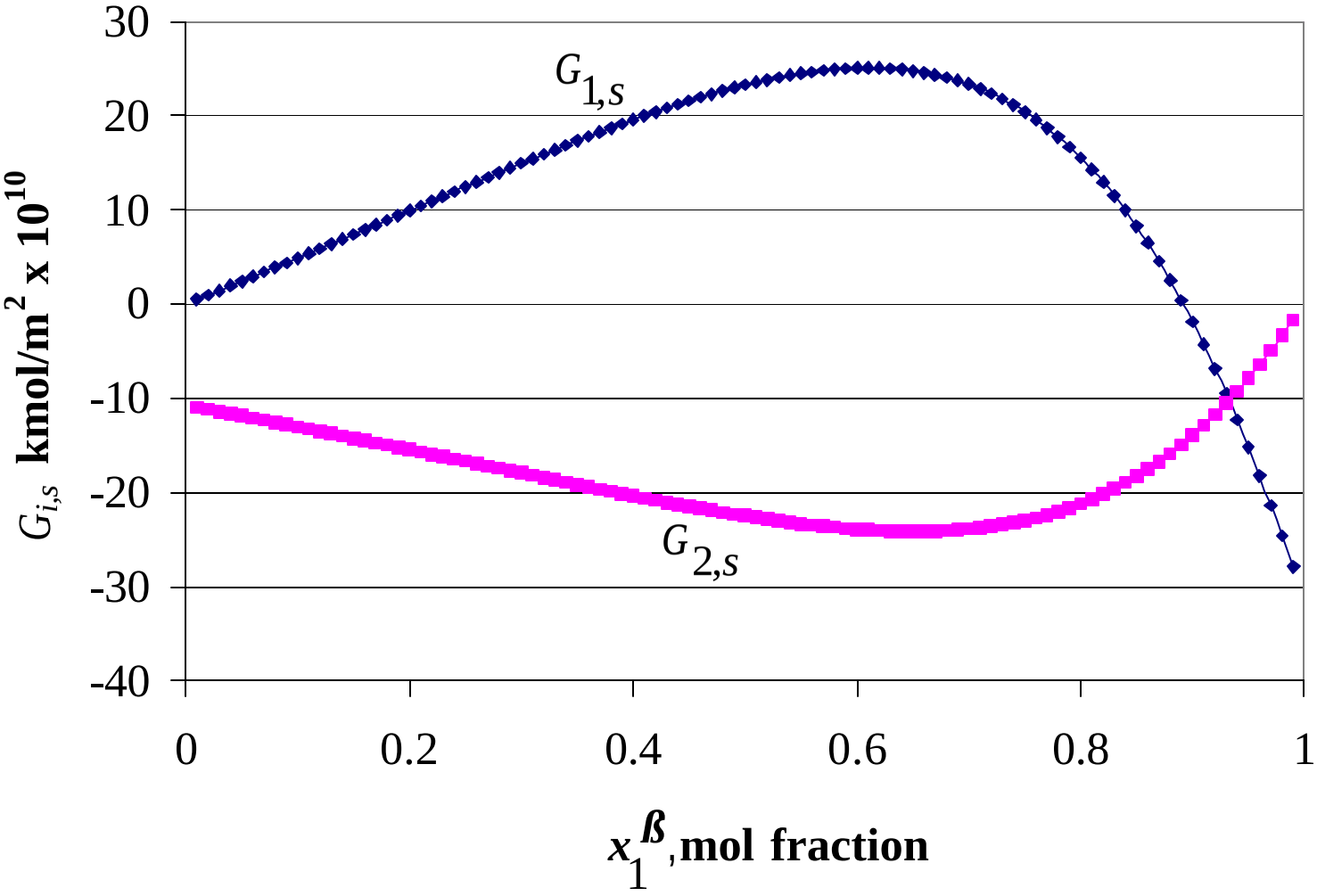

Fig. 2 – Adsorption at the Gas-Liquid Interface for Propane (1) and Normal Octane (2) Mixture vs. Mol Fraction of Propane in Liquid Phase: T = 300 K.

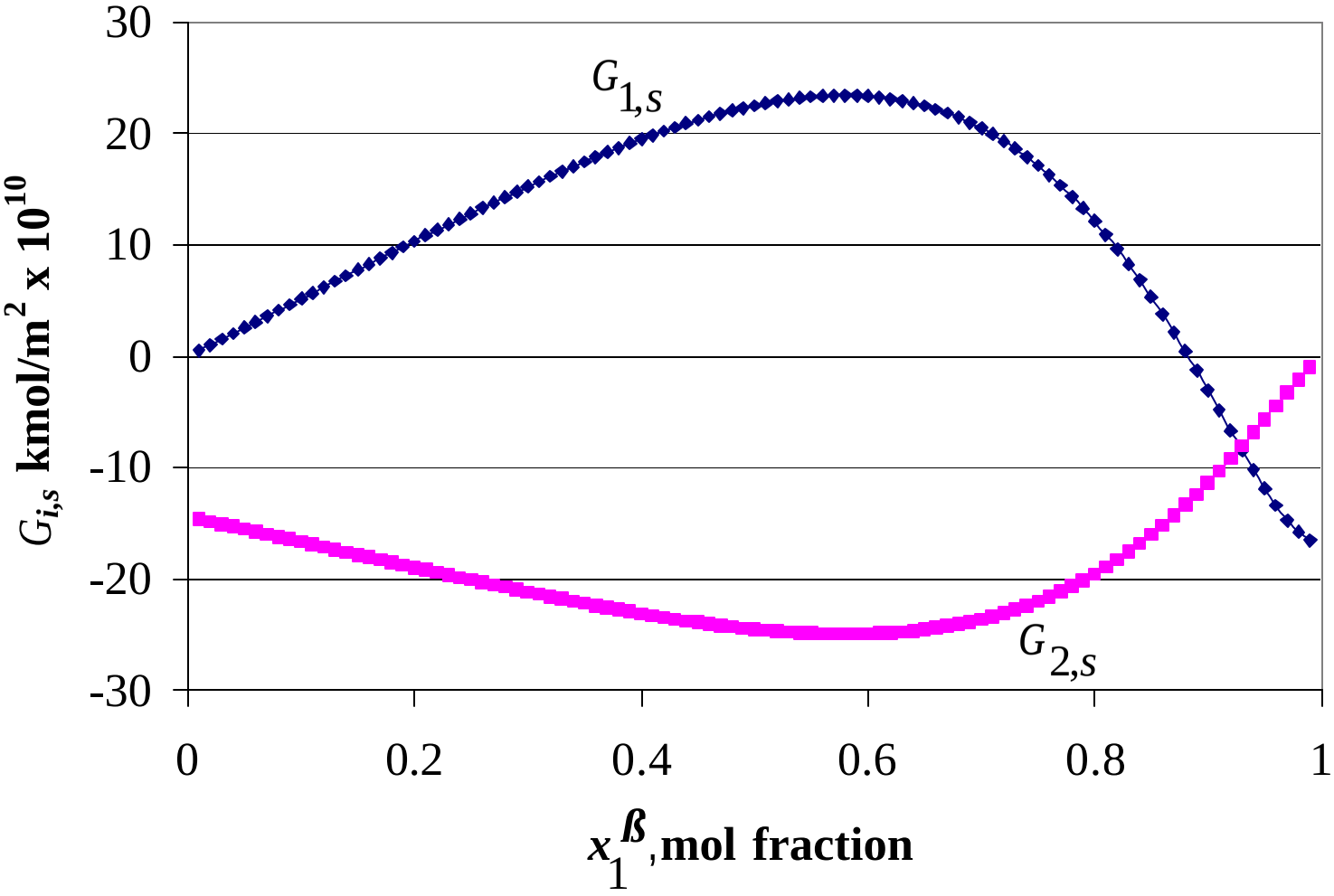

Fig. 3 – Adsorption at the Gas-Liquid Interface for Propane (1) and Normal Octane (2) Mixture vs. Mol Fraction of Propane in Liquid Phase: T = 350 K.

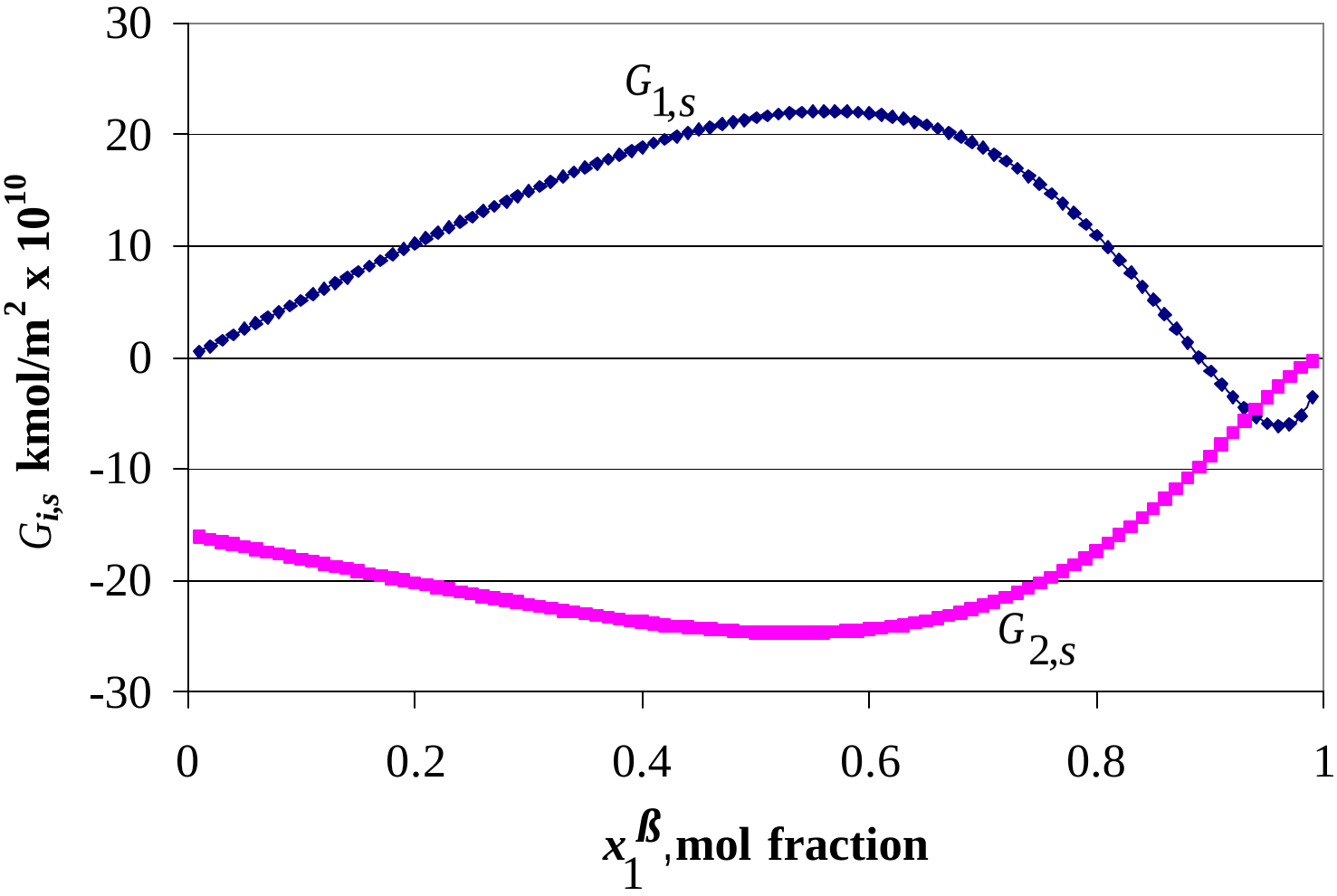

Fig. 4 – Adsorption at the Gas-Liquid Interface for Propane (1) and Normal Octane (2) Mixture vs. Mol Fraction of Propane in Liquid Phase: T = 369.8 K.

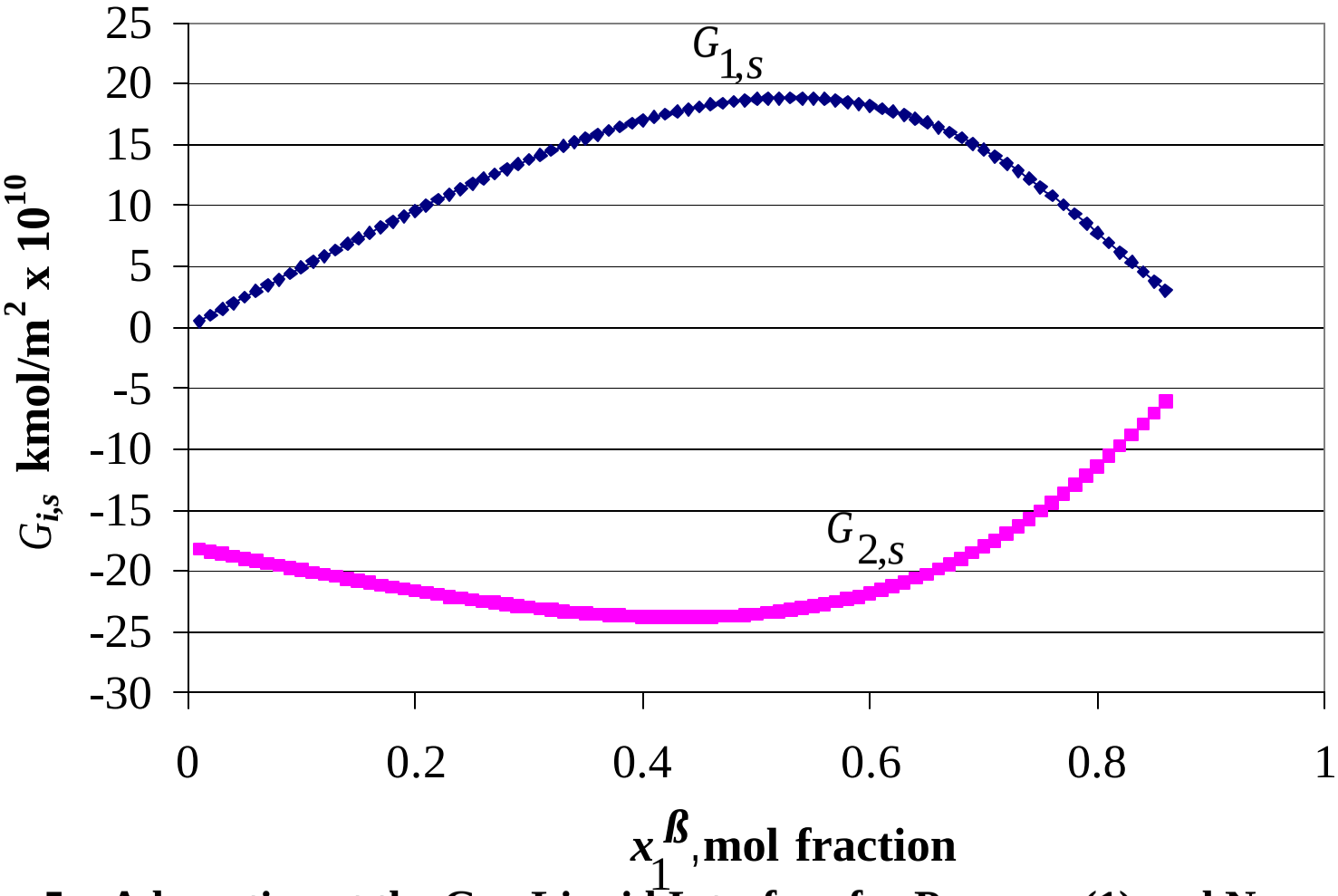

Fig. 5 – Adsorption at the Gas-Liquid Interface for Propane (1) and Normal Octane (2) Mixture vs. Mol Fraction of Propane in Liquid Phase: T = 400 K.

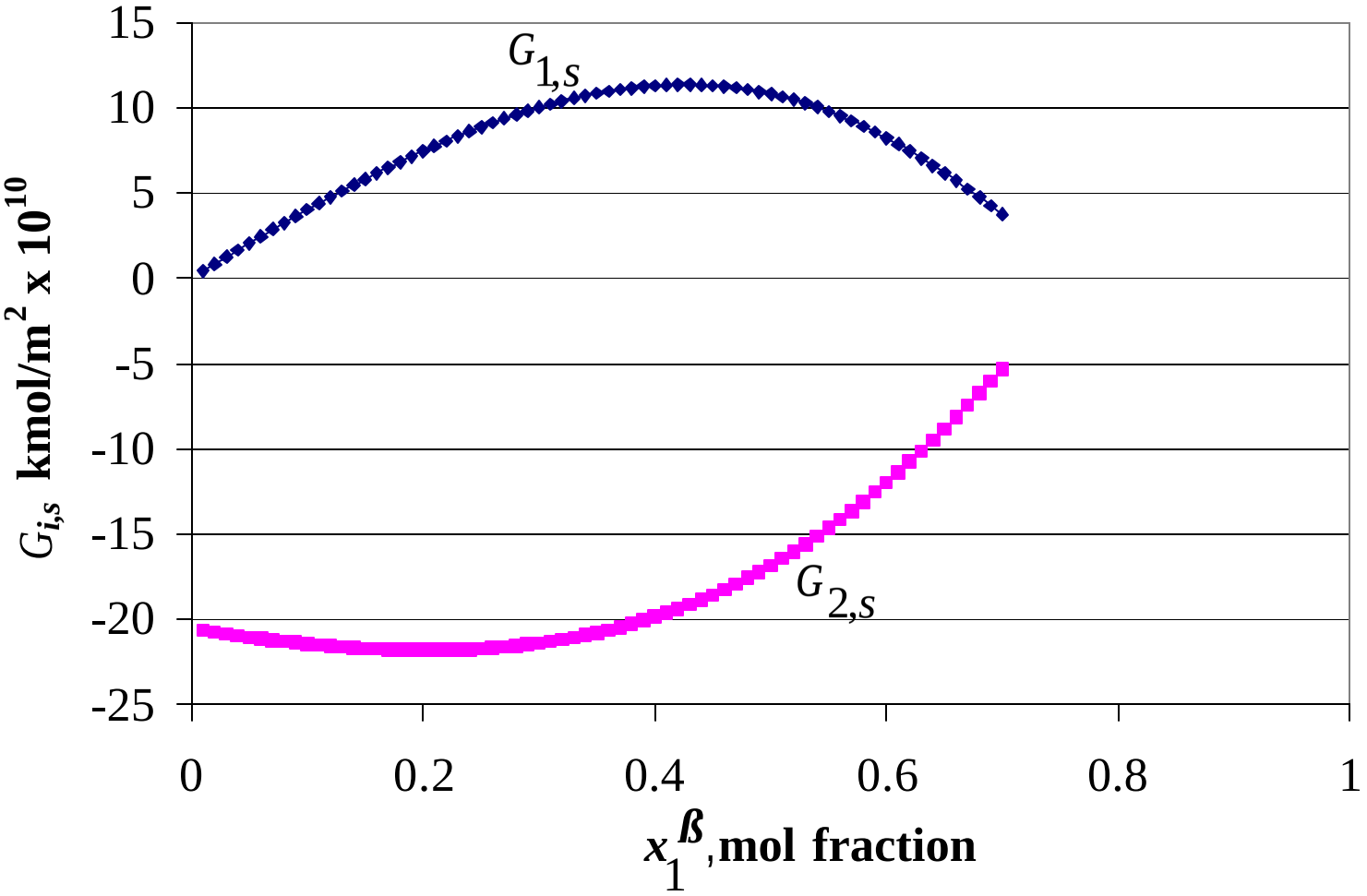

Fig. 6 – Adsorption at the Gas-Liquid Interface for Propane (1) and Normal Octane (2) Mixture vs. Mol Fraction of Propane in Liquid Phase: T = 450 K.

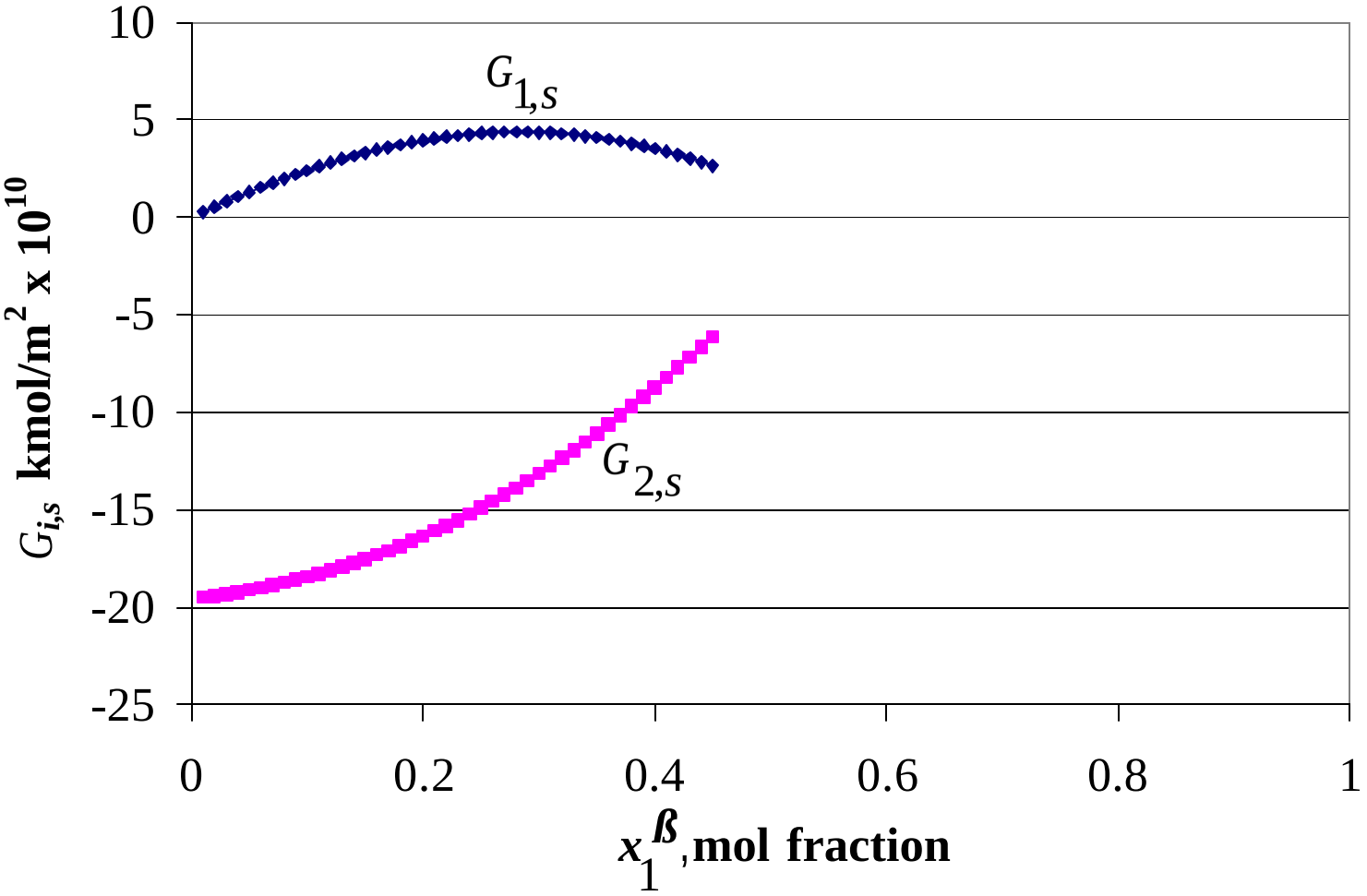

Fig. 7 – Adsorption at the Gas-Liquid Interface for Propane (1) and Normal Octane (2) Mixture vs. Mol Fraction of Propane in Liquid Phase: T = 500 K.

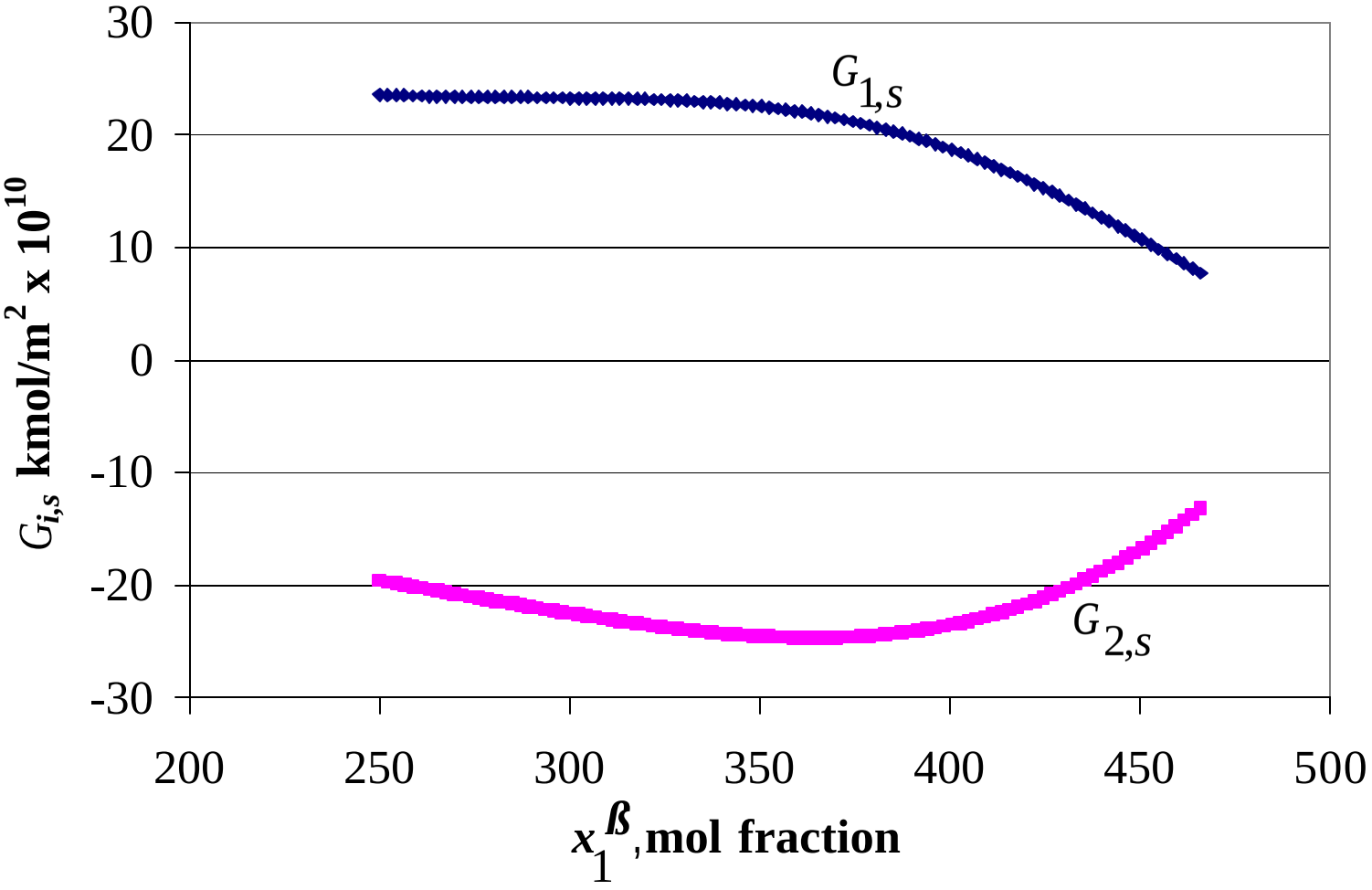

Fig. 8 – Adsorption at the Gas-Liquid Interface for Propane (1) and Normal Octane (2) Mixture vs. Temperature for the Liquid Equimolar Mixture.